

72-

DFO - Library / MPO - Bibliotheque



09039240

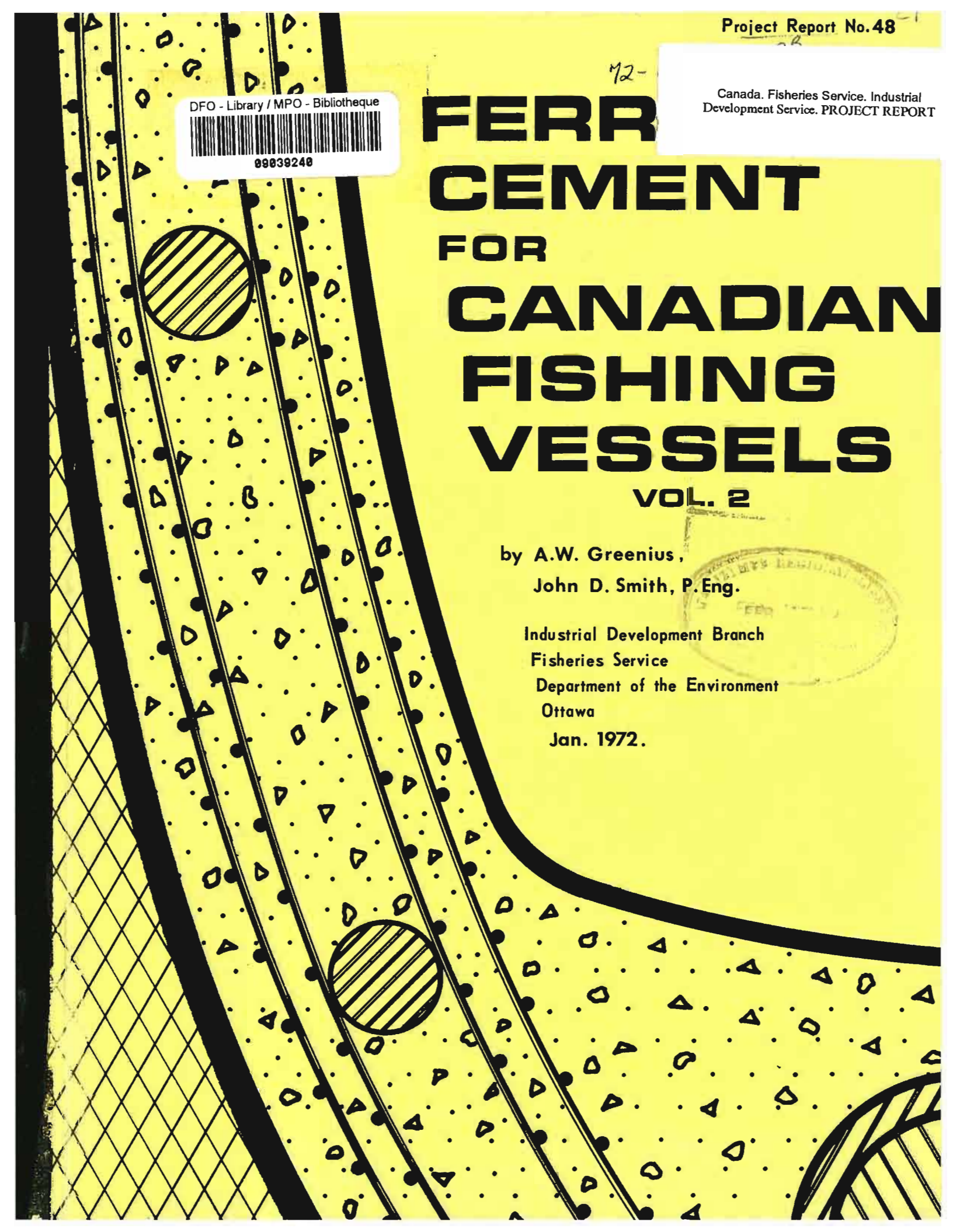
Canada, Fisheries Service, Industrial Development Service, PROJECT REPORT

FERR CEMENT FOR CANADIAN FISHING VESSELS

VOL. 2

by A.W. Greenius,
John D. Smith, P. Eng.

Industrial Development Branch
Fisheries Service
Department of the Environment
Ottawa
Jan. 1972.



FERRO-CEMENT

FOR

FISHING VESSEL CONSTRUCTION II

Prepared by

THE BRITISH COLUMBIA RESEARCH COUNCIL,

3650 WESBROOK CRESCENT,

VANCOUVER 167, CANADA

for

THE VESSELS AND ENGINEERING DIVISION,

INDUSTRIAL DEVELOPMENT BRANCH,

FISHERIES SERVICE,

ENVIRONMENT CANADA,

OTTAWA, ONTARIO.

June, 1971

Pg. 1

Conclusions reached and opinions stated by the author are not necessarily endorsed by the sponsors of this project.

Project Report No. 48.

All previous reports from the British Columbia Research Council are to be found in Section 'B' of Project Report No. 42 of The Industrial Development Branch, Fisheries Service, Department of Fisheries and Forestry, Ottawa, Ontario.

TABLE OF CONTENTS

	<u>Page</u>
INTRODUCTION	1
SUMMARY	1
Test Program	1
Mathematical Model	3
PART I - TEST PROGRAM	5
A. PANELS TO ASSESS REINFORCEMENT	5
1. Panel Construction Details	5
2. Mesh Reinforcements	6
(a) Kinds and amounts used	6
(b) Strength of mesh	7
(c) Surface bond areas	8
(d) Costs	8
3. Rod Reinforcements	9
(a) Kinds used	9
(b) Tensile strength	9
(c) Effect of welding high tensile rods	9
(d) Rod/mortar bond strengths	9
4. Strength of Panels	11
(a) Drop-impact tests	11
(b) Tensile tests	12
(c) Flexure tests	13
5. Durability	19
(a) Freeze-thaw tests	20
(b) Seawater exposure tests	23
B. PANELS TO ASSESS MORTAR ADMIXTURES	26
1. Description of admixtures used	26
(a) Pozzolans	26
(b) Water-reducing agents	27
(c) Air-entrainment agents	27
(d) Polyvinyl acetate emulsions	27

TABLE OF CONTENTS (cont'd)

	<u>Page</u>
2. Panel construction details	28
3. Characteristics of the mortars	28
(a) Workability	28
(b) Strength	29
(c) Porosity	30
(d) Durability	30
C. OTHER TESTS AND DISCUSSIONS	30
1. Interrupted mortaring	30
2. Fastening	32
3. Protective coatings	32
4. Internal soundness of panels	33
D. BIBLIOGRAPHY	34
E. TABLES AND FIGURES FOR TEST PROGRAM	35
PART II - DEVELOPMENT OF A MATHEMATICAL MODEL	93
A. INTRODUCTION	93
B. DEVELOPMENT OF THE MODEL	95
C. DISCUSSION	104
D. CONCLUSIONS AND RECOMMENDATIONS	105
TABLES AND FIGURES	107

INTRODUCTION.

The Canada Department of Fisheries and Forestry has sponsored a program to evaluate ferro-cement for fishing vessel construction. The purpose of the program is not to develop new types of ferro-cement or to assess all the possible formulations, combinations, and construction techniques which have been or may be used but is rather to obtain engineering data on "typical" ferro-cement construction as it might be undertaken on an amateur or semi-professional basis. It is also the purpose of the program to reveal any marked advantages or shortcomings of any of the several kinds of mesh and rod reinforcements, cements, sands, admixtures, mortaring, and patching techniques. In short, the program of testing has been undertaken to provide basic information for the eventual preparation of "guidelines" to aid persons wishing to make a ferro-cement boat and to aid authorities charged with the responsibility of providing certification for ferro-cement boats.

The scope of the first phase of the program reported in the Final Report, dated March 31, 1970, and its Technical Supplement, dated May 31, 1970, covered an evaluation of various sands, types of cements, and kinds of mesh.

This second phase of the program deals chiefly with the possible benefits of four mortar admixtures, an evaluation of five kinds of rods, and of three kinds of mesh when supported by rod reinforcement. In addition, Mr. John D. Smith, P. Eng.*, formerly attached to this laboratory, has developed a mathematical model to describe the behaviour of ferro-cement which should allow assessment of various ferro-cement constructions with a minimum of verifying test work.

SUMMARY.

Test Program.

Ferro-cement panels have been constructed to assess the effect of some construction variables on strength and durability.

Ten panels were used to assess the effect of four mortar admixtures, namely:

- (a) A pozzolan.
- (b) A water-reducing agent.
- (c) An air-entraining agent.
- (d) A polyvinyl acetate emulsion.

*Mr. John D. Smith is now with Defence Research Establishment Pacific at Esquimalt, B.C.

None of the admixtures appreciably improved the strength and durability (freeze-thaw and seawater cycling) of the ferro-cement. Pozzolan, in the amount added, adversely affected the freeze-thaw resistance. The air-entraining agent appeared to improve the workability slightly. It is considered that the optimum amounts of admixtures have not necessarily been used. A more extensive program may show that one or more of the above admixtures can, in fact, effect a significant improvement in the properties of the ferro-cement panels.

A series of 21 panels was constructed and tested to assess the effect of the following reinforcements on strength:

- (a) 1/2-16 ga. welded square mesh on rods.
- (b) 1/2-19 ga. hardware cloth on rods.
- (c) 1/2-22 ga. hexagonal mesh on rods.
- (d) 1/4-in. hot rolled 1020 rods.
- (e) 1/4-in. galvanized 1020 rods.
- (f) 1/4-in. nail rod.
- (g) 0.225 in. double drawn rods.
- (h) 0.225 in. deformed double drawn rods.

The strength of specimens from various combinations of rods and mesh, rod spacings, and rod/mesh orientation under tensile, flexure, and impact loadings and the durability under freeze-thaw and seawater exposures were assessed.

Rod-reinforced panels constructed of 1/2-16 ga. welded square mesh and 1/2-19 ga. hardware cloth were somewhat stronger in tension, flexure, and impact than those of 1/2-22 ga. hexagonal mesh on an equal reinforcement weight basis. A slightly thinner panel can be constructed with the square mesh materials than with the hexagonal mesh on an equal mesh weight or equal strength basis. The presence of rods in hexagonal-mesh panels tends to equalize the flexural strength of the panels in the two directions, viz. in the direction of mesh twists and across the mesh twists. Builders may find that the "workability" of the hexagonal mesh will "compensate" for the somewhat lower strength properties.

The unit costs of the three mesh materials used are about the same on an equal weight basis. On an equal strength basis, however, the 1/2-22 ga. hexagonal mesh is somewhat more expensive and will require somewhat more mortar to encase the mesh. The finished hull will be thicker and heavier.

The tensile strengths of the mesh and rod materials alone were also determined. Welding of cross-rods to double drawn material was found to reduce the strength of the material with tensile strengths near the upper limit of the range.

Tests indicated that both light rusting and removing the drawing lubricant improved the rod/mortar bond strength of double drawn rods. Hot-rolled rods with scale intact and after pickling had good bond strengths. Galvanized rods showed poor bond strengths and will require treatment with chromic acid or some other inhibitor. The long-term bond strengths have not been determined and it is considered that galvanized rods may prove superior after a lone exposure to its operating environment

Other factors such as interrupted mortaring, fastenings, and protective coatings have been considered and discussed.

A bibliography of 77 articles and books on ferro-cement is included in this report.

It is emphasized that the test results and conclusions drawn therefrom are based in most instances on tests from a single panel of any one condition of mortar formulation and reinforcing materials. This one condition may not represent the optimum combination of mortar, admixture, reinforcement, or practice.

Mathematical Model.

An attempt has been made to devise a mathematical model to obviate the need to test a great number of ferro-cement panels covering a wide range of reinforcement construction and many load conditions. The model developed in Part II by Mr. John D. Smith, P. Eng., is considered to hold promise of being a satisfactory base for a design procedure for ferro-cement in the working stress range.

A linear model, in which both mortar and steel are assumed to behave in a linear manner, resulted in a relatively simple expression for forces and moments. The expressions for the moments are:

$$M_s = \left[\frac{I_s}{h^2} + (Z - C)^2 A_s \right] \epsilon E_s h \quad \text{and} \quad M_m = \frac{C^3 E_m \epsilon h^2}{3}$$

where M_s = moment for steel
 ϵ = total strain
 h = thickness of panel
 I_s = moment of inertia of the steel
 E_s = modulus of elasticity for steel
 Z = ratio of height of centroid of steel to thickness of panel
 C = ratio of height of neutral axis to thickness of panel
 A_s = area of steel
 M_m = moment for mortar
 E_m = modulus of elasticity for mortar

A non-linear model, in which the steel is assumed to behave in a linear fashion and the mortar in a non-linear fashion, gave values for moments which agree less well with measured values obtained in another study.

An improved linear model, in which the mortar is assumed to have some tensile strength, gave values closer to the measured values.

PART I - TEST PROGRAM

A. PANELS TO ASSESS REINFORCEMENT.

1. Panel Construction Details.

Previous work on panels was oriented to determining the engineering properties of panels constructed with various types of cement and sand and various kinds of mesh reinforcement. The present work has chiefly emphasized the determination of engineering properties of ferro-cement panels containing various kinds of rod reinforcement between layers of mesh reinforcement of various kinds. Other aspects, such as the effect of rod spacing, orientation of the mesh related to rods, plastering the two sides of a panel on consecutive days, interrupted plastering, and thinner mixes have also been studied.

Four frames, 38 x 38 inches, were constructed for fabrication of the ferro-cement panels. Holes were drilled at 1-inch intervals along each side for spacing of the rods in multiples of one inch in both directions. The frames permitted plastering from both sides. A typical set-up with rods and mesh in place is shown in Fig. 1.

The panels described in Table 1 were constructed to allow a comparison, especially in the modulus of rupture and drop-impact properties of the following:

- (a) Relative strengths of panels (or test specimens) made with mesh, viz. 1/2-16 ga. welded square mesh, 1/2-19 ga. hardware cloth, and 1/2-22 ga. hexagonal mesh, when supported by high-tensile double-drawn rods spaced at 2-inch centres in both directions.
- (b) Relative strengths of panels (or test specimens) made with 1/2-16 ga. welded square mesh supported by rods spaced at 2-inch centres and with no rods.
- (c) Relative strength of panels (or test specimens) made with 1/2-19 ga. hardware cloth supported by high-tensile double-drawn rods at 2- and 4-inch centres.
- (d) Relative strengths of panels (or test specimens) made with various kinds of rods, viz. high-tensile double-drawn, galvanized 1020, bright nail wire, hot-rolled 1020, and deformed high-tensile double-drawn rods with 1/2-19 ga. hardware cloth mesh.
- (e) Relative strengths of panels (or test specimens) made with two levels of the same mesh, viz. 10 layers and 6 layers of 1/2-22 ga. hexagonal mesh supported by high-tensile double-drawn rods.

- (f) Relative strength of panels (or test specimens) made with rods of similar strength but enhanced bond strength, viz. high-tensile double-drawn rods and deformed high-tensile double-drawn rods with 1/2-22 ga. hexagonal mesh.
- (g) Relative strength and behaviour of panels (or test specimens) made by mortaring both sides on same day and on subsequent days.
- (h) Relative strength and behaviour of panels (or test specimens) made with mortar joint.

All panels 41 to 61 were made with mortar of Type II cement and Evco Dry Mortar Sand. The characteristics of the cement and sand were described in the earlier report. The cement/sand ratio used was 1:2. The cement and sand were mixed dry in the mortar mixer for about two minutes. Water in a water/cement ratio of 0.4 was added to the dry mix and the mixer was run for an additional three minutes. A slump test was made and if the slump was below three inches, a small weighed amount of water was added and the mixer was run for another two minutes. The slump was checked again. Three 2-inch test cubes were cast for one 7-day and two 28-day compression tests. The compression test results ranged from 3700 to 7275 psi for the 7-day tests and from 6250 to 9950 psi for the 28-day tests.

The mixed mortar of suitable consistency was plastered into the mesh from one side and forced through as far as possible. The panel was then plastered from the other side. Both sides were subsequently trowelled as smooth as possible. Fig. 2 shows one completed panel still in the frame. The completed panel was covered with plastic sheeting for a day or two, subsequently stripped from the frame, and cured for at least 28 days under plastic sheeting with regular wettings.

Most test panels were made in duplicate so that one panel could be cut up for large bend tests, drop-impact tests, exposure tests, etc., and the other could be used for other tests such as full size drop-impact tests, patching tests, and coating tests as desired.

2. Mesh Reinforcements.

(a) Kinds and amounts used.

Tests on various types of reinforcement mesh in the earlier work showed that expanded metal lath and firescreening were not very suitable reinforcement materials for ferro-cement construction. Difficult mortar penetration, very anisotropic properties, interlocking

of the reinforcement layers, delamination, and a tendency for the mortar to disintegrate under flexural and impact loadings were among the shortcomings encountered. The other meshes examined, namely 1/2-16 ga. welded square mesh, 1/2-19 ga. hardware cloth, and 1/2-22 ga. hexagonal mesh showed more promise although it was felt that the stiffness of the first-mentioned mesh would offer difficulties in forming smooth compound curves. The last-mentioned, hexagonal mesh, suffered from having anisotropic properties. It has an excellent ability to conform to almost any shape. All three were deemed worthy of further tests in which the customary reinforcing rods could be incorporated into the panel construction. It was felt that rods may compensate for some of the shortcomings encountered, such as the somewhat inferior impact resistance and anisotropic properties of panels constructed with hexagonal mesh reinforcement.

The panels 41 to 61 were constructed using nearly equal weights of mesh per square foot of panel, i.e. 10 layers of 1/2-22 ga. hexagonal mesh totalled 1.10 lb/sq ft of panel, 5 layers of 1/2-19 ga. hardware cloth 1.20 lb/sq ft of panel, and 2 layers of 1/2-16 ga. welded square mesh 1.12 lb/sq ft of panel. The corresponding volumes of mesh expressed as percent of the panel volume (nominal thickness 1.0 inch) are 2.70, 2.95, and 2.75 percent.

The panels 31 to 40 were constructed using 10 layers of 1/2-22 ga. hexagonal mesh.

(b) Strengths of mesh.

Tensile tests were performed on specimens of mesh. Hexagonal mesh and hardware cloth specimens were prepared by folding pieces of mesh into several 4-inch wide layers. Welded square mesh specimens were pieces 1-, 2-, and 3-wires in width. The hexagonal mesh was tested in the direction of the twists and across the twists.

The following breaking strengths of the mesh per inch width of single layer were obtained:

1/2-22 ga. hexagonal (in direction of twists)	60 lb
1/2-22 ga. hexagonal (across the twists)	21 lb
1/2-19 ga. hardware cloth	140 lb
1/2-16 ga. welded square mesh	420 lb

It will be observed that the 10 layers of 1/2-22 ga. hexagonal mesh (in direction of twists), 5 layers of 1/2-19 ga. hardware cloth, and 2 layers of 1/2-16 ga. welded square mesh have a total breaking strength of 600, 700, and 840 lb/inch width of panel. It is apparent that the 1/2-16 ga. welded square mesh is somewhat stronger per pound of steel mesh incorporated in the panels.

It should be noted that 1/2-22 ga. hexagonal mesh has four wires per inch (nominally) in the direction of the twists and only two wires per inch (nominally) in the direction across the twists. This factor accounts for at least part of the difference in strength in the two directions. It will be further apparent that the strengths of 15 lb per wire and 10.5 lb per wire for wires in the direction of twist and across twists are less than the strength of about 35 lb which would be expected for steel wire of this gauge thickness tested as a single smooth wire. The twist discontinuities and the impossibility of loading a mesh sample uniformly to develop its full strength undoubtedly account for most of this difference.

The strength data are tabulated in Table 2.

(c) Surface bond areas.

The surface bond area of the mesh per sq ft of panel and the specific bond area, defined as the ratio of the surface area of the wire to the volume of the wire (only those wires or portions thereof oriented in the direction of loading), have been calculated for the 1/2-22 ga. hexagonal mesh loaded in direction of twists, 1/2-22 ga. hexagonal mesh loaded across twists, 1/2-19 ga. hardware cloth, and 1/2-16 ga. welded square mesh. The surface bond area per sq ft of panel for equal weights of mesh in the panel is shown in Table 2. It is highest for the 1/2-22 ga. hexagonal mesh, and lowest for the 1/2-16 ga. welded square mesh since the surface area depends on the diameter of the wire. The specific surface of the 1/2-22 ga. hexagonal mesh is also higher than that of the 1/2-19 ga. hardware cloth which is, in turn, higher than that of the 1/2-16 ga. welded square mesh since this property also depends on the diameter of the mesh wire.

(d) Costs.

The various meshes were purchased locally. The price varied considerably from one supplier to another. The following unit costs, cents per square foot, are typical of recent quotations or purchase (before taxes) for single rolls or sheets:

Galvanized 1/2-22 ga. hexagonal mesh	5.7¢
Galvanized 1/2-19 ga. hardware cloth	12.0¢*
Galvanized 1/2-16 ga. welded square mesh	29.5¢

Somewhat lower costs may obtain with large-volume purchases.

*One source quoted 20¢/sq ft in 100-ft rolls!

The mesh reinforcement costs per square foot of panel for approximately equal weights of contained mesh are as follows:

10 layers 1/2-22 ga. hexagonal mesh	\$0.57/sq ft
5 layers 1/2-19 ga. hardware cloth	\$0.60/sq ft
2 layers 1/2-16 ga. welded square mesh	\$0.59/sq ft

The costs per square foot of mesh and per square foot of panel for approximately equal weights of mesh and for equal strengths of mesh are presented in Table 2.

3. Rod Reinforcements.

(a) Kinds used.

Several kinds of reinforcement rod material are available for ferro-cement construction. Their performance is affected by strength, surface finish, protective coatings, diameter and other factors. Five basic types of rod material were obtained: hot rolled 1020 1/4-in. rounds, galvanized 1020 1/4-in. rounds, bright drawn 1/4-in. nail wire, A82 double drawn C1015 0.225-in. rod, and A82 double drawn C1015 0.225-in. rod passed through dimpling rolls.

(b) Tensile strength.

The tensile properties of the several rod materials were determined and are presented in Table 3. The highest ultimate tensile strength was shown, as might be expected, by the double drawn rods and the lowest by the galvanized 1020 rods.

(c) Effect of welding high tensile rods.

The longitudinal stringer reinforcement rods in a hull are often welded to the vertical reinforcement rods. A loss of strength is anticipated at welds in high strength double drawn rods. A typical arc-weld of a cross rod to a test specimen rod resulted in a reduction in strength from 100,000 to about 90,000 psi for the higher strength A82 double drawn material. A similar weld in the lower strength A82 double drawn material did not diminish the tensile strength. In this latter case, the break was some distance from the weld. The results are presented in Table 3.

(d) Rod/mortar bond strengths.

The effect of scale, pickling, drawing lubricant, rusting, and deforming on the bond (pull out) strength was assessed by a series of tests. Mortar was packed around hairpin-shaped rod specimens as shown in Fig. 3. The length of embedment of each arm was 6 inches.

The duplicate mortar specimens were tested under tensile loading after a curing period of 28 days. Usually one arm of one hairpin started to slip and the withdrawing load dropped. The maximum load attained at first slippage was divided by the embedded surface area of the two arms of the hairpin. However, in the case of one test with galvanized rods, both arms slipped and in the case of both tests with the deformed double-drawn rods the block split, presumably due to the wedging action of the deformation impressions. Fig. 4 shows two mortar blocks after testing. The unbroken bonds of the specimens were tested 3 1/2 months later. Each hairpin was sawn at the bend and each arm was tested separately. The deformed double-drawn rods again split the mortar blocks. A very corroded rod reclaimed from panels submitted by a local boat manufacturer broke before the bond failed in these latter tests. The test results are shown in Table 4. The order of rating of the bond strengths obtained was the same in both tests (28-day and 4 1/2 months). The bond strengths in the latter were slightly improved although it is considered that some of the improvement may be related to the different testing technique used. The galvanized rod showed bond strengths of about 45 lb per sq in. of encased bond surface, much below that of any other rods. The deformed double-drawn rod had the highest bond strength, 655 lb per sq in. of surface, of any of the new rod materials used.

The markedly inferior bond strength observed in the galvanized rod specimens is at variance with most reported work which shows that the bond of concrete to galvanized reinforcement is substantially the same as that of ungalvanized reinforcement. Much of the work has been concerned with common deformed concrete reinforcement bar in which the raised bumps act as keys to increase the effective bond strength. However, it is generally recognized that some concrete (and mortar) mixes and reactive galvanized steel surfaces may show a substantial reduction in bond strength. Where low bond strength is expected, the Zinc Institute Inc. recommends the use of a passivating treatment such as dipping the galvanized rod in an 0.2 to 1 percent chromic acid solution. Alternatively, the rod may be dipped for 10 to 20 seconds in sodium dichromate (20 oz per U.S. gal) and sulphuric acid (S.G. 1.84) (0.5-1.0 percent by volume).

Removal of the light coating of drawing lubricant effected a considerable improvement in the bond strength of the double-drawn rod. Cast concrete may be effective in chemically cutting any residual drawing lubricant on the reinforcing rods (as has been stated) but the results of the present tests show that the residual lubricant had an adverse effect on the bond strength. Lightly rusting of the rod by exposure to the atmosphere for a few days (in a moist climate) effectively improved the bond strength.

Rods deformed by dimpling gave higher bond strengths but the wedge-splitting action encountered may cause delamination of panels and hulls under single or cyclic loads.

Hot rolled rods had bond strengths only exceeded by those of the deformed rod. Pickling diminished the bond strengths slightly.

4. Strength of Panels.

(a) Drop-impact tests.

Drop-impact tests were performed on five panels, No. 44, 45, 46, 48, and 55, to show the effect of kinds of mesh and the presence and spacing of rods on the resistance to impact. The panels tested are described in Table 1.

The test apparatus and procedure have been described in a previous report. The larger panels tested in this study required a larger supporting frame, viz. 31 x 31 inches vs the 24 x 26 in. and 12-in. diam frames used earlier. The impact tup weighed 50 lb and was dropped from a height of 10 feet as before.

The resistance to the 500 ft-lb drop-impact was assessed by the amount of deformation or dishing of the panel, by the visual appearance of the top surface, and by type and extent of cracking in the bottom (convex tension) surface. None of the panels sustained any visible damage to their top surfaces. The rod-reinforced panel 44 containing 3 + 2 layers of 1/2-19 ga. hardware cloth sustained less deformation than similar panels containing 1 + 1 layers of 1/2-16 ga. welded square mesh or 5 + 5 layers of 1/2-22 ga. hexagonal mesh. The extent of cracking, defined by the diameter of a circle encompassing all the cracks (both radial and rectilinear), was also lower for panel 44. As may be expected the presence of rods effected a significant improvement in the impact resistance of the panels.

The test results are tabulated in Table 5. The appearance of the bottom surface of the several panels is shown in Fig. 5 to 9.

All three meshes (1/2-19 ga. hardware cloth, 1/2-16 ga. welded square mesh, and 1/2-22 ga. hexagonal mesh), when used in equal amounts, provide considerable resistance to impact loadings when reinforced with rods. The cracking, away from the centre of impact, was generally very fine. On these single tests, the panel containing 1/2-19 ga. hardware cloth showed somewhat better impact resistance but the panels containing 1/2-16 ga. welded square mesh and 1/2-22 ga.

hexagonal mesh were deemed generally acceptable. Rods, especially when spaced at 2-in. centres, served to prevent extensive propagation of open cracks. The panels tested showed no cracking in the top surface and no water leakage would have occurred if the impact load had occurred below the water line of a ferro-cement hull of these constructions.

The drop-impact test, which is described more fully in an early report, has an energy of 500 ft-lb when dropped from a height of 10 feet. The height gives a velocity at impact approximately equal to a boat speed of 15 knots. The earlier report showed that the chosen energy produced significant damage to 2 x 6-inch wood planks and to 1/4-inch steel floor plate on a 12-inch span. The test produced significant damage but not complete destruction of the 30-inch panels of the various mesh constructions described. The test allowed quantitative and descriptive ratings of the several panels.

The impact tests reported herein allow a comparative rating of ferro-cement panels of various constructions but do not provide a comparison of ferro-cement with other materials. However, it can be stated that a 36 x 36-inch piece of 3/4-inch fir plywood tested under the same conditions showed splintering and delamination of the bottom surface over an area about 10 inches in diameter. The top surface was essentially undamaged except for a slight (1/16 to 1/8 in.) concavity. A 2 x 10 in. fir plank (flat grain on the same span (31 inches)) cracked lengthwise and transversely. The permanent deflection was about 1/4 in. No glass fibre reinforced laminate panels have been tested but the resilience of such panels is likely to be high. It is interesting to record again that Gibbs and Cox, Inc.* reported using a laminate tester in which the weight of the impactor could be varied from 7 to 150 lb. A dropping height of 20 feet gave an impact energy ranging from 140 to 3,000 ft-lb.

(b) Tensile tests.

Tensile testing was confined to panels 41, 42, and 43. One 4-inch wide specimen (containing two lengthwise rods) was cut in each direction from the 24-inch square panel remaining after separation of the bend test specimens. Simple grips which could be clamped to the specimens were made from steel floor or checker plate. (It is difficult to grip straight ferro-cement tensile specimens unless shoulders are "cast" or other provisions made.) The distance between the grips was about 7 inches. All six tensile specimens, except 41E, broke at a transverse rod three inches from one end of

*Gibbs and Cox, Inc., Marine Design Manual for Fiberglass Reinforced Plastics, McGraw-Hill Book Company, Inc., New York, 1960.

the specimens and near the grip. The load at first crack and the maximum load at ultimate failure are presented in Table 6.

The highest breaking strengths, 3,860 and 3,900 lb, were obtained in the specimens containing 1/2-16 ga. welded square mesh. The equivalent strengths per inch width of specimen are 965 and 975 lb, respectively. The lowest strengths, 2,600 and 3,100 lb, were given by the specimens containing 1/2-22 ga. hexagonal mesh. The equivalent strengths are 650 and 775 lb, respectively.

The breaking strengths of unencased mesh equivalent to that in the tensile test specimens are 3,360 lb for 1/2-16 ga. welded square mesh, 2,800 lb for 1/2-19 ga. hardware cloth, and 2,400 and 840 lb for 1/2-22 ga. hexagonal mesh in lengthwise and crosswise directions, respectively. These values, augmented by the tensile strength of the mortar (which is small) and the rod/mortar bond strength should be close to the breaking strengths of the tensile specimens. The Actual Breaking Strengths and the Summed Breaking Strengths are shown in Table 6 for comparison. It will be observed that the Actual Breaking Strengths are close to the Summed Strength (mesh breaking strength + rod/mortar bond strength) except in the case of 43D (1/2-22 ga. hexagonal mesh specimen with twists across the direction of tensile loading). The Actual Breaking Strength greatly exceeded the Summed Strength for this specimen. The reason has not been pursued but it is likely related to the fact that the summed strength of the equivalent numbers of single wires making up the mesh will be considerably higher than the strengths obtained from hexagonal mesh specimens. For example, the strength of a single 22 ga. wire at a tensile strength of 50,000 psi will have a breaking strength of about 33 lb compared with the determined mesh strength of about 11 lb per wire when tested across the direction of twist and 15 lb per wire when tested in the direction of twist. Substitution of the assumed value for a single wire gives Summed Breaking Strengths for the hexagonal mesh specimen 43D of 3,250 lb and for 43E of 6,130 lb, both considerably above the Actual Breaking Strengths obtained in the tests.

(c) Flexure tests.

Two 12-inch wide specimens were cut from adjacent sides of the 36-in. square test panels 41, 42, 43, 47, 49, 50, 51, 52, 53, 54, 56, 57, 58, 59, 60, and 61. Except in panel 58, the axes of rod and mesh were coincidental and in the lengthwise and transverse directions of the bend test specimens. In panel 58, the axes of the rods were in the lengthwise and transverse directions of the bend specimens but the mesh was at 45° to the rods and hence to the specimen bend direction. An additional bend test specimen was cut diagonally from the 24-inch square remaining in panel 58. The mesh in this specimen (58D) was in the lengthwise and transverse direction of the specimen but the

rods were at 45° . Because the mesh fabric width was only 36 inches, it was necessary to lap the layers of mesh when laid diagonally. This lap was located near the span centre of the diagonal bend specimen 58D and allowed the effect of laps to be assessed at the same time. In panels 60 and 61 also, one of each of a pair of bend specimens was cut to place a mortar joint at mid-span of the specimens.

The 12-inch wide specimens were tested in third point loading on roller supports. The test span was 21 inches. The loading was applied through a spherical self-aligning head in a Tinius Olsen Universal Testing Machine of 60,000 lb capacity. The 1,200-lb and 12,000-lb ranges were used as required. The mid-span deflection was measured by a Mercer dial gauge (0.001 in., 2.0 in.) between the underside of the test specimen and the machine table. The deflection was recorded for 100-lb increments of load until the deflections increased rapidly with only small load increments. The bottom (tensile) surface of the specimen was observed for the first sign of a crack. The load at first visible crack and the maximum load held were recorded. Loading was continued until the load dropped significantly. Generally, a deflection over one inch was obtained before loading was stopped.

The flexural strength at the first visible crack and the modulus of rupture (flexural strength at the maximum load held) have been calculated. These results and a description of the mode of failure are presented in Table 7. Load-deflection curves have been drawn for the various bend tests. These are presented in various combinations in Fig. 10 to 13 for easy comparisons.

Two of the flexure specimens (49B and 52B) were tested somewhat differently from the others in that they were subjected to a bending load, were unloaded to zero, and were then reloaded to the maximum load held. Specimen 49B was loaded to 2,800 lb (deflection 0.200 in.) at which point the load dropped slightly indicating the maximum load had been nearly attained. Fine cracks had been observed. The machine was unloaded to zero. The residual no-load deflection was 0.05 in. The specimen was reloaded until the ultimate load was obtained. Specimen 52B was loaded to 2,000 lb (deflection 0.275 in.) at which point the slope of the load/deflection curve was flattening rather rapidly. No cracks were observed at this time. The machine was unloaded and the deflection gauge returned nearly to 0. The specimen was subsequently reloaded until the ultimate load was obtained. The slope of the load/deflection curves is considered later.

Examination of the flexural test results presented in Table 7 and the load-deflection curves presented in Fig. 10 to 13

allow certain comparisons to be made and conclusions to be drawn. Although the conclusions drawn are valid for the test results obtained in the present program, they are drawn in most instances from results obtained on a single test. The conclusions are therefore considered to be tentative conclusions, not to be applied unreservedly. Although attempts have been made to standardize the construction of panels, variations in mesh location and compactness, in mortar density (soundness), and in other aspects will provide variations in the quality and in the strengths of apparently similar panels. More replication is required to randomize the inherent variability so that conclusions of greater general validity can be drawn.

Within the limitations set forth above the effect of the following factors are discussed and conclusions are drawn:

(i) Mesh reinforcement.

The maximum loads in bending (average of two tests, one in each direction) carried by the flexural modulus of rupture specimens is 3,020, 2,570, and 2,675 pounds for 1 + 1 layers of 1/2-16 ga. welded square mesh, 3 + 2 layers of 1/2-19 ga. hardware cloth, and 5 + 5 layers of 1/2-22 ga. hexagonal mesh, respectively. (These panel specimens contained equal weights of mesh and contained double-drawn rods at 2-in. spacing in each direction). The load/deflection curves for flexural specimens from these panels 42, 41, and 43, are shown in Fig. 10 and 11. The load-carrying capacity of the panel with the 1/2-16 ga. welded square mesh construction is slightly better than for the other two constructions. Placement of the 1/2-19 ga. hardware cloth with three layers in the tension side would have enhanced its load-carrying capacity.

The modulus of rupture values (calculated for a nominal thickness of 1.0 inch) in Table 8 show the superiority of the 1/2-16 ga. welded square mesh. However, panels constructed as above but with the mesh layers more tightly laced (stapled or clipped) and a layer of mortar 1/16 in. thick could have overall thicknesses as low as 0.825, 0.95, and 1.075 in., respectively. Actual specimen thickness measurements (excluding any surplus thickness of mortar on the surface) are 0.9, 1.0, and 1.1, in., respectively. The average moduli of rupture (transverse and longitudinal) calculated on this basis are 6,525, 4,500, and 3,865 psi, indicating the fairly marked superiority of the panel specimens which contain the

1/2-16 ga. welded square mesh material. The average modulus of the panel specimens which contain the 1/2-19 ga. hardware cloth is also higher than that of the 1/2-22 ga. hexagonal mesh specimens. Bending loads carried by the 1/2-19 ga. hardware cloth panel specimens and by the 1/2-22 ga. hexagonal mesh specimens may also be compared in Fig. 12 and 13 for panels 53 and 57. On a minimum thickness basis, the modulus of rupture of the panel specimen containing 2 + 3 layers of 1/2-19 ga. hardware cloth is inferior to that of the specimen containing 5 + 5 layers of 1/2-22 ga. hexagonal mesh when the rods in the "tension side" are in the transverse direction and is markedly superior when the rods are in the lengthwise direction. Once again, the presence of rod reinforcements appears to eliminate the strength differences encountered when hexagonal mesh panels without rods were tested in the direction of the mesh twists and across the mesh twists.

Since the weights and hence the volumes of the mesh (and rods) in the panels of the three constructions described above are almost identical, the differences in thickness represent the extra weight of mortar necessary to fill the spaces between the mesh layers. It is apparent that panels with square mesh materials (in the constructions used herein) generally give somewhat higher values for flexural modulus of rupture than do panels with hexagonal mesh and, at the same time, may be up to 0.2 inch thinner (and hence lighter).

(ii) Location of rods in panels.

The modulus of rupture of panels reinforced with welded square mesh materials (including hardware cloth) is higher for bend specimens in which the rods in the tension side are in the lengthwise direction than for specimens in which the rods are in the transverse direction, Fig. 14 and 15. The panels reinforced with hexagonal mesh showed nearly equal strengths for specimens with "tension side" rods in the lengthwise and transverse directions, Fig. 16.

The presence of rod reinforcement appears to balance the anisotropic strength properties inherent in the hexagonal mesh reinforcement material and manifest in the panels containing hexagonal mesh reinforcement but no rod reinforcement. It is not

known whether this equalization of strengths in the two directions is due to the rod/mortar bond, the inherent "soft geometry" of the mesh, or to some other cause.

(iii) Rod spacing.

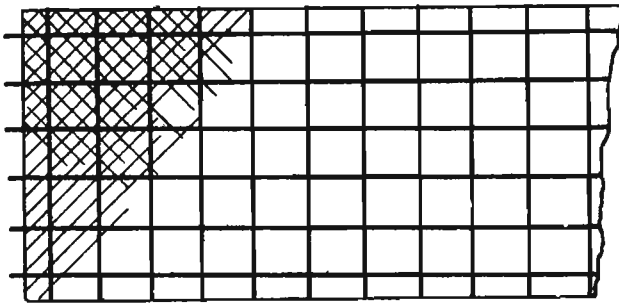
The panels described in the earlier report were made without rods in order that the effect of using various types of mesh could be measured without the masking effect of rod reinforcement. The layers of mesh used in those panels were laid one upon another throughout the whole thickness of the panel whereas in ferro-cement construction the mesh reinforcement is placed in the outer portions of the panels, the rods acting as spacers to place the mesh in the more highly stressed portions of the panel. Direct comparison of new panels containing rods with the old panels with no rods is therefore not possible. The present panels with and without rods on 2-in. centres were geometrically identical except for the presence or absence of rods between the mesh layers. Fig. 17 shows that "tension side" rods in the lengthwise direction of the test specimen gave a three-fold increase in the load carrying capacity in flexure. Fig. 18 shows that "tension side" rods in the transverse direction gave a two-fold increase.

The closer is the rod spacing the greater is the load-carrying capacity and the higher is the ultimate modulus of rupture in flexure when the rods in the "tension" side of the flexure specimens are in the lengthwise direction of the specimens, Fig. 19. The rod spacing appears to have little effect when the rods in the "tension" side of the flexure specimens are in the transverse direction of the specimen, Fig. 20.

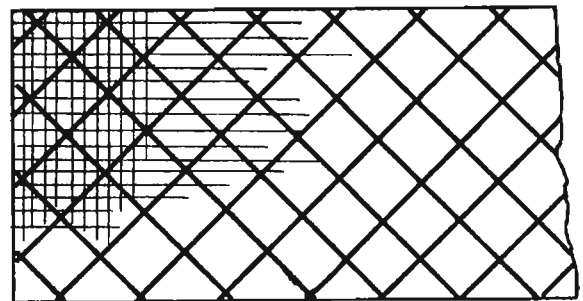
(iv) Orientation of rods and mesh.

The load-carrying capacity of flexure specimens containing 3 + 2 layers of 1/2-19 ga. mesh oriented at 45 degrees to the double-drawn rods spaced on 2-inch centres is reduced by about 40 percent when the rods are in the direction of the flexure specimen, Fig. 21 and 22. The load-carrying capacity of the flexure specimen oriented at 45 degrees to the rods

and in the line of the mesh wires is similar to the capacities of the specimens oriented in the direction of the rods and 45 degrees to the mesh wires, Fig. 23. Sketches (a) and (b) below show the two conditions.



(a) Rods lengthwise and transverse.
Mesh at 45 degrees.



(b) Rods at 45 degrees.
Mesh lengthwise and transverse.

(v) Kind of rods.

Panel specimens containing 1/4-in. diameter hot rolled bars carried higher loads in flexure than any of the other rods, Fig. 24 and 25. The apparent inferiority of the panel specimens containing the much stronger double-drawn rods is believed due to the poorer rod/mortar bond characteristics of this rod rather than to differences in diameter. The larger diameter of the hot rolled rods does, however, place the mesh reinforcement farther from the centre-line of the panel specimens thereby enhancing the load-carrying ability. A much greater bond area between mortar and rod such as would exist in a hull and the fixing of the rod ends in a hull may enhance the load-carrying capacity of ferro-cement panels containing the strong double-drawn rods.

(vi) Repeated loading.

Loading the flexural specimens to a point close to the ultimate load, unloading to 0, and reloading until the ultimate load is reached appears to have only a small effect on the load/deflection curve of the specimen. Both specimens showed only a small change in the slope of the curve, Fig. 26 and 27. In each case, the reloading produced a load/deflection curve of more constant slope. The deflection of specimen 52B returned to 0 when the load was removed. A permanent set was obtained in specimen 49B after the load was removed. The original deflection at load had been similar. The cause of the difference in behaviour is not known but the presence of fine visible cracks in specimen 49B and no visible cracks in 52B, the use of galvanized 1020 rods in 49B and high tensile double drawn rods 52B, and indications of loss of rod/mortar bond (rod slippage) in 49B are possible factors.

5. Durability.

The durability of concrete has been defined* as "its resistance to deteriorating influences of internal and external factors to which it is exposed within the duration of life expected from the structure". It follows that the requirements for a durable concrete will depend on the type of structure, the type of exposure or service condition, and the required service life. The service conditions to which the concrete is subjected include weathering, chemical action, and wear. The characteristics of greatest importance in the performance of ferro-cement hulls are weathering resistance and chemical resistance. It has been pointed out that disintegration of concrete by weathering is caused mainly by the disruptive action of freezing and thawing and by expansion and contraction, under restraint, resulting from temperature variations and alternate wetting and drying. Although the results of laboratory tests to measure the durability of concrete are difficult to correlate with service performance, tests conducted over many years have shown that freeze-thaw tests can distinguish between durable and non-durable types of concrete.

*Zoldners, N.G., Durability of Concrete, Canadian Pit and Quarry, Vol. 6 No. 10, October 1965, pp 34-36.

Seawater is mildly corrosive to concrete (mortar) mainly because of the soluble sulphate salt in the water. It is generally recommended that concrete for use in seawater be made with Portland cements which contain not more than 8 percent tricalcium aluminate. ASTM Types II and IIA, IV, and V meet this requirement. A low water/cement ratio and entrained air will increase the resistance of the concrete to attack by seawater. Under most conditions Portland cement concrete provides good protection of embedded steel reinforcement against corrosion because of its high alkalinity. Inadequate covering of the steel, honeycombing, cracking, and other shortcomings may allow ingress of corrosives which can lead to serious corrosion. A minimum cover of 2 to 3 inches is generally recommended for concrete for marine structures. A thick cover over the reinforcement layers in ferro-cement boat construction is not possible and seldom will exceed 1/8 in. In isolated areas, the mesh may be exposed during the fairing of the hull before a final coating of some kind is applied. Ferro-cement mortar with its low water/cement ratio, absence of coarse aggregate, and its trowelled finish should be much less permeable than structural concrete. Moisture and chlorides which penetrate the mortar, however, will form rust. Rust formation results in a 13-fold volume expansion and spalling pressures will be developed. It is reported* that the white corrosion products formed on galvanized reinforcement produces too small a volume of zinc corrosion products to cause cracking or spalling.

Although much research and exposure testing has been undertaken over many years on structural concrete, a relatively small amount of research has been reported on the durability of ferro-cement. The freeze-thaw and seawater exposure tests on panel coupons containing various cements, additives, and meshes (galvanized vs ungalvanized), in this study are not comprehensive but are intended to show any differences in behaviour between the various ferro-cement mortar mixes and constructions.

(a) Freeze-thaw tests.

The size of available specimens did not permit freeze-thaw tests according to the requirements of ASTM Designation C290-67**. The tests carried out do, however, allow a comparative evaluation of the various specimens tested.

*Frazier, K.S., Value of Galvanized Reinforcing in Concrete Structures, Materials Protection, 4, May 1965, pp 53-55.

**ASTM Des. C290-67: Resistance of Concrete Specimens to Rapid Freezing and Thawing in Water.

Twelve 3 x 5-inch weighed unreinforced coupons representing a variety of mortars, with and without admixtures*, as described in Table 8, were placed on wire mesh in shallow trays in the test chamber**. The chamber was programmed to provide six freeze-thaw cycles per day. The temperature in the water-filled trays cycled from 10 C to -4 C. The temperature of the chamber itself cycled over a much wider range from 25 C to -12 C. The cycling program was continued for 350 cycles.

Visual observations were recorded at intervals throughout the test program. At the end of the program the specimens were dried four hours at 200 F and weighed. The visual observations and weight-loss measurements of spalling loss are recorded in Table 8. The coupon from panel 33 containing 25 percent pozzolan replacement of the cement showed severe deterioration and breakdown. The coupon from panel 40 containing polyvinyl acetate emulsion showed a slight spalling of the top surface. Damage to the other coupons was insignificant. Coupons from panels 33, 35, 37, and 40, are shown in Fig. 28. A close-up photograph of a severely damaged coupon (panel 33), a lightly damaged coupon (panel 40), and an undamaged coupon (panel 35), is shown in Fig. 29.

Eleven test coupons, approximately 3 x 4 inches, from various mesh-reinforced panels, described in Table 9, were subjected to 76 cycles of freezing and thawing in a similar program. The sawn edges of these coupons had been coated with an epoxy formulation to prevent entry of water through the sawn edges. The visual observations of the coupons after 36 cycles and 76 cycles are presented in Table 9. Fig. 30 shows the condition of the coupons after 76 cycles. The coupons from panels 5, 17, 19, and 23, were seriously damaged. The damage was in the form of delamination, disintegration, or both of the top layer (1/4 in. thick) of the coupons. The coupon from panel 25 which showed light flaking of the top surface early in the test cycle did not deteriorate further. It is believed that trowelling may have deposited a thin layer of cement on the top surface.

* Admixtures are described in section B.

**Environmental Chamber Model ELHH-27-MRLC-1, Associated Testing Laboratories, Inc.

The observations and conclusions drawn are summarized as follows:

(i) Unreinforced coupons made from all five types of cement used (I, II, III, V, and Aluminous) resisted 350 freeze-thaw cycles without apparent damage.

(ii) The unreinforced top layer of reinforced coupons containing cement of types I, II, III, and V showed serious damage in a 76-cycle freeze-thaw program. The coupon containing aluminous cement showed no apparent damage.

(iii) The mesh-reinforced bottom portions of the coupons above containing types I, II, III, and V were not visibly damaged.

(iv) In the 350-cycle test program of unreinforced coupons containing no admixture, a water reducing agent, and an air-entraining agent showed no visible damage, the coupon containing pozzolan showed severe damage and the coupon containing the pva emulsion showed light spalling.

(v) In the 76-cycle test none of the reinforced coupons from the present series of panels 31, 33, 35, 37 (with and without additives) showed any deterioration. However, another coupon from the earlier series of panels (panel 5) (without additive) disintegrated badly.

(vi) The freeze-thaw tests show some inconsistencies. One coupon containing additive failed, another did not. One coupon of Type II cement mortar (no additive) failed, another did not. Admixtures have not consistently changed the resistance to freeze-thaw deterioration. Although pozzolans can improve concretes and mortars, investigations by others have shown that concrete containing pozzolan may have reduced resistance to freezing and thawing if the concrete is incompletely cured and may have reduced strength and durability. Authorities recommend that the pozzolan be checked in combination with the cement and aggregate (or sand) used to assess the advantages or disadvantages in respect to quality.

(vii) The 76-cycle tests suggest that mesh reinforcement confers improved resistance to disintegration in a freeze-thaw environment.

(viii) Further tests to confirm any possible deleterious effect of pozzolan and to include variations in the amount of admixtures and greater replication of tests are required.

(b) Seawater exposure.

A simple immersion-drying apparatus (Fig. 31) was constructed to expose ferro-cement coupons in seawater followed by drying in front of a fan. Two gear-reducers in tandem and a combination of V-pulleys were used to rotate a pair of coupon-holding wheels at 1 revolution every 4 hours (1 hour immersion, 3 hours drying). Each wheel holds 12 coupons in slots in its outer rim. The coupons, approximately 3 x 4 inches and weighing about 300 to 500 g, were sawn from panels representing various mixes and meshes (panels 4 to 25). Nine coupons were tested in duplicate, one was a single test. Five coupons were from panels 31 to 40, with various mortar additives. The sawn edges of each coupon were coated with an epoxy compound to ensure that water entered only from the flat trowelled or mould surfaces. The seawater used in the bath was filtered seawater from the Vancouver Public Aquarium which obtains its supply from Burrard Inlet. Vancouver tap water was used as make-up for the high evaporative losses. Checking showed that the salinity was maintained. The tests, performed at room temperature throughout, were continued for 350 exposure cycles.

Near the end of the cycling tests the coupons were weighed just before emerging from the 1-hour soak in seawater and again at the end of the 3-hour drying period. The coupons were weighed again at the end of the run after 20 hours at 200 F. The weight loss from the 3-hour drying cycle was negligible. The weight loss on oven drying ranged from 0.7 to 1.6 percent for coupons from panels 4 to 25 and from 1.2 to 2.0 for coupons from panels 31 to 40. The relatively low weight loss (or weights of absorbed water) is believed to be at least partially due to clogging of the pores and voids on prolonged soaking. Clogging may be caused by the formation of cement gels. This postulation appears to be confirmed by a subsequent absorption test in which three coupons from the 350 cycle immersion test and three coupons not previously immersed were soaked one hour

and then dried at 200 F. The cycled coupons gained an average of 1.0 percent, the uncycled coupons 2.7 percent.

The physical condition of the panel coupons after 350 seawater immersion cycles was evaluated by the visible appearance and by comparing the scratch hardness and the penetration hardness of coupons exposed to the wetting and drying cycle with hardness of uncycled coupons.

Coupons from two panels No. 6 containing 1/2-22 ga. hexagonal mesh, and No. 9 containing 1/2-16 ga. welded square mesh with zinc coating removed, showed red-brown rust stains in the bottom surface of the coupon, Fig. 32. The bottom surface is the surface cast against the plastic sheet and contains a layer of partially exposed mesh. Many bottom surfaces showed a slight white rust pattern. The appearance of top surfaces was essentially unchanged except for a general overall yellowing.

Comparing the scratch hardness of exposed and unexposed coupons revealed no detectible differences. Penetration hardness tests on the top and bottom surfaces using a 1/8-in. ball and 60 kg load also showed no real differences.

The descriptions of the visual appearance and the average hardnesses are given in Table 10.

In addition, five three-inch wide bend test specimens (8D, 10D, 5H, 8H, and 10H), which had been previously tested in bending to such an extent that damaged mortar exposed a large amount of the reinforcing mesh, were immersed in seawater for 48 hours. The severe cracking damage of the specimens allowed easy penetration of the seawater into the specimens and contact with the exposed mesh. A copious yellow-white encrustation covered the wires and filled the cracks of 8D (galvanized 1/2-19 ga. hardware cloth). Heavy yellowish white encrustations in the cracks and severe red rust staining of the mesh was observed on 10D (3/8-19 ga. mesh coppered or liquor-finished to provide temporary corrosion resistance). These specimens are shown in Fig. 33 and 34. The specimens 5H and 8H containing galvanized 1/2-22 ga. hexagonal mesh and galvanized 1/2-19 ga. hardware cloth showed a yellowish deposit on the wires or on the crack pattern in the mortar over the wires. Specimen 10H (containing coppered or liquor-finished 3/8-19 ga. mesh) showed severe rusting on all exposed wires. Specimens 8H and 10H are shown in Fig. 35.

The observations and conclusions from the seawater exposure tests are summarized as follows:

(i) The absence of serious corrosion in any of the sound 24 test coupons tested through 350 cycles of alternate immersion and drying is believed due to the lack of interchange of solution. The inherent difficulty of removing liquid from fine capillaries and voids and the probable clogging action of the seawater in the capillaries and voids are believed responsible for the apparent absence of serious corrosion.

(ii) Temperatures considerably above ambient temperature or very much longer drying periods at ambient are required to effectively remove moisture from the capillaries and voids of ferro-cement mortar.

(iii) Ungalvanized wire mesh exposed on the surface of the test coupons will rust and stain the surface of the coupons. Rust stains were evident after a few cycles but did not appear to be substantially worse after 350 cycles.

(iv) Ungalvanized wire one diameter (0.0625 in.) below the surface of the coupon did not rust even after 350 immersion cycles. The under side of the wires exposed to the surface did not rust where the wire/mortar bond was good.

(v) Wire mesh galvanized with a very light coating also developed red rust on wires exposed in the surface of the test coupons.

(vi) Galvanized wires exposed on the surface of the test coupons developed a "white rust" deposit during curing of the mortar. This deposit was only slightly increased by the seawater immersion tests.

(vii) The layer of sound mortar required to provide good protection of the steel mesh need not be thick. A layer 1/16 in. thick provided good protection in the present tests. Fine surface cracks which may be opened under static or cyclic loading may require a greater thickness of mortar for protection of the wire mesh against corrosion.

(viii) None of the mortars, regardless of the type of cement, sand, and additives used, deteriorated (as measured by scratch and penetration hardness tests) even after exposure to 350 immersion and drying cycles.

(ix) Heavy corrosion products will form on galvanized and ungalvanized mesh (or rod) materials in ferro-cement materials damaged enough to provide access of a corrodent such as seawater. The preliminary exposure tests suggest that galvanizing minimizes the attack but corrosion of the mesh could be severe. Rapid cleaning of the mesh and patching of the mortar or the removal and replacement of the mortar mesh in the damaged area with subsequent remortaring will be necessary to restore the ferro-cement.

B. PANELS TO ASSESS MORTAR ADMIXTURES.

1. Description of admixtures used.

Admixtures fulfill an important function in modern concrete technology, conferring special properties to the concrete mix. Selection of admixtures is difficult, however, because of variations in the behaviour of the various formulations available across the land and it is generally recommended that tests be run on mortars to which an admixture is added to determine any adverse side effects.

In this study, four admixtures have been used, viz. a pozzolan, a water-reducing agent, an air-entraining agent, and a polyvinyl acetate emulsion.

(a) Pozzolans.

Pozzolans are described as siliceous or siliceous and aluminous materials which possess little or no cementitious value but which will, in finely divided form and in the presence of moisture, react chemically with calcium hydroxide at ordinary temperatures to form compounds with cementitious properties. Pozzolans may be used to improve workability and quality of concrete, to reduce the cost, or to minimize the reaction between certain aggregates and the alkalis in the cement. Pozzolans may also reduce heat generation during curing and the permeability of concrete.

No recommendations for optimum proportions of pozzolan materials in rich cement/sand mortars have been found. The American Concrete Institute Manual of Concrete Practice (Part 1) 1967 states that "some indication of suitable proportions for use of cementitious and pozzolanic admixtures in concrete is given by specifications for blended cements. Federal (U.S.) specifications for Portland-pozzolan cement require that the percentage of pozzolan by weight be between 15 and 35 percent". Pozzolan calcined and ground from shale deposits in the Gulf Island of B.C. replaces 25 percent of the cement in the mixes prepared for ferro-cement panels in this study.

(b) Water-reducing agents.

Water-reducing agents are considered to lower the mix water requirement which results in an increased compressive strength. For the same strength, therefore, it is possible to reduce the cement content. The basic ingredient of the common water-reducing admixtures is either salts of lignosulphonic acid or hydroxycarboxylic acids. The water-reducing agent used in the present study is described as an aqueous solution of metallic salts of lignin sulfonic acids which contains a catalyst to counteract the hydration-retarding action. The admixture was added at 6.5 fluid ounces per sack of cement, a rate which has given good results in normal concrete.

(c) Air-entrainment agents.

Air-entrainment agents have a proven reputation for producing concretes which can resist damage by frequent wetting and by cycles of freezing and thawing. Many specifications require concretes which contain about 6 percent entrained air. Air-entraining agents are generally formulated from wood resins, sulphonated hydrocarbons, and synthetic detergents. The air-entraining agent used in the present study is described as an aqueous solution of purified and modified triethylamine salts of a sulfonated hydrocarbon and which contains a catalyst to promote more rapid and complete hydration of the Portland cement. The admixture was added at 3/4 fluid ounce per sack of cement, a rate reported suitable for normal concretes.

(d) Polyvinyl acetate emulsions.

Polyvinyl acetate emulsions have been used to toughen concrete. The added polymer, in the right proportion, fills

the voids in the cement gel structure and exerts a binding effect on this gel structure. The air spaces, formed by air entrainment, are not filled.

A 1:5 emulsion/cement ratio for the emulsion used is reported to improve the workability of concrete mixes and to allow a lower water/cement ratio to be used. The cost of the polyvinyl acetate emulsion is over 20¢/lb, making it a relatively expensive addition.

Recommended additions of 5 lb of a polyvinyl emulsion were added to panels made in this study. Water was added to produce a slump of 3 to 3 1/2 inches (the emulsion + water/cement ratio used was 0.48). The workability of the mixes used was not good. Additional tests would be required to obtain the optimum ratios for good workability and other properties.

2. Panel construction details.

Ten 30-inch panels (31 to 40) reinforced with 12 layers of 1/2-22 ga. hexagonal mesh laid into the bottom of the plastic-lined form moulds were constructed as described in the 1969-70 report. Each panel was made in duplicate. As before, a three-inch strip along one side of each panel contained no reinforcement and was used to determine the modulus of rupture of unreinforced mortar.

Type II cement and Evco Dry Mortar Sand were used throughout in a ratio of 1:2 by weight except for panels 33 and 34 in which pozzolan replaced 1/4 of the cement. The water/cement ratio was maintained at 0.4 except where a very low slump value was obtained and extra water added. Three 2-inch mortar cubes were cast for 7-day and 28-day compression tests. The panels were cured under plastic sheeting with regular wettings for at least 28 days before sectioning for various tests. Panel construction details, water/cement ratio, cement/sand ratio, slump, workability, mortar compression strength, and the modulus of rupture values are summarized in Table 11.

3. Characteristics of the mortars.

(a) Workability.

Workability has been subjected to several means of assessment such as the cone slump test (as used in this work) (ASTM Designation C143) and the flow table test (ASTM Designation C124).

All such tests can undoubtedly provide a measure of the workability for various applications. For the present work the ease (or difficulty) of working the mortar into the mould containing the layers of mesh and inspection of the back of the panel after stripping from the mould are probably the best means of assessing the workability. In panels 31 to 40, an attempt has been made to use a water/cement ratio of 0.4. In general, if a slump below 3 inches was obtained (a level which experience has shown gives mesh penetration difficulties), a small amount of water was added to the mix. Although the assessment of workability by the ease of penetrating the mesh and by inspection of the backs of the panels is subjective, it is concluded that both the water-reducing agent and the air-entrainment agent have improved the workability of the mortar. The pozzolan and polyvinyl acetate emulsion, in the amounts used, did not improve workability. The description of the workability of each mix is presented in Table 11.

The amounts of the various admixtures used are the amounts recommended by suppliers' literature for normal concrete practice. The proportions used may not be optimum for the rich cement/sand mortars used in ferro-cement work.

(b) Strength.

Except in the case of the polyvinyl acetate emulsion the additives in the amounts used did not effect substantial changes in the compression strength or the modulus of rupture of the mortar specimens. Compare the values in Table 11 and Table 3-S of Technical Supplement, dated March 31, 1970. The average compression strengths at 28 days for mortars containing no additives, pozzolan, water-reducing agent, and air-entraining agent, ranged from 5,500 to 6,575 psi. The compression strength of the mortar containing the pva emulsion was markedly lower than the compression strength of the other mortars but the optimum addition for mortars may not have been attained. The modulus of rupture in bending for all mortars tested ranged from about 700 to 1,100 psi. The number of samples tested was too small for an analysis of variation to be undertaken. However, the range in modulus of rupture encountered was similar to that found in the Technical Supplement, P.4.

It is concluded that the additives in the proportions used have not effected a significant improvement in the compressive strength and modulus of rupture of the mortar.

(c) Porosity.

Visual examination of the sawn cross-sections of the five panels indicated that panels containing the water-reducing agent and the air-entraining agent had a more uniform void distribution than did the other panels. The panel containing the polyvinyl acetate additive appears to be most dense except for compaction voids. Fig. 36 shows sections of the five panels 31, 33, 35, 37, and 40.

Water absorption tests on these same specimens showed weight gains ranging from 3.9 for the specimen containing the water-reducing agent to 6.7 percent for the specimen containing the air-entraining agent after soaking bone dry specimens in water for four hours as shown in Table 12. It should be remarked that the size, distribution, and shape of the voids are considered to be more important than the total void volume on the permeability of concrete (or mortar).

(d) Durability.

The effect of additives on durability test results has been considered in detail under another section. Briefly, 350 wetting-drying cycles of mesh reinforced coupons from the five panels 31, 33, 35, 37, and 40, in seawater produced no apparent deterioration as assessed by visual observation and scratch and penetration hardness tests. The results of freeze-thaw tests were less conclusive. Mesh-reinforced coupons from panels 31, 33, 35, and 37 in one freeze-thaw test lasting 76 cycles showed no apparent damage. (The coupon from panel 40 was inadvertently omitted from the test cycling.) Unreinforced coupons from all five panels were given 350 freeze-thaw cycles in another test. The coupon containing pozzolan disintegrated badly, the coupon containing the polyvinyl acetate emulsion showed slight spalling of the top surface. The other three coupons showed no apparent change. The weight losses reflect the visual appearances.

The test results are reported fully in Tables 8 and 9.

C. OTHER TESTS AND DISCUSSIONS.

1. Interrupted mortaring.

Although small boats may be plastered or mortared by

a competent crew in a day it may be difficult to finish a large boat in a single day. Some builders have changed their practice to mortaring over two or more days.

Three panels, 59, 60, and 61, were constructed to determine what problems could result by interrupted mortaring. Panel 59 containing 3 + 2 layers of 1/2-19 ga. hardware cloth on double-drawn rods at 2-inch centres was mortared from one side only on one day. The other side was lightly wetted and mortared on the next day. Panel 60, which contained 5 + 5 layers of 1/2-19 ga. hardware cloth on double-drawn rods at 2-inch centres, was fully mortared from both sides but on completion of mortaring a two-inch wide strip of mortar 12 inches from one edge was blown out with an air gun. The edges were lightly wetted and the strip remortared the next day. Fig. 37 shows the surface of the finished meshed patch joint. Panel 61 was mortared from both sides except for a 12-inch wide strip which was finished the next day.

Section of panel 59 to prepare the 12 x 24 inch flexure specimens revealed some slight sponginess in the centre of the panel. Some sections, however, showed a good bond between the two layers of mortar. The flexure specimens did not delaminate during the test and the preliminary test suggests that a mortar of good mesh penetrability will bond satisfactorily.

Sectioning panel 60 revealed large open areas where the two mortar layers failed to join, Fig. 38. The lack of penetration is attributed to the many layers of mesh used and to a mortar which was slightly too stiff. The cured panel sounded hollow when tapped with a hammer but preliminary tests with an Audigage thickness gauge were not promising as a means of detecting "hollow" panels. The flexure test specimens cracked at the joint but the panel was generally of very poor quality. The panel points out the need for an instrument to indicate when penetration is inadequate.

The flexure test specimen of panel 61 cracked at the joint but exhibited only a slightly lower modulus of rupture than the flexure test remote from the joint.

The modulus of rupture values for the several specimens from panels 59, 60, and 61 and the modes of failure are given in Table 7. Although the test program was limited, it appears as if interrupted mortaring should not result in localized weaknesses if proper care is taken.

Panel 52 was mortared using a mix with a slightly higher water/cement ratio (0.45) of slightly higher slump (4 1/2 in.). The mortar penetrated well but the flexural modulus of rupture was

lower than the corresponding panel. The compression strength of the test cubes was normal.

2. Fastenings.

Various brackets, bumper strips, and marine fittings must be attached to the hull and deck of boats. Ferro-cement construction requires different techniques than those used for steel, aluminum, fibreglassed, and wooden boats. Welding cannot be used unless steel plates or bars are incorporated into the steel reinforced skeleton before mortaring. The possibility of using powder-actuated bolts has been raised.

Preliminary tests on a ferro-cement test panel were carried out in this laboratory by a representative of one of the major powder-actuated tool manufacturers.

The panel thickness of one inch was less than the minimum thickness of concrete considered necessary to receive threaded studs or nails placed by powder-actuated tools without spalling and cracking.

Eight 1/4-20NC studs with 1/8-inch shanks were placed in the panels with various power settings. Some slight spalling and cracking of both top and bottom surfaces of the panel occurred at the studs. The spalling would require surface patching to restore the smooth appearance. The withdrawal resistance ranged from a few pounds to 1,000 pounds. The results were not entirely promising but additional tests appear to be warranted.

3. Protective coatings.

The resistance to chemical attack of concrete and mortar and the reinforcement encased within can be maximized by close control of cement and sand proportions, mixing, and placing. Tests have shown that sound ferro-cement mortar, especially when made from a cement such as Type II with enhanced sulphate resistance, is reasonably resistant to attack by seawater. The fine voids, capillaries, and fine cracking may allow seawater to enter the mortar with possible eventual disintegration of the ferro-cement. Such disintegration may occur from leaching (effluorescence) resulting from alternate wetting and drying, from the expansion forces from freezing and thawing, or from the expansion forces from the formation of voluminous corrosion products on the steel reinforcement. An exterior coating appears to be necessary for its protective value as well as its cosmetic value. An interior protective coating may be required for a ferro-cement vessel if the vessel is operating in an aggressive service.

The American Concrete Institute has published a guide* on coatings for the protection of concrete against chemical attack. There are about 20 basic film-forming materials available for use in the manufacture of coatings but there are many variations in the formulations of these basic coatings which may make substantial changes in the performance of the coatings. The coating must provide an impermeable barrier, adhere well under adverse conditions of vapour and hydraulic pressures, and meet many other requirements.

Tests done in this laboratory using a modified polyester coating on ferro-cement lasted only 200 hours in the salt spray test whereas the same material lasted over 2,000 hours on a steel substrate. Much attention should be paid to the preparation of the mortar surfaces for best adhesion.

Acrylic latex and alkyd resins have been used but the experience seems to be limited. Chlorinated rubber-based paints are finding considerable favour at the present time in view of their rather successful application to concrete floors and swimming pools.

Much screening and service testing remain to be done before any coating can be recommended with reasonable assurance.

4. Internal soundness of panels.

It is considered that a device to check internal soundness of panels or hulls before setting and curing would be most desirable. A preliminary test using a Branson Audigage on cured panels to show centreline voids (or form surface voids) was not promising. It has recently been announced** that a lead zirconate titanate crystal transducer has been developed and will be marketed as part of a portable ultrasonic unit for on-site inspection of concrete structures. The possible use of ultrasonic devices for field testing of ferro-cement should be explored although such devices may not find much use in amateur or semi-professional boatbuilding.

*Guide for the Protection of Concrete against Chemical Attack by Means of Coatings and Other Corrosion-Resistant Materials, J. American Concrete Institute, Proc. Vol. 63, No. 12, Dec. 1966, pp 1305-1393.

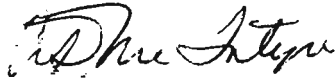
**Ultrasonics, Jan. 1970, p. 4.

D. BIBLIOGRAPHY.

Additional articles related to various aspects of ferro-cement construction have been received during the present program. Nearly 80 articles, ranging from one page to whole books, are retained in the library of B.C. Research. The complete compilation is shown in Table 13.



A.W. Greenius
Division of Engineering



A.D. McIntyre, Deputy Head,
Division of Applied Physics

AWG/mc

E. TABLES AND FIGURES FOR TEST PROGRAM.TABLE 1. Panel Construction Details.

Panel No.	Description
41, 44	Rods - high tensile double-drawn rods, 0.225 in. dia., spaced at 2-inch centres in each direction. Mesh - 1/2-19 ga. hardware cloth, 3 layers on one side of rods, 2 layers on the other side.
42, 45	Rods - high tensile double-drawn rods, 0.225 in. dia., spaced at 2-inch centres in each direction. Mesh - 1/2-16 ga. welded square mesh, 1 layer on each side of rods.
43, 46	Rods - high tensile double-drawn rods 0.225 in. dia., spaced at 2-inch centres in each direction. Mesh - 1/2-22 ga. hexagonal mesh, 5 layers on each side of rods.
47, 48	Rods - none (rods were initially placed at 6-inch centres but were pulled from panel after initial set). Mesh - 1/2-16 ga. welded square mesh, 1 layer on each side of rods.
49	Rods - galvanized 1020 rods, 1/4-in. dia., spaced at 2-inch centres in each direction. Mesh - 1/2-19 ga. hardware cloth, 3 layers on one side of rods, 2 layers on other side.
50	Rods - bright nail 1015 rods, 0.250 in. dia., spaced at 2-inch centres in each direction. Mesh - 1/2-19 ga. hardware cloth, 3 layers on one side of rods, 2 layers on other side.

TABLE 1 (cont'd)

Panel No.	Description
51	<p>Rods - hot rolled 1020 rods, 1/4-in. dia., spaced at 2-inch centres in each direction.</p> <p>Mesh - 1/2-19 ga. hardware cloth, 3 layers on one side of rods, 2 layers on the other side.</p>
52	<p>Rods - high tensile double-drawn rods, 0.225 in. dia., spaced at 2-inch centres in each direction.</p> <p>Mesh - 1/2-19 ga. hardware cloth, 3 layers on one side of rods, 2 layers on other side.</p> <p>Mortar - a thinner mortar was used, followed by brushing to roughen panel surface, allowing to set for 1 hour and resurfacing with mortar.</p>
53	<p>Rods - deformed high tensile double-drawn rods, 0.225 in. dia., spaced at 2-inch centres in each direction.</p> <p>Mesh - 1/2-19 ga. hardware cloth, 3 layers one side, 2 layers on the other side.</p>
54	<p>Rods - deformed high tensile double-drawn rods, 0.225 in. in dia., spaced at 4-inch centres in each direction.</p> <p>Mesh - 1/2-19 ga. hardware cloth, 3 layers on one side of rods, 2 layers on other side.</p>
55	<p>Rods - high tensile double-drawn rods, 0.225 in. in dia., spaced at 4-inch centres in each direction.</p> <p>Mesh - 1/2-19 ga. hardware cloth, 3 layers on one side of rods, 2 layers on other side.</p>
56	<p>Rods - high tensile double-drawn rods, 0.225 in. dia., spaced at 2-inch centres in each direction.</p> <p>Mesh - 1/2-22 ga. hexagonal mesh, 5 layers on each side of rods.</p>
57	<p>Rods - deformed high tensile double-drawn rods, 0.225 in. dia., spaced at 2-inch centres in each direction.</p> <p>Mesh - 1/2-22 ga. hexagonal mesh, 5 layers on each side of rods.</p>

TABLE 1 (cont'd)

Panel No.	Description
58	<p>Rods - high tensile double-drawn rods, 0.225 in. dia., spaced at 4-inch centres in each direction.</p> <p>Mesh - 1/2-19 ga. hardware cloth, 3 layers on one side of rods and 2 layers on other side of rods.</p> <ul style="list-style-type: none"> - mesh direction oriented at 45 degrees to direction of rods. - mesh width required a diagonal lap extending from point on one side 2 feet from corner to point 2 feet from corner in adjacent side.
59	<p>Rods - high tensile double-drawn rods, 0.225 in. dia., spaced at 2-inch centres in each direction.</p> <p>Mesh - 1/2-19 ga. hardware cloth, 3 layers on one side, 2 layers on other side of rods.</p> <p>Mortar - plastered from one side only on the first day; plastered the other side on the next day.</p>
60	<p>Rods - high tensile double-drawn rods, 0.225 in. dia., spaced at 2-inch centres in each direction.</p> <p>Mesh - 1/2-19 ga. hardware cloth, 5 layers on one side, 5 layers on other side of rods.</p> <p>Mortar - plastered whole panel from both sides.</p> <ul style="list-style-type: none"> - removed 2-inch wide strip of wet mortar across full width of panel and 12 inches from edge with air blast. - plastered in 2-inch wide strip on the next day.
61	<p>Rods - high tensile double-drawn rods, 0.225 in. dia., spaced at 4-inch centres in each direction.</p> <p>Mesh - 1/2-22 ga. hexagonal mesh, 3 layers on each side of rods.</p> <p>Mortar - plastered only 12-inch wide strip along one side on first day.</p> <ul style="list-style-type: none"> - plastered remainder of panel on next day.

TABLE 2. Unit Weights, Breaking Strengths, Bond Areas, and Approximate Costs of Various Mesh Reinforcements on Equal Weight and Equal Strength Basis.

Type of Mesh	Mesh Weight		Breaking Strength		Bond Area ⁽¹⁾		Cost	
	lb/sq ft mesh	lb/sq ft panel	lb/lin. in. mesh	lb/lin. in. panel	sq in./sq ft panel	spec. surface in. ² /in. ³ mesh	\$/sq ft mesh	\$/sq ft panel
1/2-22 ga. hexagonal mesh (in direction of twists)	0.11	1.10 ⁽²⁾ (10 layers)	60	600 (10 layers)	300 (10 layers)	120	0.057	0.57 (10 layers)
	0.11	1.54 ⁽³⁾ (14 layers)	60	840 (14 layers)	420 (14 layers)		0.057	0.80 (14 layers)
1/2-22 ga. hexagonal mesh (across twists)	0.11	1.10 (10 layers)	21	210	195 (10 layers)	160	0.057	0.57 (10 layers)
	0.11	1.54 (14 layers)	21	294	266 (14 layers)		0.057	0.80 (14 layers)
1/2-19 ga. hardware cloth	0.24	1.20 ⁽²⁾ (5 layers)	140	700	190 (5 layers)	96	0.120	0.60 (5 layers)
	0.24	1.44 ⁽³⁾ (6 layers)	140	840	228 (6 layers)		0.120	0.72 (6 layers)
1/2-16 ga. welded square mesh	0.56	1.12 ^(2,3) (2 layers)	420	840	118 (2 layers)	62	0.295	0.59 (2 layers)

(1) Calculated only for wires in direction of loading.

(2) 10 layers, 5 layers, and 2 layers = approximate equal weight of mesh.

(3) 14 layers, 6 layers, and 2 layers = approximate equal strength of mesh.

TABLE 3. Tensile Test Results for Reinforcement Rods used in Test Panels.

Description of Rod	Dia. in.	U.T.S.	Elong. % in 8 in.	R.A. %
Hot rolled 1020	0.250 by 0.265 (oval)	70,000	23.5	67.3
		69,700	24.0	66.8
Galvanized 1020	0.220 by 0.276 (oval)	50,600	24.4	71.3
		49,300	25.1	69.0
Bright nail wire	0.250	73,400	(2)	63.9
		72,700	8.5	64.8
A82 double ⁽¹⁾ drawn 1015	0.225	100,000	(2)	49.5
		99,000	(2)	58.5
		102,000	3.0(3)	52.0
A82 double ⁽¹⁾ drawn 1015 with cross weld		89,000	1.25(4)	
A82 double drawn 1015	0.225	78,800	10.0	63.6
A82 double drawn 1015 with cross weld	0.225	80,000	7.5(5)	62.5
A82 deformed double drawn 1015	0.225 nom.	82,600	4.0	-
		85,000	3.8	-

(1) ASTM Designation A82 requires that the cold drawn rod must have a minimum tensile strength of 80,000 psi.

(2) Broke outside gauge length.

(3) Broke close to gauge mark.

(4) Broke at cross weld.

(5) Broke 1/2 inch from weld.

TABLE 4. Rod/Mortar Bond Strengths.

Type of Reinforcing Rod	Bond Strength, lb/sq in. of embedded rod surface	
	28 days	4 1/2 months
Hot rolled rod (1020)(scale intact)	406	580
Hot rolled rod (1020)(pickled)	300	555
Double-drawn rod (as received)	135	280
Double-drawn rod (drawing lubricant removed)	188	330
Double-drawn rod (lightly rusted)	286	518
Deformed double-drawn rod (clean)	651	660
Galvanized 1020 rod	33	57
Reclaimed rod (badly corroded)	480	700

TABLE 5. Results of Drop-Impact Load Tests on 36-inch Panels.

Panel No.	Description of Panels Materials listed in order from top to bottom of panel, i.e. from impact surface to tension surface.	Dishing in 1/16 in.	Diameter of circle encompassing cracks in.	Rectilinear crack, extension from centre in.	Description of Bottom Surface
44	2 layers 1/2-19 ga. hardware cloth. Double-drawn rods at 2 in. Double-drawn rods at 2 in. 3 layers 1/2-19 ga. hardware cloth	4	12	17	Very fine radial cracks One fine rectilinear crack
45	1 layer 1/2-16 ga. welded square mesh Double-drawn rods at 2 in. Double-drawn rods at 2 in. 1 layer 1/2-16 ga. welded square mesh	8	15 x 18	6	Fine radial cracks Fine rectilinear cracks
46	5 layers 1/2-22 ga. hexagonal mesh Double-drawn rods at 2 in. Double-drawn rods at 2 in. 5 layers 1/2-22 ga. hexagonal mesh	9	30	0	Radial cracking
48	2 layers 1/2-19 ga. hardware cloth Lengthwise and transverse rods removed from panel before setting 3 layers 1/2-19 ga. hardware cloth	18	32	18	Fine radial cracking One rectilinear crack open 1/16"
55	2 layers 1/2-19 ga. hardware cloth Deformed double-drawn rods at 4 in. Deformed double-drawn rods at 4 in. 3 layers 1/2-19 ga. hardware cloth	10	24	17	Radial cracking Fine rectilinear crack Centre spalling over 6 in. dia.

TABLE 6. Tensile Strengths of Panel Specimens and Comparison with Summed Strengths (Total Mesh Strength + Rod/Mortar Bond Strength) (All specimens 4 in. wide, 1 in. nom. thick. Loads in lb)

Panel Test Specimen No.	Panel Descriptions	Load, lb		Remarks	Total Mesh Strength lb	Total Rod/Mortar Bond Strength lb	Summed Strength* lb
		At first crack	Max at final failure				
41D	3 layers 1/2-19 ga. hardware cloth Double-drawn rods at 2 in. 2 layers 1/2-19 ga. hardware cloth	3100	3540	Main transverse crack at edge of grip.	2800	850	3650
41E	3 layers 1/2-19 ga. hardware cloth Double-drawn rods at 2 in. 2 layers 1/2-19 ga. hardware cloth	3200	3400	Main transverse crack at edge of grip, one other fine crack.	2800	850	3650
42D	1 layer 1/2-16 ga. welded square mesh Double-drawn rods at 2 in. 1 layer 1/2-16 ga. welded square mesh	2900	3860	Main transverse crack at edge of grip, three fine cracks in gauge length.	3360	850	4210
42E	1 layer 1/2-16 ga. welded square mesh Double-drawn rods at 2 in. 1 layer 1/2-16 ga. welded square mesh	2400	3900	Main transverse crack at edge of grip occurred at 3600 lb	3360	850	4210
43D	5 layers 1/2-22 ga. hexagonal mesh Double-drawn rods at 2 in. 5 layers 1/2-22 ga. hexagonal mesh (mesh twists across load direction)	2400	2600	Main transverse crack at edge of grip, one fine crack in centre of gauge length.	840	850	1690
43E	5 layers 1/2-22 ga. hexagonal mesh Double-drawn rods at 2 in. 5 layers 1/2-22 ga. hexagonal mesh (mesh twists in load direction)	2900	3100	Main transverse crack near edge of grip.	2400	850	3250

*No allowance made of mortar strength.

TABLE 7. Results of Bend Tests in Third-Point Loading.
 (Specimen width 12 in., length > 24 in., span 21 in.)
 (Modulus of rupture values in brackets for minimum practical panel thickness)

Panel Test Specimen No.	Description of Specimens Material listed in order from top to bottom of specimen, i.e. from compression to tension sides.	Load at First Observed Crack lb	Maximum Load lb	Modulus of Rupture psi	Remarks
41A	3 layers 1/2-19 ga. hardware cloth Lengthwise double-drawn rods at 2 in. Transverse double-drawn rods at 2 in.	1100	2240	3930 (3930)	No rods slipping Main crack under load point Several fine cracks
41B	3 layers 1/2-19 ga. hardware cloth Transverse double-drawn rods at 2 in. Lengthwise double-drawn rods at 2 in. 2 layers 1/2-19 ga. hardware cloth	1700	2900	5080 (5080)	Rods slipping (bond failure) Major cracks under load points
42A	1 layer 1/2-16 ga. welded square mesh Lengthwise double-drawn rods at 2 in. Transverse double-drawn rods at 2 in. 1 layer 1/2-16 ga. welded square mesh	1300	2800	4910 (6050)	Rod slipping (bond failure) Main crack under one load point
42B	1 layer 1/2-16 ga. welded square mesh Transverse double-drawn rods at 2 in. Lengthwise double-drawn rods at 2 in. 1 layer 1/2-16 ga. welded square mesh	1950	3240	5680 (7000)	Rods slipping Fine cracks under both load points
43A	5 layers 1/2-22 ga. hexagonal mesh Lengthwise double-drawn rods at 2 in. Transverse double-drawn rods at 2 in. 5 layers 1/2-22 ga. hexagonal mesh (bending across mesh twists)	1800	2650	4650 (3830)	No rods slipping Major crack under one load point Fine crack under other load point
43B	5 layers 1/2-22 ga. hexagonal mesh Transverse double-drawn rods at 2 in. Lengthwise double-drawn rods at 2 in. 5 layers 1/2-22 ga. hexagonal mesh (bending in direction of mesh twists)	1400	2700	4740 (3900)	Rods slipping (bond failure) Major crack under one load point

TABLE 7. (cont'd)

Panel Test Specimen No.	Description of Specimens Material listed in order from top to bottom of specimen, i.e. from compression to tension sides.	Load at First Observed Crack lb	Maximum Load lb	Modulus of Rupture psi	Remarks
47A	1 layer 1/2-16 ga. welded square mesh Lengthwise rods removed from panel Transverse rods removed from panel 1 layer 1/2-16 ga. welded square mesh	1100	1600	2800	Several fine cracks between load points
47B	1 layer 1/2-16 ga. welded square mesh Transverse rods removed from panel Lengthwise rods removed from panel 1 layer 1/2-16 ga. welded square mesh	900	1300	2280	Fairly fine cracks between load points
49A	2 layers 1/2-19 ga. hardware cloth Lengthwise galvanized 1020 rods at 2 in. Transverse galvanized 1020 rods at 2 in. 3 layers 1/2-19 ga. hardware cloth	1300	1530	2680	No rods slipped Main crack under one load point Several fine cracks between load points
49B	2 layers 1/2-19 ga. hardware cloth Transverse galvanized 1020 rods at 2 in. Lengthwise galvanized 1020 rods at 2 in. 3 layers 1/2-19 ga. hardware cloth	1300	2800	4910	Rods slipping (bond failure) Several fine cracks between load points
50A	3 layers 1/2-19 ga. hardware cloth Lengthwise bright nail wire rods at 2 in. Transverse bright nail wire rods at 2 in. 2 layers 1/2-19 ga. hardware cloth	1300	2350	4120	Rods lipping (bond failure) Main crack under one load point Several cracks between load points
50B	3 layers 1/2-19 ga. hardware cloth Transverse bright nail wire rods at 2 in. Lengthwise bright nail wire rods at 2 in. 2 layers 1/2-19 ga. hardware cloth	2320	2400	4210	Rods slipping (bond failure) Uniform cracking between load points - smooth bend.

TABLE 7. (cont'd)

Panel Test Specimen No.	Description of Specimens Material listed in order from top to bottom of specimen, i.e. from compression to tension sides.	Load at First Observed Crack lb	Maximum Load lb	Modulus of Rupture psi	Remarks
51A	2 layers 1/2-19 ga. hardware cloth Lengthwise hot rolled 1020 rods at 2 in. Transverse hot rolled 1020 rods at 2 in. 3 layers 1/2-19 ga. hardware cloth	900	2900	5080	Rods did not slip Uniform cracking between load points Smooth bend
51B	2 layers 1/2-19 ga. hardware cloth Transverse hot rolled 1020 rods at 2 in. Lengthwise hot rolled 1020 rods at 2 in. 3 layers 1/2-19 ga. hardware cloth	1500	3600	6310	Rods did not slip Top spalling Major crack under one load point Several cracks between load points
52A	2 layers 1/2-19 ga. hardware cloth Lengthwise double drawn rods at 2 in. Transverse double drawn rods at 2 in. 3 layers 1/2-19 ga. hardware cloth	1300	1870	3270	No rods slipping Uniform cracking between load points Smooth bend
52B	2 layers 1/2-19 ga. hardware cloth Transverse double drawn rods at 2 in. Lengthwise double drawn rods at 2 in. 3 layers 1/2-19 ga. hardware cloth	2000	2050	3600	No rods slipping Several fine cracks under one load point
53A	2 layers 1/2-19 ga. hardware cloth Lengthwise deformed d-d rods at 2 in. Transverse deformed d-d rods at 2 in. 3 layers 1/2-19 ga. hardware cloth	1100	1840	3230 (3230)	No rods slipping Some top spalling Fine cracks between load points Smooth bend
53B	2 layers 1/2-19 ga. hardware cloth Transverse deformed d-d rods at 2 in. Lengthwise deformed d-d rods at 2 in. 3 layers 1/2-19 ga. hardware cloth	1900	3080	5400 (5400)	No rods pulled Slight top spalling Main cracks at load points

TABLE 7. (cont'd)

Panel Test Specimen No.	Description of Specimens Material listed in order from top to bottom of specimen, i.e. from compression to tension sides.	Load at First Observed Crack lb	Maximum Load lb	Modulus of Rupture psi	Remarks
54A	3 layers 1/2-19 ga. hardware cloth Lengthwise deformed d-d rods at 4 in. Transverse deformed d-d rods at 4 in. 2 layers 1/2-19 ga. hardware cloth	1000	1460	2560	Rods slipping (bond failure) Major crack under one load point Several fine cracks between load points
56A	5 layers 1/2-22 ga. hexagonal mesh Lengthwise double drawn rods at 2 in. Transverse double drawn rods at 2 in. 5 layers 1/2-22 ga. hexagonal mesh (bending in direction of mesh twists)	900	1460	2560	Rods slipping (bond failure) Major and fine cracks between load points
56B	5 layers 1/2-22 ga. hexagonal mesh Transverse double drawn rods at 2 in. Lengthwise double drawn rods at 2 in. 5 layers 1/2-22 ga. hexagonal mesh (bending across line of mesh twist)	1000	1450	2540	Rods slipping (bond failure) Major cracks under load points Several fine cracks between load points
57A	5 layers 1/2-22 ga. hexagonal mesh Lengthwise deformed d-d rods at 2 in. Transverse deformed d-d rods at 2 in. 5 layers 1/2-22 ga. hexagonal mesh (bending in direction of twists)	1400	2720	4760 (3940)	Rods slipping Fine cracks under both load points and between load points
57B	5 layers 1/2-22 ga. hexagonal mesh Transverse deformed d-d rods at 2 in. Lengthwise deformed d-d rods at 2 in. 5 layers 1/2-22 ga. hexagonal mesh (bending across mesh twists)	1200	2540	4450 (3680)	Rods slipping (bond failure) Slight top spalling Major crack under one load point

TABLE 7. (cont'd)

Panel Test Specimen No.	Description of Specimens Material listed in order from top to bottom of specimen, i.e. from compression to tension sides.	Load at First Observed Crack lb	Maximum Load lb	Modulus of Rupture psi	Remarks
58A	3 layers 1/2-19 ga. hardware cloth Lengthwise double-drawn rods at 2 in. Transverse double-drawn rods at 2 in. 2 layers 1/2-19 ga. hardware cloth (mesh laid at 45° to rod direction)	500	1220	2140	Rods slipping (bond failure) Fine cracks between load points
53B	3 layers 1/2-19 ga. hardware cloth Transverse double-drawn rods at 2 in. Lengthwise double-drawn rods at 2 in. 2 layers 1/2-19 ga. hardware cloth (mesh laid at 45° to rod direction)	1600	1800	3150	Rods slipping (bond failure) Slight top spalling Many cracks under each load point
58D	3 layers 1/2-19 ga. hardware cloth Diagonal double drawn rods at 2 in. Diagonal double drawn rods at 2 in. 2 layers 1/2-19 ga. hardware cloth (mesh laid at 45° to rod direction) (contains 4-inch mesh lap at midlength)	1000	1440	2520	Rods slipping (bond failure) Main crack under one load point Several fine cracks over span except in centre where 4-inch lap has reinforced specimen
59A	2 layers 1/2-19 ga. hardware cloth Lengthwise double-drawn rods at 2 in. Transverse double-drawn rods at 2 in. 3 layers 1/2-19 ga. hardware cloth (interrupted mortaring)	800	1580	2760	Rods pulling Fine uniform cracking over span between load points
59B	2 layers 1/2-19 ga. hardware cloth Transverse double-drawn rods at 2 in. Lengthwise double-drawn rods at 2 in. 3 layers 1/2-19 ga. hardware cloth (interrupted mortaring)	1300	1700	2980	Rods slipping (bond failure) Fine uniform cracking over span between load points

TABLE 7. (cont'd)

Panel Test Specimen No.	Description of Specimens Material listed in order from top to bottom of specimen, i.e. from compression to tension sides.	Load at First Observed Crack lb	Maximum Load lb	Modulus of Rupture psi	Remarks
60A Joint	5 layers 1/2-19 ga. hardware cloth Lengthwise double-drawn rods at 2 in. Transverse double-drawn rods at 2 in. 5 layers 1/2-19 ga. hardware cloth (interrupted mortaring)	700	1760	3080	Rods pulled Delamination Single crack at one side of joint Fine crack near load point
60B	5 layers 1/2-19 ga. hardware cloth Transverse double-drawn rods at 2 in. Lengthwise double-drawn rods at 2 in. 5 layers 1/2-19 ga. hardware cloth (interrupted mortaring)		1100	1930	Rods slipped Delamination starting at 700 lb Fine cracking between load points
61A Joint	3 layers 1/2-22 ga. hexagonal mesh Lengthwise double-drawn rods at 4 in.	600	1070	1870	Rods pulling Main crack at joint Several fine cracks between load points
61A No joint	Transverse double-drawn rods at 4 in. 3 layers 1/2-22 ga. hexagonal mesh (interrupted mortaring) (bending in direction of mesh twists)	700	1300	2280	Main crack between load points Several fine cracks between load points
61B	3 layers 1/2-22 ga. hexagonal mesh Transverse double-drawn rods at 4 in. Lengthwise double-drawn rods at 4 in. 3 layers 1/2-22 ga. hexagonal mesh (interrupted mortaring) (bending across mesh twist)	600	900	1870	Rods slipping (bond failure) Major crack under one load point

TABLE 8. Assessment of Unreinforced Test Coupons Exposed to 350 Freeze-Thaw Cycles.

Coupon Test Panel No.	Description of Test Panel			No. of Cycles	Visual Appearance	Weight Loss % of Original Dry Weight
	Cement	Sand	Mesh		Description	
16	II	Evco Dry Mortar Sand	None	350	No significant change	0
17	I	" "	"		No significant change	0
19	III	" "	"	350	No significant change	0.8
23	V	" "	"	350	No significant change	0
24	Aluminum	" "	"	350	No significant change	0
25	II	Del Monte	"	350	Slight powdering of coupon	0.7
26	I	Evco Dry Mortar Sand	"	350	No significant change	1.1
31	II + no additive	" "	"	350	No significant change	1.2
33	II + pozzolan	" "	"	50-100 350	Some crumbling at one corner Coupon crumbled badly	26.2
35	II + water reducing agent	" "	"	350	No significant change	1.1
37	II + air entraining agent	" "	"	350	No significant change	2.2
40	II + pva emulsion	" "	"	100-125 125-150 350	Slight flaking of surface Slight spalling of top surface Slight spalling of top surface	4.9

TABLE 9. Assessment of Mesh-Reinforced Test Coupons Exposed to 76 Freeze-Thaw Cycles.

Coupon Test Panel No.	Description of Test Panel			Visual Appearance	
	Cement + Additive	Sand	Mesh Reinforcement	No. of Cycles	Description
5	II	Evco Dry Mortar sand	1/2-22 ga. hexagonal	36	No visible change
				76	Top unreinforced layer of mortar completely disintegrated. Bottom reinforced portion is sound.
17	I	Mortar sand	"	36	No visible change
				76	Some disintegration of unreinforced layer. Bottom reinforced layer is sound.
19	III	Mortar sand	"	36	No visible change
				76	Top unreinforced layer of mortar completely disintegrated. Bottom reinforced layer is sound.
23	V	Mortar sand	"	36	No visible change
				76	Some disintegration of unreinforced layer. Bottom reinforced layer is sound.
24	Aluminous	Mortar sand	"	36	No visible change
				76	Coupon appears to be completely sound.
25	II	Del Monte	"	36	Slight flaking of top surface
				76	Slight flaking of top surface, bottom reinforced layer is sound.
31	II + no additive	Evco Dry Mortar sand	"	36	No visible change
				76	No apparent damage
33	II + pozzolan	Mortar sand	"	36	No visible change
				76	No apparent damage
35	II + water reducing agent	Mortar sand	"	36	No visible change
				76	No apparent damage.
37	II + air entraining agent	Mortar sand	"	36	No visible change
				76	No apparent damage
37A	" "	Mortar sand	"	36	No visible change
				76	No apparent damage

TABLE 10. Assessment of Test Coupons Exposed to 350 Seawater Immersion and Drying Cycles.

Coupon Test Panel No.	Description of Test Panel			Visual Appearance after 350 Cycles				Penetration Hardness Value			
								Exposed Coupon		Virgin Coupon	
	Cement	Sand	Mesh	Top	Bottom	Top	Bottom	Top	Bottom		
4-F ⁽¹⁾	II	Evco D.M.	1/2-16 welded ⁽²⁾	No change	No change	107	105	105	106		
5-F	II	"	1/2-22 hex	"	"	108	106	96	102		
6-F	II	"	1/2-22 hex ⁽³⁾	"	Red rust spots at wires	107	101	101	105		
8-F	II	"	1/2-19 hardware	"	Slight white rust on wires	106	105	105	103		
9-F	II	"	1/2-16 welded ⁽⁴⁾	"	Red rust spots at wires	113	97	104	92		
17-F	I	"	1/2-22 hex	"	No change	109	96	90	95		
19-F	III	"	"	"	"	102	103	102	90		
23-F	V	"	"	"	Slight white rust on wires	95	103	102	105		
24-F	Aluminous	"	"	"	" " " "	112	113	109	109		
25-F	II	Del Monte	"	"	" " " "	100	105	96	91		
31-D	II	Evco D.M.	"	"	" " " " (5)	98	98	90			
33-D	II+ ⁽⁶⁾	"	"	"	" " " " (5)	99	99	89			
35-D	II+ ⁽⁷⁾	"	"	"	" " " " (5)	105	106	103			
37-D	II+ ⁽⁸⁾	"	"	"	Heavy white rust on wires ⁽⁵⁾	91	97	85	77		
40-D	II+ ⁽⁹⁾	"	"	"	" " " " (5)	65	62	54	56		

(1) Panels 4-17, 23-25 incl. tested in duplicate.

(2) All mesh galvanized after weaving or welding except as noted in (3) and (4).

(3) Wires galvanized before weaving.

(4) Galvanizing stripped from mesh.

(5) Original panels had light to heavy white rust pattern on wires from the original curing.

(6) 1 pt pozzolan: 3 pts cement.

(7) 62 cc water reducing agent: 25 lb cement: 50 lb sand.

(8) 7 cc air entrainment agent: 25 lb cement: 50 lb sand.

(9) 5 lb polyvinyl emulsion: 5 lb H₂O.

TABLE 11. Summary of Test Panel Construction Data with Various Admixtures.
(12 layers of 1/2-22 ga. galvanized hexagonal mesh, Type II cement, Evco Dry Mortar Sand)

Panel No.	Admixture	Cement/ Sand Ratio	Water/ Cement Ratio	Slump in.	Compression Strength, psi		Mod. of Rupture (unreinforced) psi	Remarks
					7-day	28-day		
31	No additives	1:2	0.4	2 1/2	5900	6950	1120 930	A rather stiff mix, difficult to penetrate mesh.
32		1:2	0.4	2	4300	6450 6520		
33	Pozzolan replaced 25% of cement, i.e. pozzolan/cement ratio = 1:3	1:2	0.42	2 1/2	4550	7200 7850	840 680	A rather stiff mix, difficult to penetrate mesh.
34		1:2	0.45	3 1/2	3575	6225 4975		A more workable mix with easier penetration of mesh.
35	Water-reducing agent at recommended rate of 6.5 fl. oz per sack of cement	1:2	0.35	2	7725	5500 4700	1100 1015	A rather stiff mix, difficult to penetrate mesh.
36		1:2	0.37	3	5825	5875 5875		A more workable mix with easier penetration of mesh.
37	Air-entraining agent at recommended rate of 3/4 fl. oz per sack of cement	1:2	0.40	3	4900	6100 5100	835 735	Good workability and easier penetration of mesh.
		1:2	0.40	3	5454	6050 7200		
39	Polyvinyl/acetate emulsion pva/water 1:1 polyvinyl/acetate emulsion pva/water 1:1.44	1:2	0.48*	3	3500	3650 3775	850 790	Rather stiff mixes, difficult to penetrate mesh.
40		1:2	0.49*	3 1/2	2250	3000 3400		

*includes pva emulsion.

TABLE 12. Effect of Admixture on Absorption Properties.

Panel No.	Description of Panel				Absorption of Water, Percent of Dry Weight
	Cement	Sand	Water/Cement Ratio	Admixture	
31	Type II 25 lb	Evco Dry Mortar Sand 50 lb	0.4	Nil	5.2
33	Type II 18 3/4 lb	"	0.4	Pozzolan 6 1/4 lb	5.6
35	Type II 25 lb	"	0.4	Water-re- ducing agent 6.5 oz/sack	3.9
37	Type II 25 lb	"	0.4	Air entrain- ment agent 3/4 oz/sack	6.7
40	Type II 25 lb	"	0.2	Polyvinyl acet. emul. pva/cement ratio 0.2	5.8

TABLE 13. BIBLIOGRAPHY.

o.	Author and Affiliation	Title	Journal and Citation (volume, date, paging)	Narrative	Tables	Diags, Figs.	Scale Drawings	Performance	Photographs	Costs
1	Saga Technical Associates (designers, publishers)	Bibliographic introduction to ferrocement.	Toronto, Saga 1969?	x	x	x	x	x	x	
2	Bozakiadov, V.F. et al. Shipbuilding Publishing House, Leningrad.	Ship hulls made of reinforced concrete.	Leningrad, 1968 Translation pub. by CFSTI AD680 042, 1968	x	x	x	x	x	x	
3	Canby, Charles D. U. of Michigan, Dept. of Naval Architecture & Marine Engineering.	Ferro-cement, with particular reference to marine applications.	Ann Arbor, 1969 Departmental No. 014	x	x	x		x		
4	Lin, T.Y. & Associates, Consulting Engineers (For U.S. Naval Civil Engineering Lab., Calif)	Ferro cement panels v. 1	Report No. CR 69.008 CFSTI AD850630, 1968	x	x	x		x	x	
5	Geymayer, H.G. U.S. Corps of Engineers.	Strain meter & stress meters for embedment in models of mass concrete structures.	Tech. Report No. 6-811, U.S. Army Engineer Water-Ways Exper. Station Vicksburg, Mass.	x	x	x		x	x	
6	_____	Use of epoxy or polyester resin in tensile zone of composite concrete beams.	Tech. Report No. C-69-4, U.S. Army Engineer Water-Ways Exper. Station Vicksburg, Mass.	x	x	x		x	x	
7	Gibbs & Cox, Inc.	Marine design manual for Fiberglass reinforced plastics.	New York, McGraw Hill 1960	x	x	x	x		x	
8	Harper, Ross et al Consultants.	Boatbuilding in ferro-cement	The Authors, Vancouver, B.C., 1967(?)	x			x			
9	Hartley, R.T. Builder	Boatbuilding with Hartley 3rd ed.	Auckland, N.Z., the author, 1967.	x	x	x	x		x	x
10	Jackson, G.W. & W.M. Sutherland.	Concrete boatbuilding.	London, Allen & Unwin, 1969	x	x	x	x	x	x	
11	Mowat, Dallas N. Univ. of Calgary, Dept. of Civil Engineering.	Flexural testing of ferr-cement planks	M.Sc. Thesis, 1970.	x	x	x		x	x	
12	Muhlert, Hans F. Univ. of Michigan, Dept. of Naval Architectur & Marine Engineering.	Analysis of ferro-cement in bending.	Ann Arbor, 1970 Departmental No. 043	x	x	x		x		
13	Samson, John and Wellens, Geoff Samson Marine Design Enterprises Ltd.	How to build a ferro-cement boat.	Vancouver, Samson Marine Design Enterprises, 1968.	x		x	x		x	

TABLE 13. (cont'd)

No.	Author and Affiliation	Title	Journal and Citation (volume, date, paging)	Narrative	Tables	Diags, Figs.	Scale Drgs.	Performance	Photographs	Costs
14	Anon	Chinese build concrete boats	Concrete Products v. 69(12) Dec 66 p. 36-37.	x					x	x
15	"	Concrete barges multiply in Gulf.	Concrete Products v. 70 Jan. 1967 p. 56-58.	x					x	
16	"	Concrete-hulled pilot launch for Bahrain.	Shipbuilding & Shipping Rec. 1966 v. 49:437.	x				x	x	
17	Anon	Construction of an 18M ferro-cement hyperbolic hull - Communist China.	U.S. Joint Publications Res. Service. JPRS 4167, 1960	x	x					
18	"	Ferrocement	Concrete construction 1966, v. 11:355	x						
19	"	Ferro-cement: does it have a future in the work boat field?	The Work Boat. Feb. 1969.	x		x			x	x
20	"	Progress in ferro-cement.	Yachting Monthly. Sept. 1967 p. 120-124.	x		x	x		x	
21	"	Seacrete stern trawlers.	Fishing News International v. 7, 1967, p. 69-70	x				x	x	
22	"	Thin-shelled reinforced concrete in the U.K.	Engineering 1963 8 Feb. 232-3.	x					x	
23	"	YM and Ferro	Report from Yachting Monthly 1969?	x		x	x		x	
24	Allen, R.T.L. & Terrett, F.L. Cement and Concrete Assoc.	Durability of concrete in coastal protection work	Conference on coastal engineering. 1968. Chap 75: 1200-1207.	x				x		
25	Barnes, Sam.	Concrete boats.	Machine Design. April 1968, p 44-45	x		x				
26	Bellport, B.P. U.S. Reclamation Bureau.	Combating sulphate attack on concrete on Bureau of Reclamation projects.	In: Symposium on Performance of Concrete. Toronto, University Press 1968, p 77-92.	x	x				x	x
27	Burgess, John.	Seacrete Method developed by British yard.	Fishing News International v. 8, May 1968: 44-45.	x				x	x	x
28	Cassie, W. Fisher.	Lambot's boats.	Concrete (London) v.1 1967; 380-82.	x					x	
29	Cement & Concrete Assoc. of Australia.	Ferrocement boats.	Concrete Information No. C-39, 9 pp 1968?	x	x				x	
30	Fondriest, F.F. & Birkimer, Donald L.	Control of cracking in concrete.	Battelle Technical Review Sept/Oct 1968: 3-9.	x		x			x	
31	Fyson, John F. Supr. of Boatbuilding FAO Regional OH Bangkok.	Ferro-cement construction for fishing vessels Pts 1-3.	Fishing News Internat. v.8, April 1968; 51-55, May 39-43, June 30-32 (or FAO reprint).	x						x
32	Gaul, R.W. & E.D. Smith	Effective & practical repair of cracked concrete.	In: Epoxies with concrete. Am. Concrete Inst. Pub. SP-21, 1968 p. 29-36.	x		x			x	
33	Gardner, John. Tech. Editor.	Ferro-cement makes strong hull; micro-balloons help lick resin sag.	National Fisherman. March 1967, p. 8a	x					x	

TABLE 13. (cont'd)

No.	Author and Affiliation	Title	Journal and Citation (volume, date, paging)	Narrative	Tables	Diags, Figs.	Scale Drgs.	Performance	Photographs	Cases
34	Gibson, Peter. Correspondent.	Fishboats in Ferro-cement.	Western Fisheries 1968. January 25, 26, 28.	x					x	
35	Gt. Brit. Building Research Station.	Zinc-coated reinforcement for concrete.	Digest #109. Watford 1969.	x		x			x	
36	Hagenbach, T.M. Seacrete Ltd.	Ferro-cement boats.	Conf. on fishing vessel constrn. Mat'ls. Montreal, 1968. p 365-371.	x					x	x
37	Hurd, M.K. Am. Concrete Inst.	Ferro-cement boats.	Am. Concrete Inst. J. 1969: March p 202-4.	x					x	
38	Iorns, Martin. Fibersteel Corp.	Cement boatbuilding problems aired.	National Fisherman. May 1967.	x						
39	_____	Ferro-cement advice from an expert.	National Fisherman. June 1967, June 1967, p 7B, 23B, 24B.	x					x	
40	Kaiser Cement.	Ferro-cement seagoing architectural concrete.	Oakland, Cal. Kaiser undated. 7 pp.	x					x	
41	Kelly, A.M. & Mouat, T.W. B.C. Research, Vancouver.	Ferro-cement as a fishing vessel construction material.	Paper presented at Conf. on Fishing Construction Materials. Montreal, 1968.	x	x	x		x	x	
42	Kristinsson, G.E. Commercial Marine Services, Ltd., Montreal.	The growing acceptance of Ferro-cement as a first-class boat-building material.	Sea Harvest Ocean Sci. Dec 69/Feb 70. 32-34.	x			x			
43	¹ Lachance, L. & ² P, Fugere. ¹ Laval University. ² Consulting Eng.	Construction of a ferro-shotcrete motor-sailer hull.	L'Ingenieur, March 1970. v. 56. (translation available)	x	x				x	x
44	Mather, B.	Field & laboratory studies of the sulphate resistance of concrete.	In: Symposium on the performance of concrete. Toronto, Univ. Press 1968. p 66-76.	x	x	x				
45	Mathews, S.T. Ship Division N.R.C.	Main hull girder loads on Great Lakes bulk carrier.	Soc. Naval Architects & Marine Engineers. Spring Meeting, 1967. Proceedings Paper No. 11.	x	x	x		x		
46	Morgan, Rowland G. U. of Bristol.	Underwater concrete.	Underwater Science & Technol. J2, 1970, June, 74-80.	x		x			x	
47	_____	Concrete as a shipbuilding material	International Marine & Shipping Conf. (London) 1969. Section 11, Materials. p 9-14.	x					x	
48	Nervi, Pier Luigi. Nervi & Bertoli (Rome)	Concrete and structured form.	Engineering, 1955. 601-603.	x					x	
49	_____	Ferro-cement: its characteristics & potentialities.	L'Ingegnere 1951 (trans.)	x		x			x	
50	_____	Ferro-cements: chapter 4 of his Structures.	McGraw Hill, 1956	x		x	x		x	

TABLE 13. (cont'd)			Narrative	Tables	Diags, Figs.	Scale Dwg's.	Performance	Photographs	Costs
No.	Author and Affiliation	Title	Journal and Citation (volume, date, paging)						
51	Nervi, Pier Luigi, Nervi & Bertoli (Rome).	Precast concrete offers new possibilities for design of shell structures.	American Concrete Institute J. v. 25: 537-548, 1953.	x		x			x
52	_____	Thin reinforced concrete members from Thorn exhibition hall.	Civil Engineering 1951, v. 46:25-31.	x		x			
53	Oberti, Guido. Prof.	The penstock of Castelbello (Transl.)	Energia Elettrica 1953. v. XXX No. 5. 17 p.	x	x			x	x
54	_____	Some conclusions about deformability & resistance in tension ferro-cement.	Undated paper (Transl.)	x	x			x	
55	Rath, Dick.	Concrete boats - are they for real?	Boating Oct 1967. 37-42.	x			x		x
56	Romualdi, J.P. Battelle Development.	Two-phase concrete and steel material.	U.S. Patent 3,429,094 Feb 25, 1969.	x	x	x		x	
57	Ross, Stanley.	Concrete floats: smooth sailing ahead.	Concrete products. v. 66, 1963 Oct: 29-32.	x					x
58	Schutz, B.J.	Epoxy resin adhesives for bonding concrete to concrete.	In: Epoxies with concrete Am. Concrete Inst. Pub. SP-21. Detroit, 1968 p. 19-28.	x		x			x
59	Stevenson, H.I.	Use of concrete ships for mill log pond breakwater at Powell River.	Unpublished notes. 1964.	x					
60	Swenson, E.G. Div. Building Res., N.R.C.	Admixtures in concrete NRC Tech. Paper No. 181.	National Research Council Ottawa.	x					
61	Tuthill, Lewis H. U.S. Reclamation Bureau. _____ and Coff, L.	Concrete operations in the concrete ships program. Discussion & closure.	Am. Concrete Inst. J. 1945 v. 16: 137-180. _____ Supp. Nov. 1945 180-1 - 180-5.	x	x	x		x	x
				x					x

TABLE 13. (cont'd)			Narrative	Tables	Dwgs. Figs.	Scale Dwgs.	Performance	Photographs	Costs
	Author and Affiliation	Title	Journal and Citation						
62	Collen, L.D.G. Trinity College, Dublin.	Some Notes on the Characteristics of Ferro-cement.	Civil Engineering and Public Works Review (U.K.) v. 54:195-196, Feb.1959	x		x		x	x
63 63a	Collen, L.D.G. Trinity College, Dublin.	Some Experiments in Design and Construction with Ferro-cement.	Bulletin of the Institution of Civil Engineers of Ireland. v. 86:39-58, Jan. 1960	x	x	x	x	x	x
64	Vivian, H.E. C.S.I.R.O. Melbourne, Aust.	Some Chemical Additions and Admixtures in Cement Paste and Concrete.	Fourth International Symposium on the Chemistry of Cement, Wash. D.C., 1960 pp 909-926.	x				x	
65	Anon.	Ferro-cement Boats.	Portland Cement Association, 1969.	x				x	x
66	Samson, J. Samson Marine Design Enterprises Ltd., Vancouver, B.C.	Ferro-cement Boat Construction.	Proc. Conf. on Fishing Vessel Construction Material, Montreal, Oct. 1-3, 1968, pp 267-279.	x		x	x	x	
67	Fraser, D.J. Commercial Marine Services Ltd. Montreal.	Estimated Hull Work and Material Content for 100 ft Combination Fishing Vessel in Different Materials.	ibid, pp 305-321.	x	x	x	x	x	x
68	Hedges, L., and E. Perry, Naval Architects & Civil Engineers, N.S.W., Australia.	Ferro-cement Fishing Vessels.	ibid, pp 427-429	x	x				
69	Gardner, J., Editor, National Fisherman; F.G. Wolff, Marine Consultant, Bristol, Pa.	Consultant finds Ferro-cement has Limitations.	National Fisherman - 50, No. 10, Feb. 1970, pp 4-B, 15-B, 16-B.	x					x
70	Gardner, J., Editor, National Fisherman, R.W. Waddell and T.W. Beckett (Saga Technical Associates).	Need for Ferro-cement Background Stressed.	ibid, Mar. 1969, pp 4-B, 22-B	x					x
71	Daranandana, N., et al., Technological Research Group, Bangkok.	Ferro-cement for Construction of Fishing Vessels. Report No. 1.	Res. Proj. No. 21/14, Dept. of Fisheries, Ministry of Agriculture, Applied Scientific Research Corporation of Thailand.	x	x	x			x

TABLE 13. (cont'd)			Narrative	Tables	Dwgs. Figs.	Scale Dwgs.	Performance	Photographs	Costs
Author and Affiliation	Title	Journal and Citation							
72 Betts, J., President, International Amateur Boat Builders Society.	Ferro cement: Promise or Put-on?	Amateur Boat Building, Van. 1968 pp 20, 31.	x						
73 Spratt, G.W.	Research and Development in Ferro-cement Usage.	Mimeo, Mar. 1969.	x						
74 Collins, J.F., and J.F. Claman, U.S. Navy.	Ferro-cement for Marine Application - An Engineering Evaluation.	Paper prepared for presentation before the New England Section of the Society of Naval Architects and Marine Engineers, M.I.T., March 1969, 66 pp. 21 refs.	x	x	x		x	x	x
75 Shah, S.P., University of Illinois, Chicago, U.S.A.	Ferro Cement as a New Engineering Material.	Paper prepared for presentation before the Annual Convention of the Canadian Capital Section of American Concrete Institute, Ottawa, Dec. 1970, 37 pp, 9 refs.	x	x	x		x	x	
76 Masubuchi, K.	Chap. 9 Concrete (includes Ferro-Cement in Marine Engineering)	Materials for Ocean Engineering, Book, First Edit. The M.I.T. Press, Massachusetts Institute of Technology, Cambridge, Mass. Feb. 1970 pp 205-219.	x	x	x		x		
77 Benford, J.R. and H. Husen (Jay R. Benford & Associates, Inc., Friday Harbor, Washington, U.S.A.) (in B.C. Research library)	Practical Ferro-Cement Boatbuilding.	Book, published by J.R. Benford, Box 456, Friday Harbor, Wash., U.S.A. 1970. \$10.00	x	x	x	x		x	x

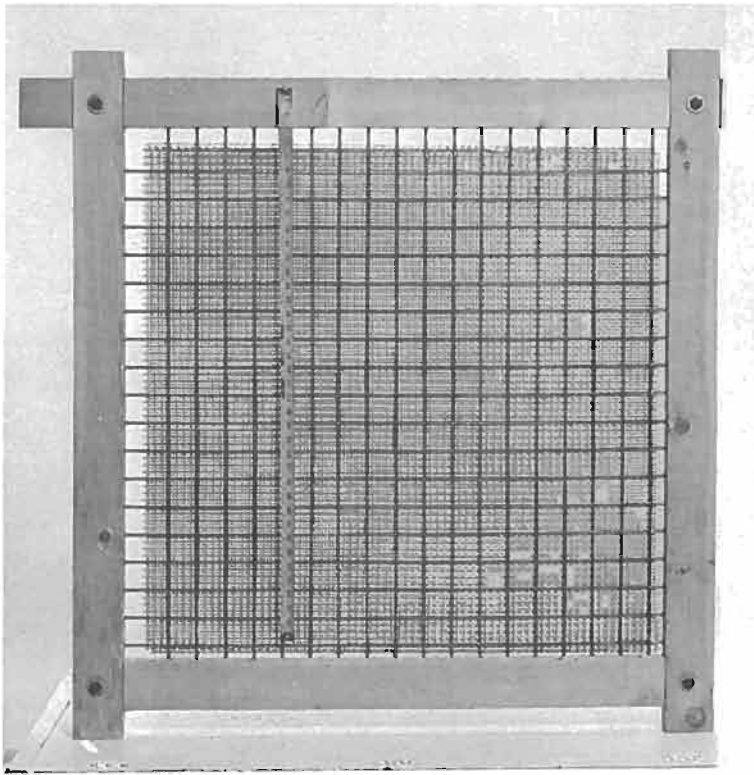


Fig. 1 Frame holding 1/4-inch rods and mesh for 36-inch panels plastered from both sides.

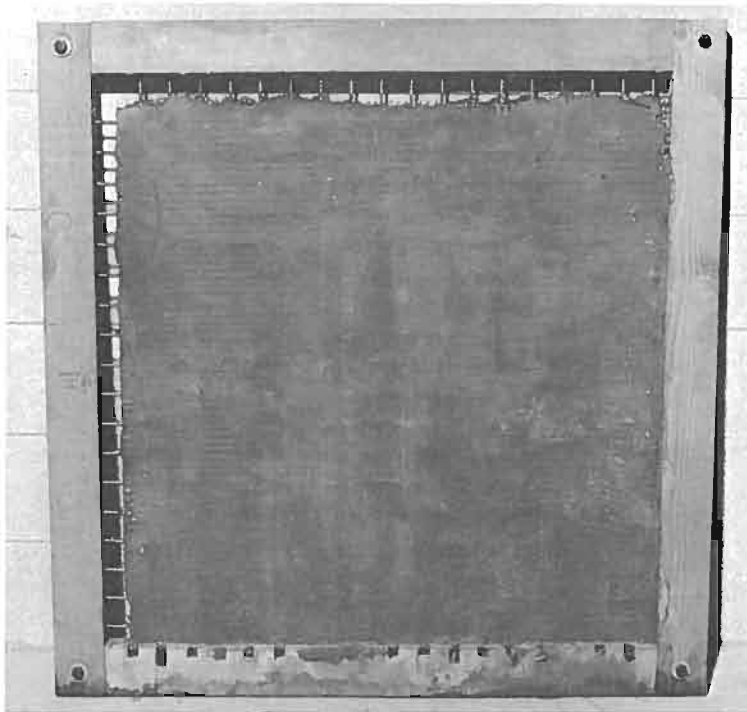


Fig. 2 Plastered 36-inch panel.

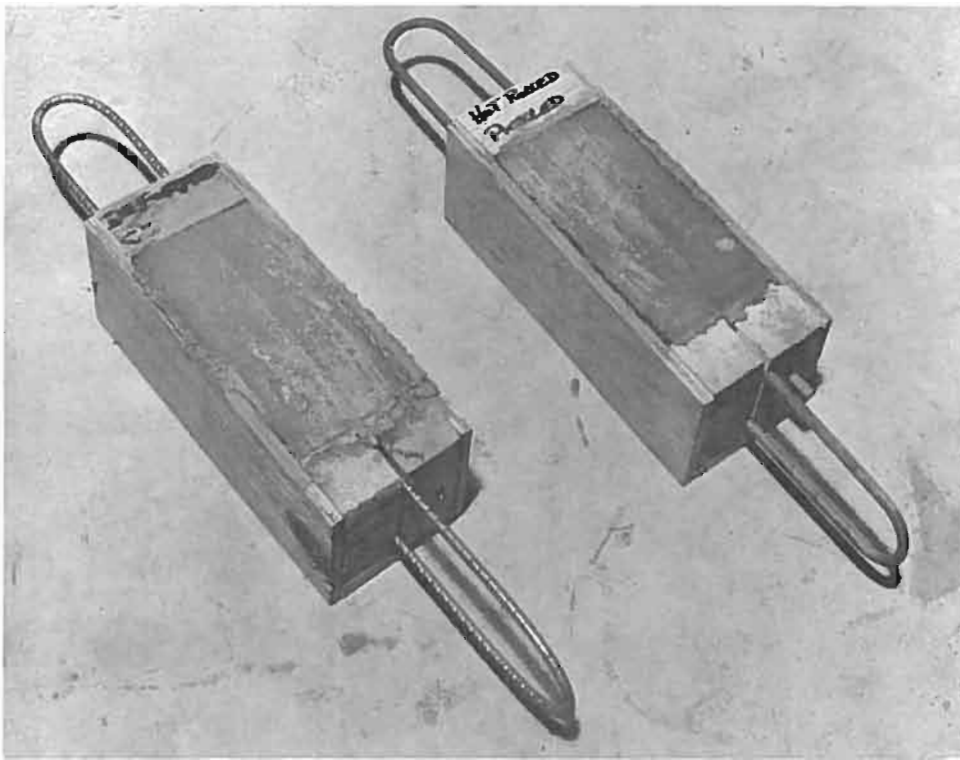


Fig. 3 Hair-pin specimens for rod/mortar bond tests.

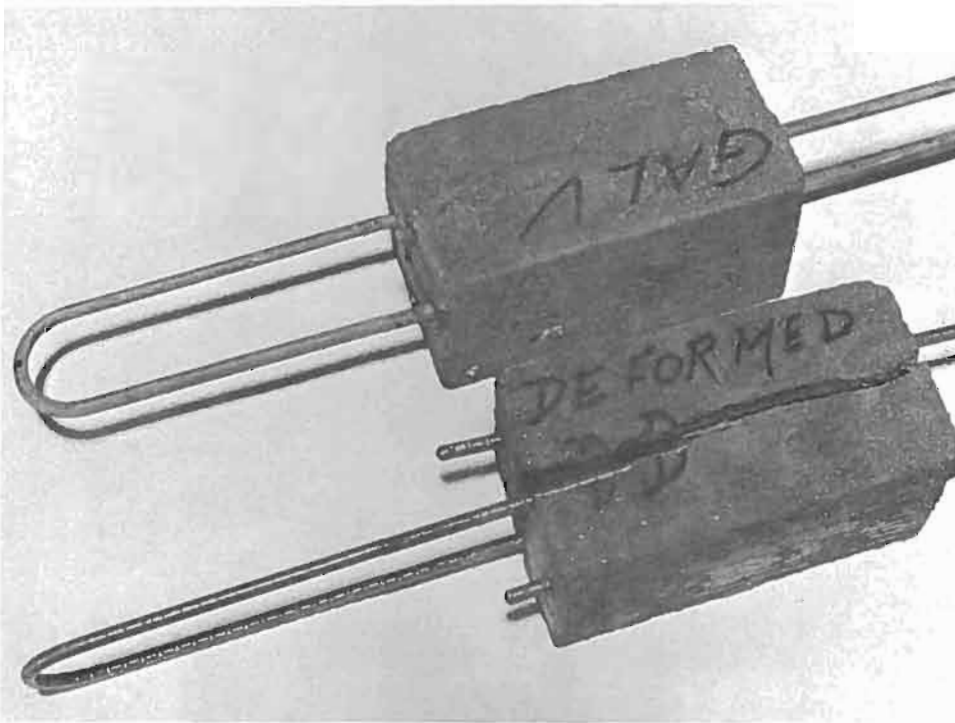


Fig. 4 Rod/mortar bond tests showing splitting of mortar block by deformed double-drawn rod.

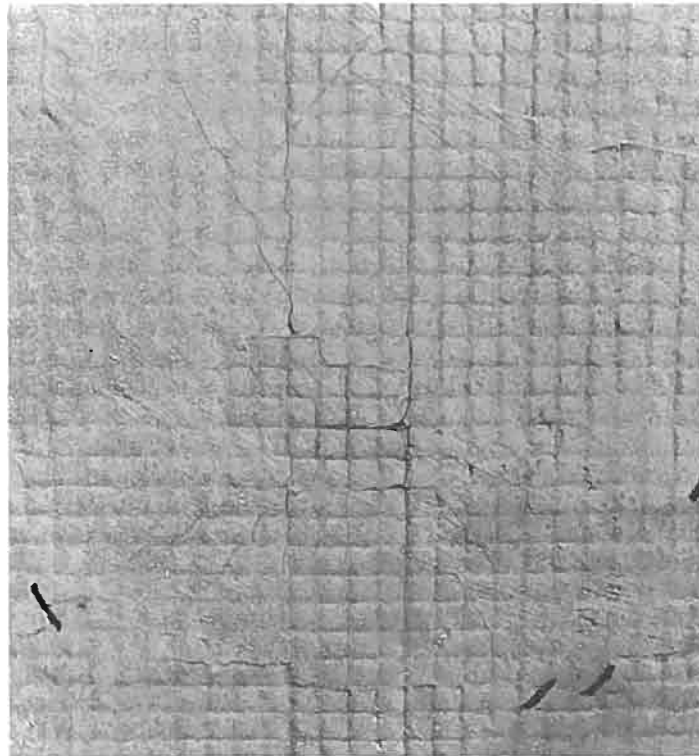
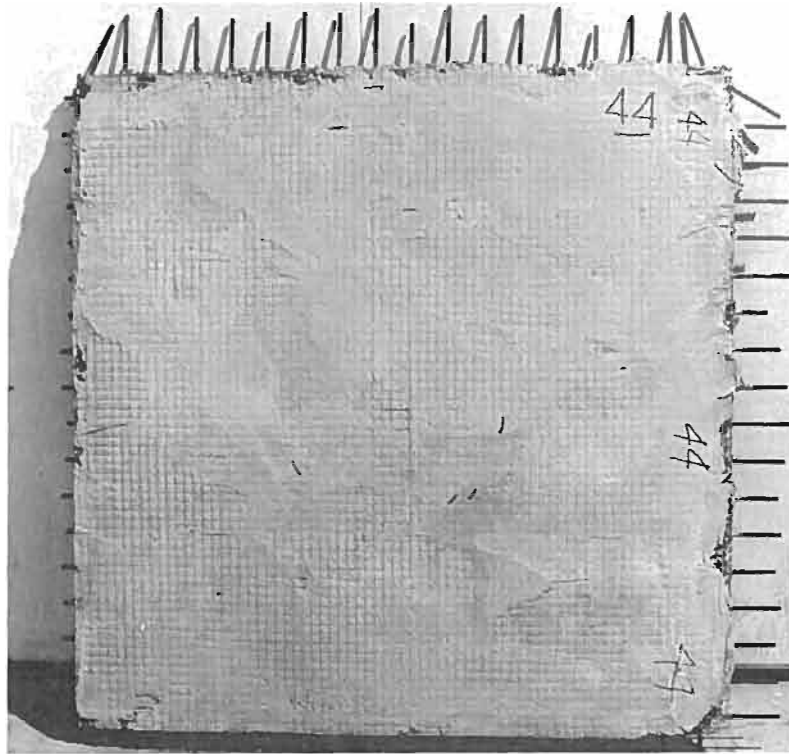


Fig. 5 (a) and (b). Bottom side of panel 44 after drop-impact test. (3 + 2 layers 1/2-19 ga. hardware cloth, double-drawn rods at 2 in.) (Compare with Fig. 6 and 7 and with Fig. 8).

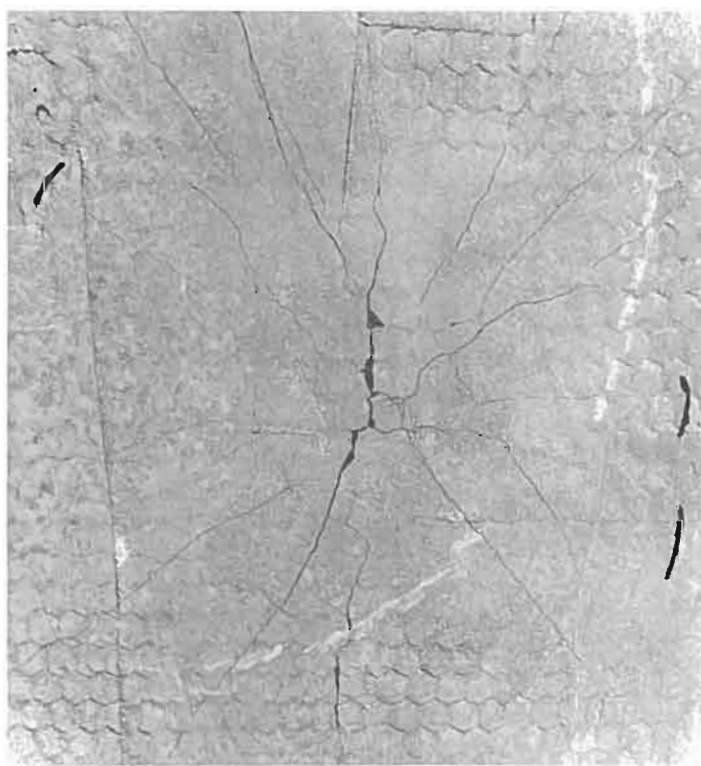
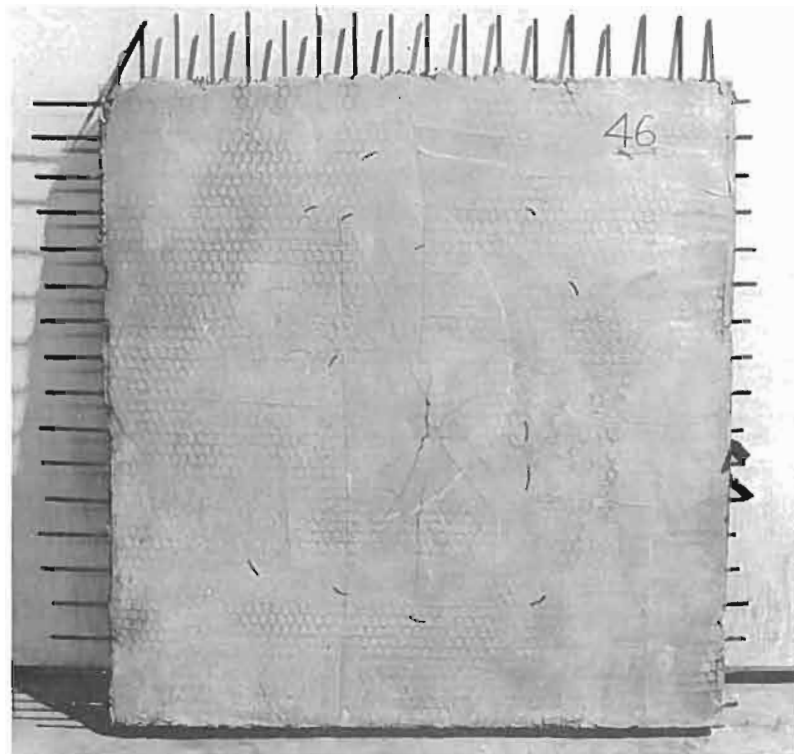


Fig. 6 (a) and (b). Bottom side of panel 46 after drop-impact test. (5 + 5 layers 1/2-ga. hexagonal mesh, double-drawn rods at 2 in.) (Compare with Fig. 5 and 7).

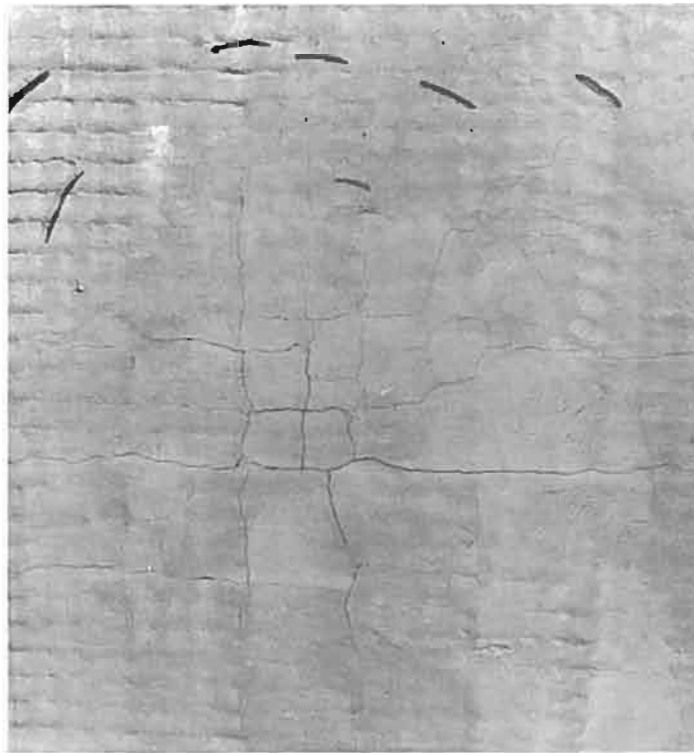
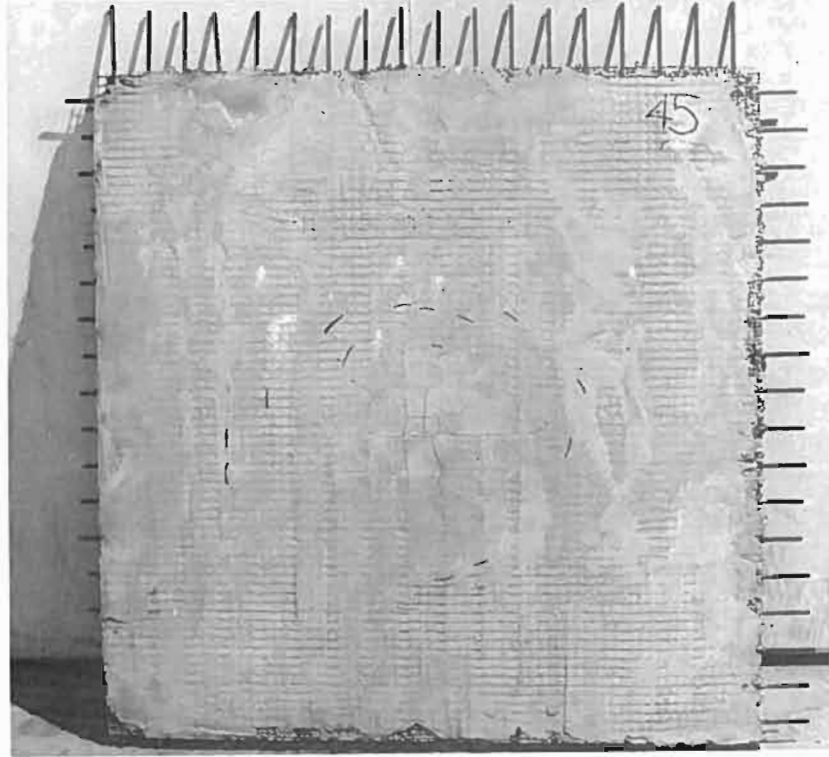


Fig. 7 (a) and (b). Bottom side of panel 45 after drop-impact test. (1 + 1 layers 1/2-16 ga. welded square mesh, double-drawn rods at 2 in.) (Compare with Fig. 5 and 6)

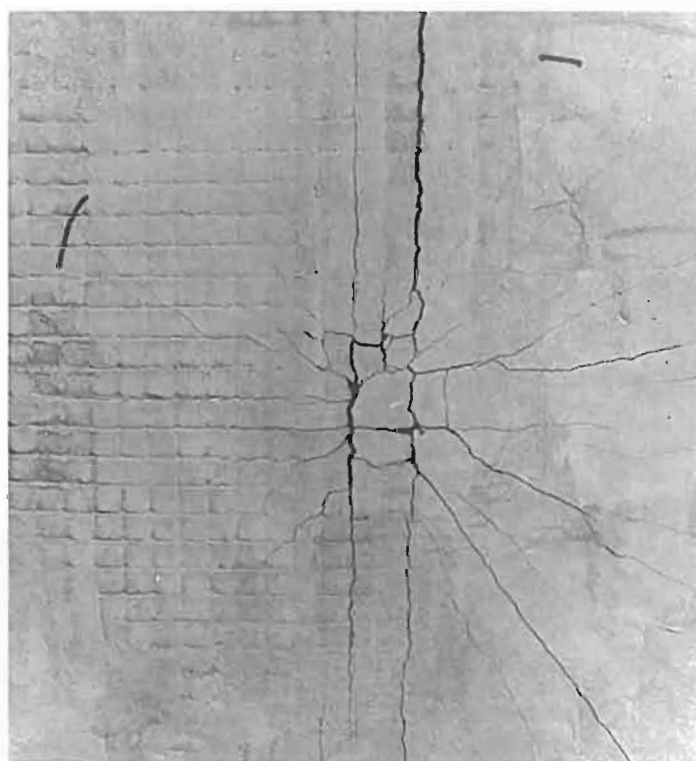
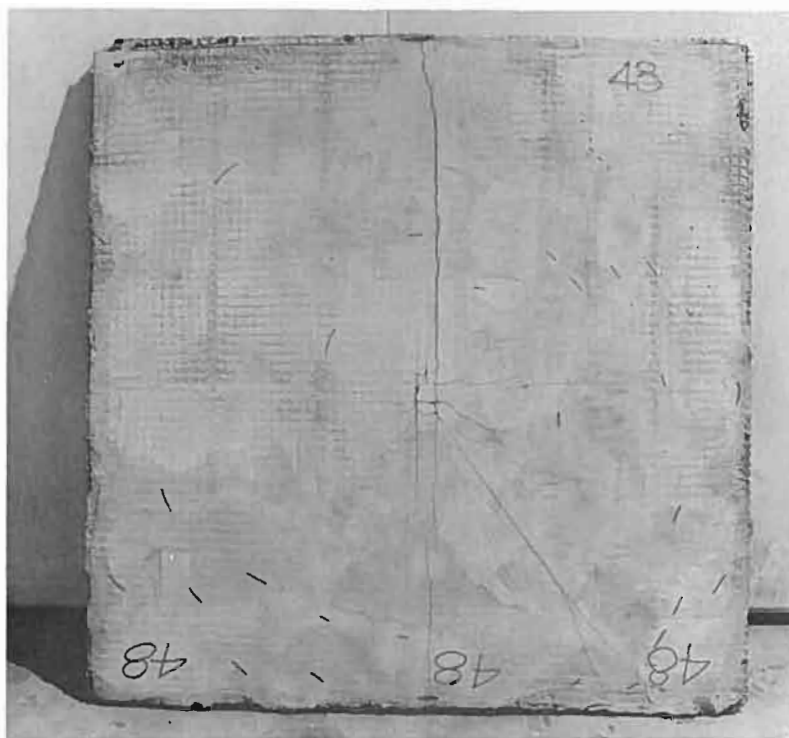


Fig. 8 (a) and (b). Bottom side of panel 48 after drop-impact test. (1 + 1 layers 1/2-16 ga. welded square mesh, no reinforcing rods)
(Compare with Fig. 5)

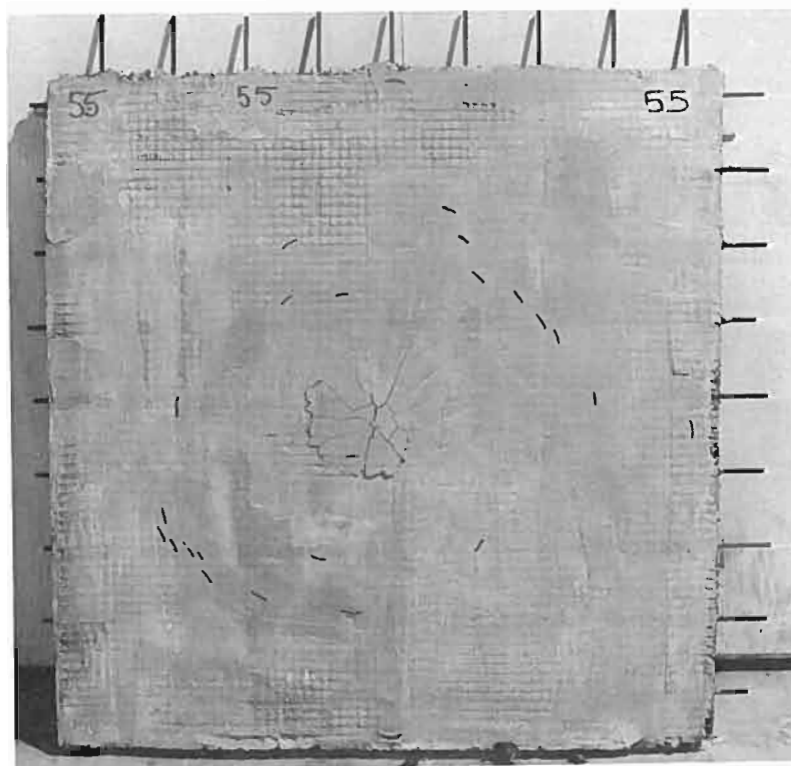


Fig. 9 (a) and (b). Bottom side of panel 55 after drop-impact test. (3 + 2 layers 1/2-ga. hardware cloth, deformed double-drawn rods at 4 in.) (Compare with Fig. 5)

69-4125

Fig. 10 to 27.

Effect of various parameters on load-deflection curves (load-carrying capacity) of flexure test specimens cut from panels of various constructions.

Flexure specimens - length 24 in.
- width 12 in.
- thickness 1 in. nom.

Span length - 21 in.
Loading - third point

69-4125

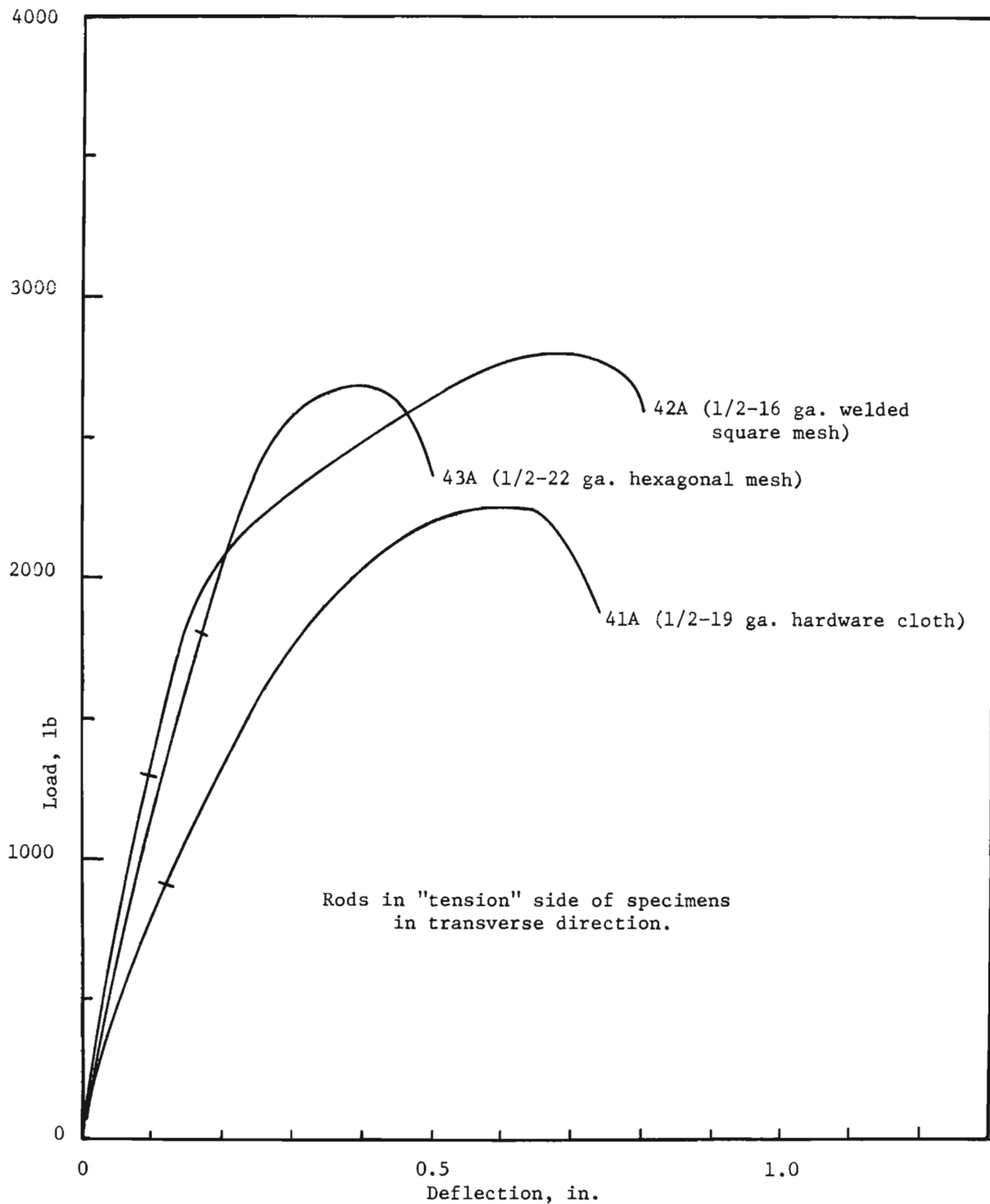


Fig. 10. Effect of mesh reinforcement on flexural strength.

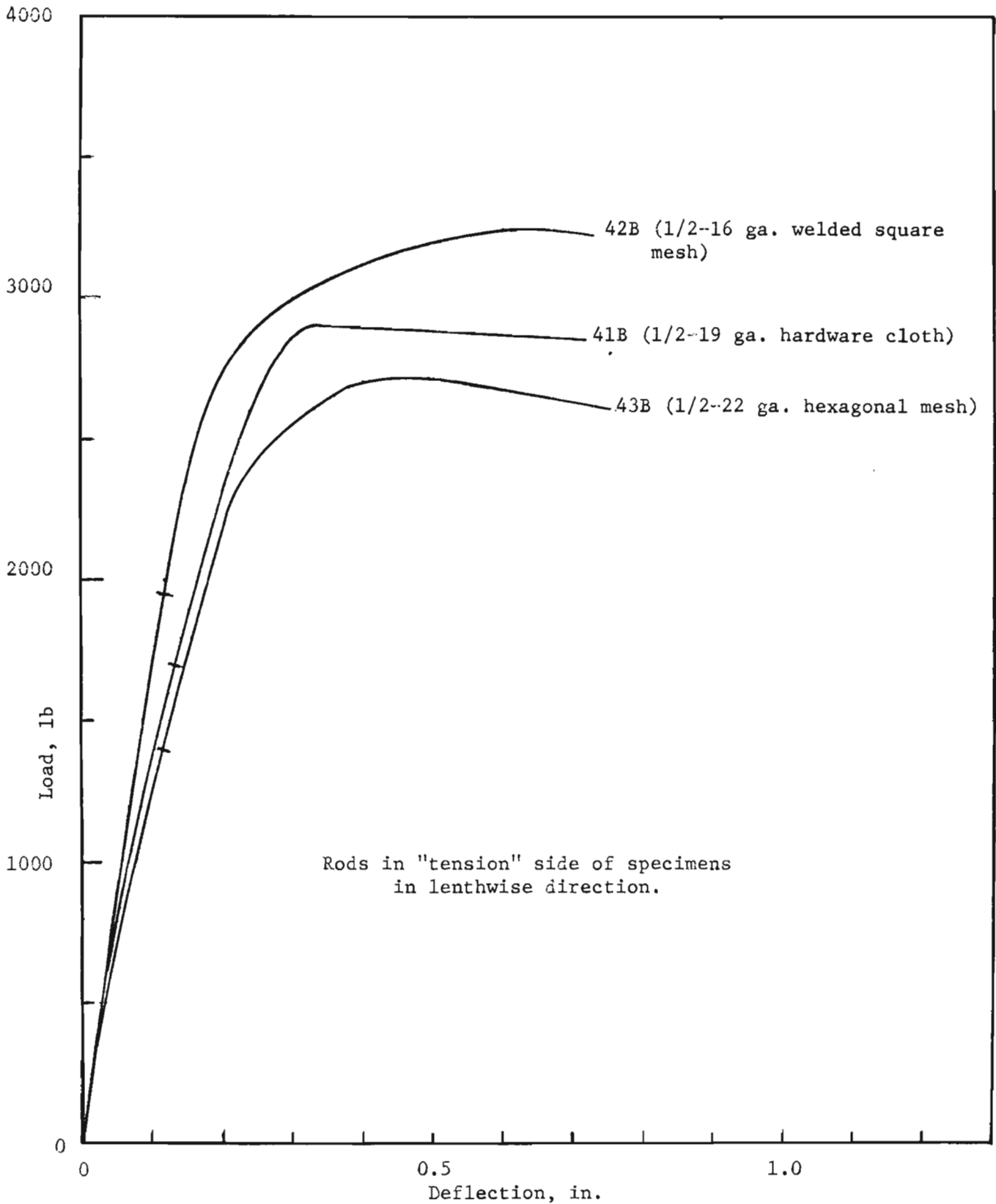


Fig. 11. Effect of mesh reinforcement in flexural strength.

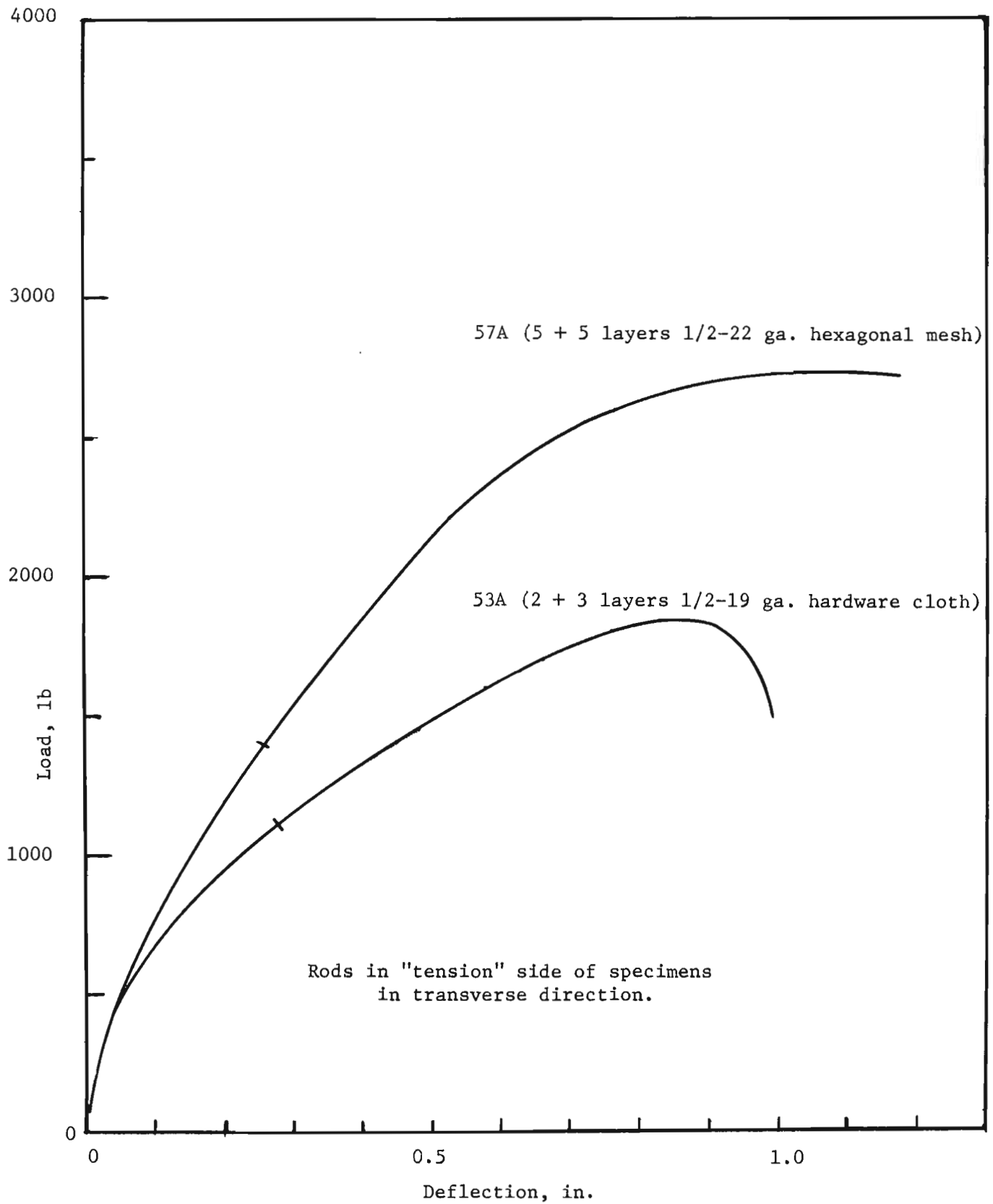


Fig. 12. Effect of mesh reinforcement on flexural strength.

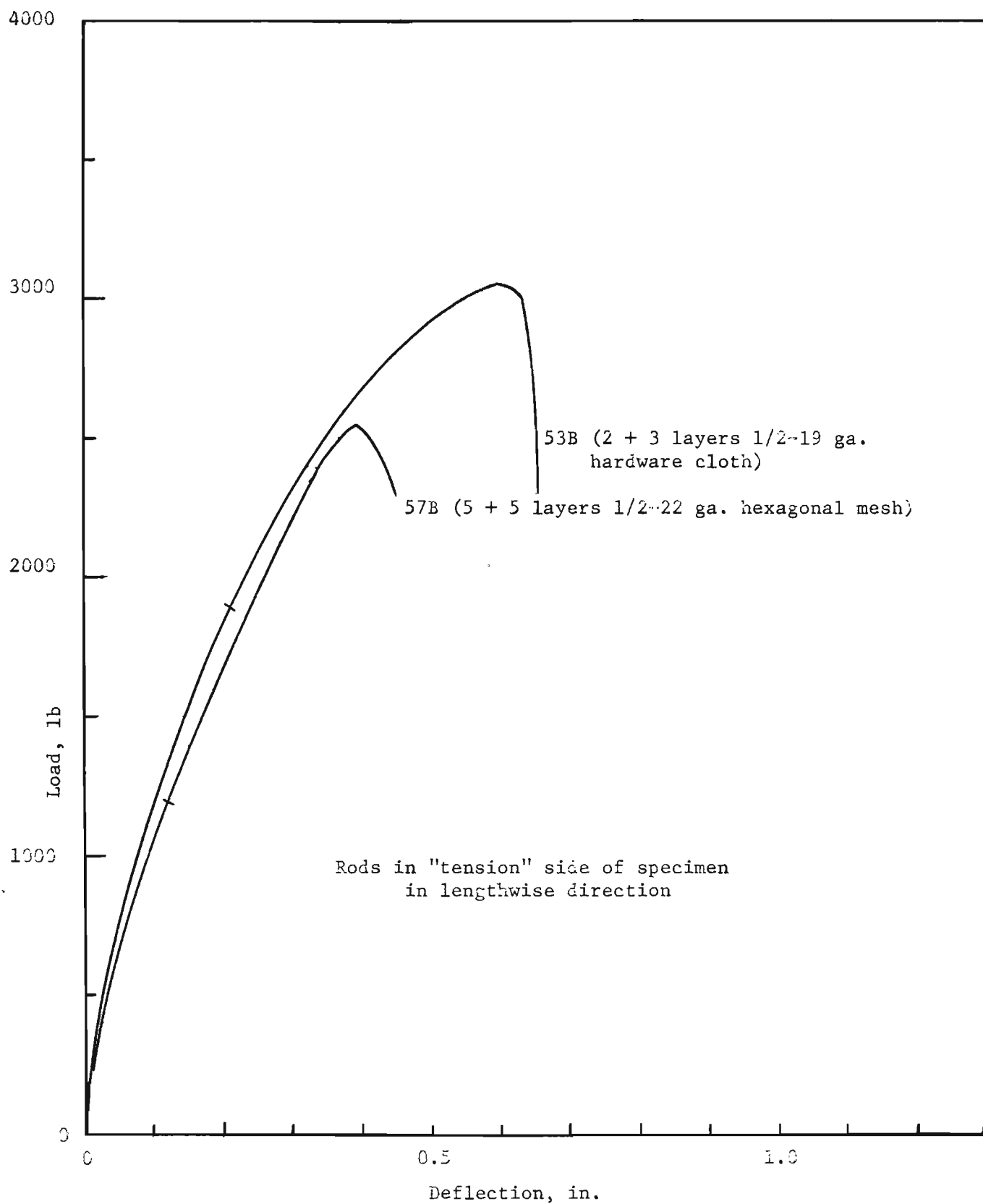


Fig. 13. Effect of mesh reinforcement on flexural strength.

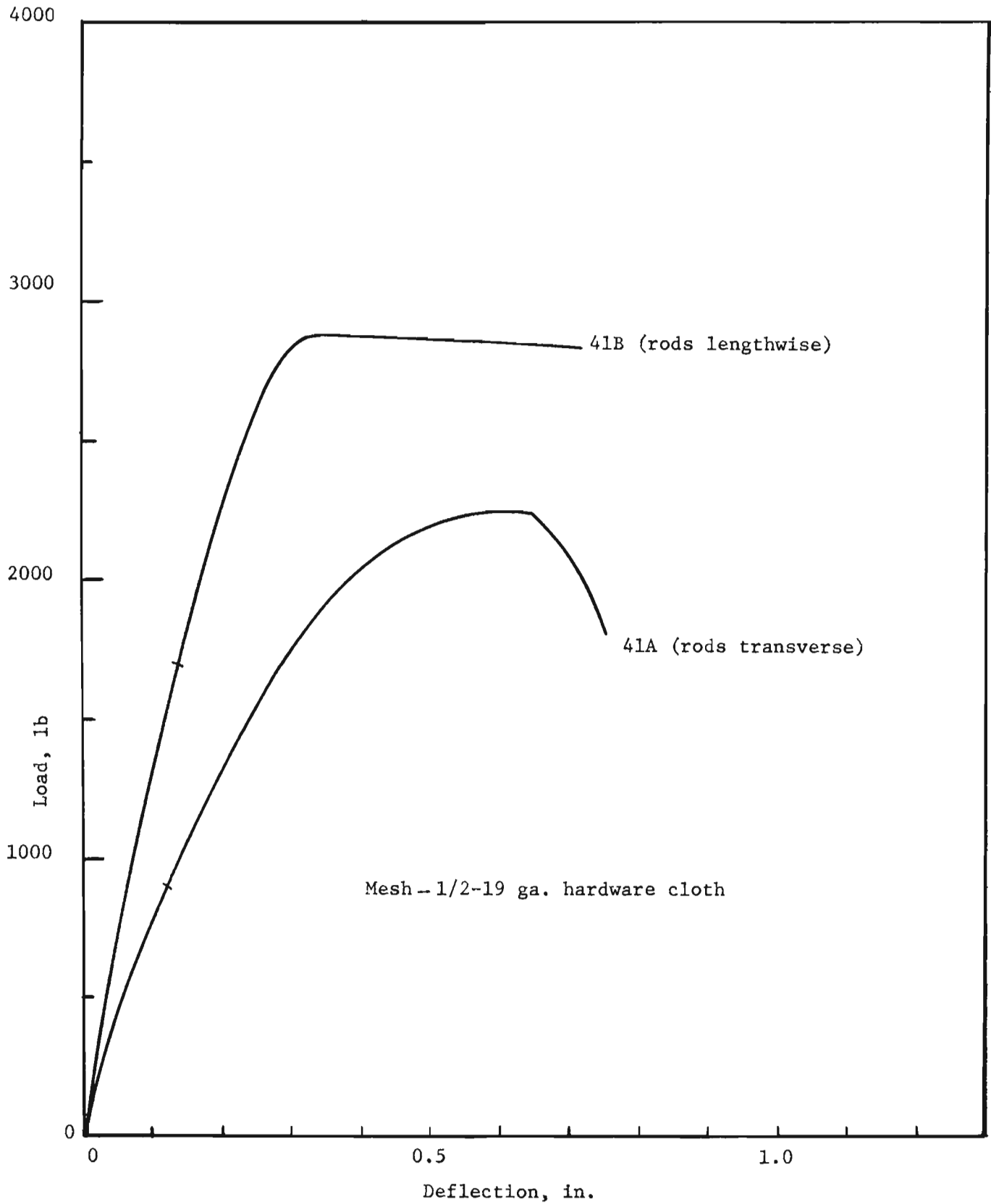


Fig. 14. Effect of orientation of "tension-side" rods on flexural strength.

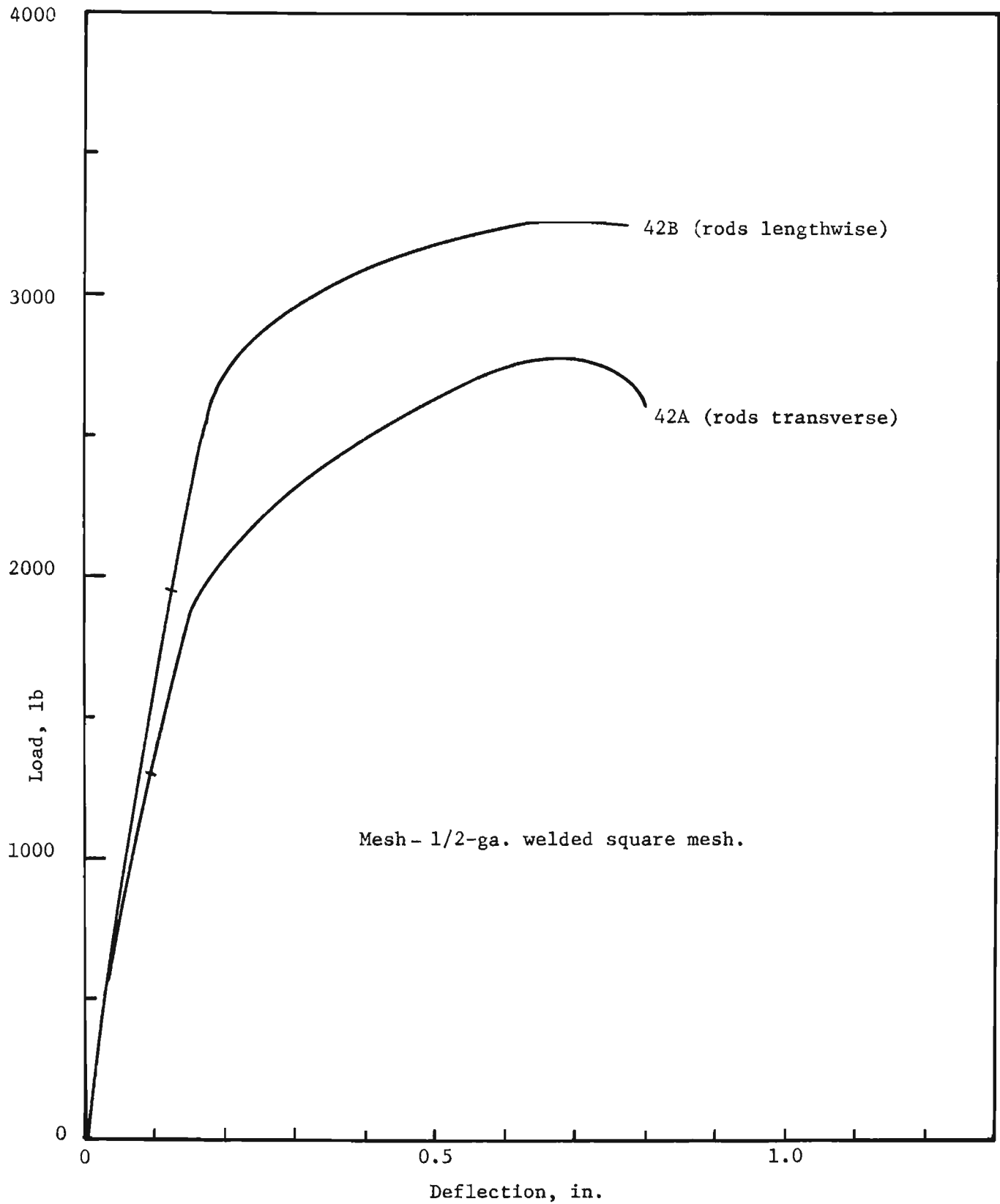


Fig. 15. Effect of orientation of "tension-side" rods on flexural strength.

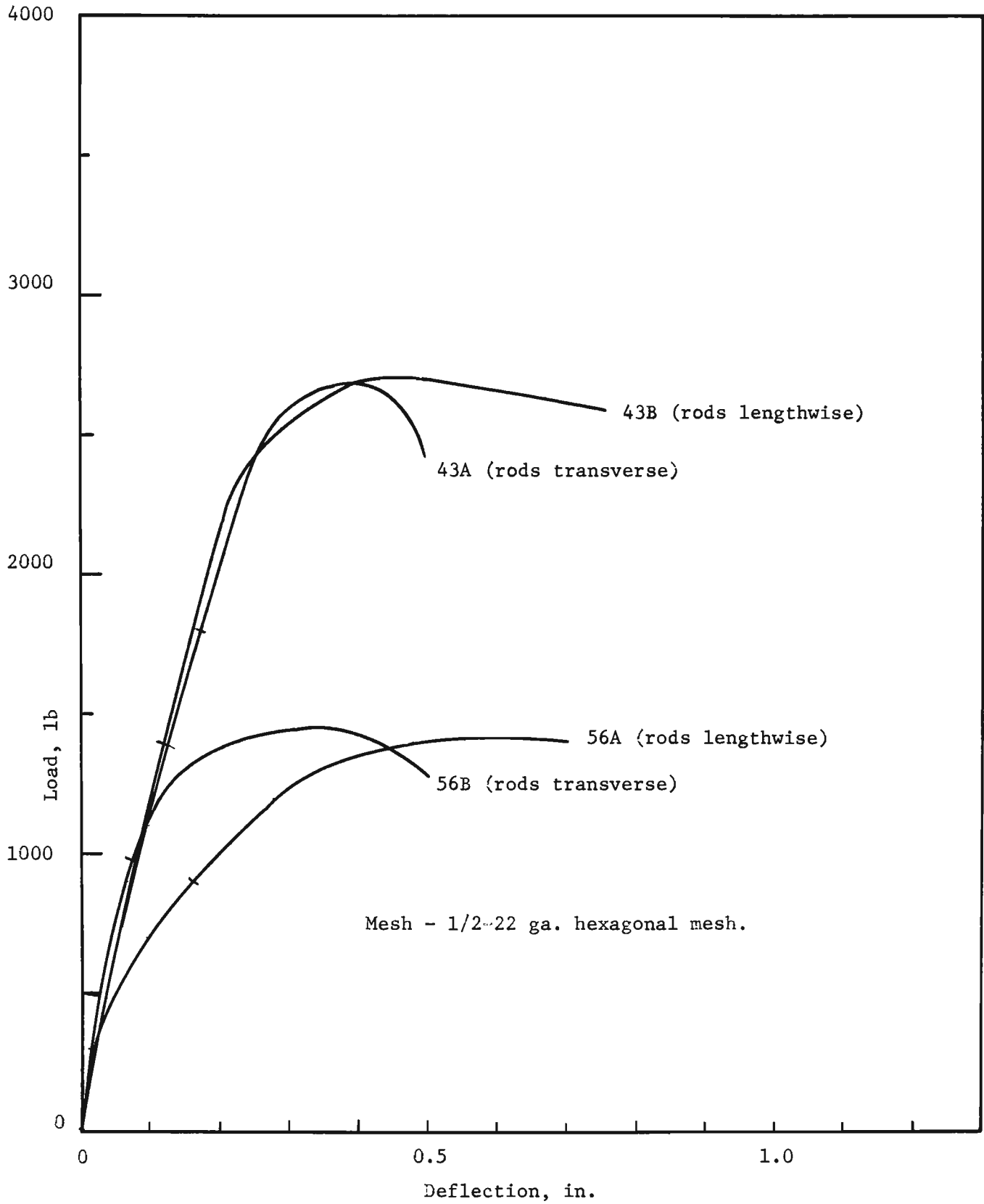


Fig. 16. Effect of orientation of "tension-side" rods on flexural strength.

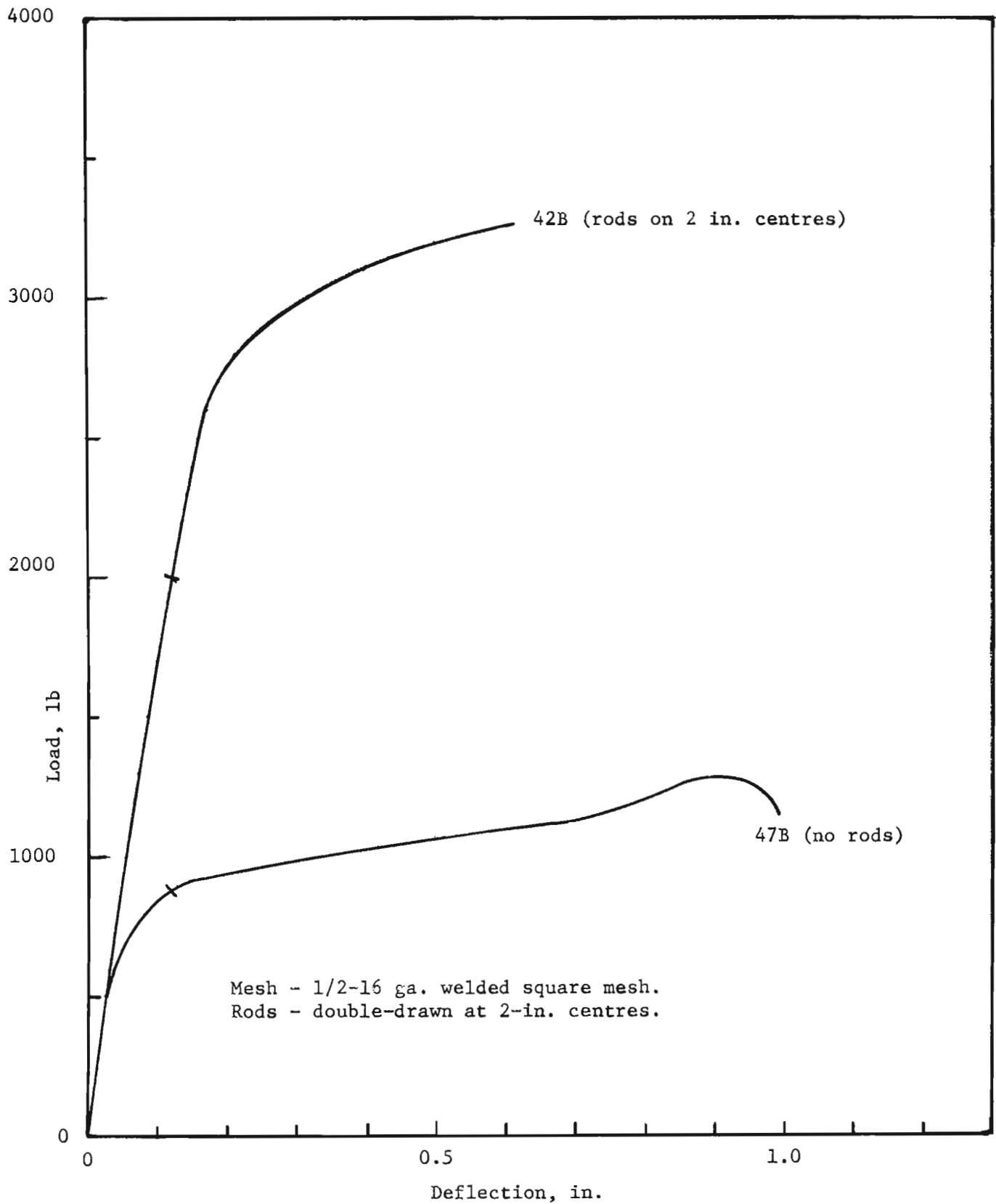


Fig. 17. Effect of rods on flexural strength.

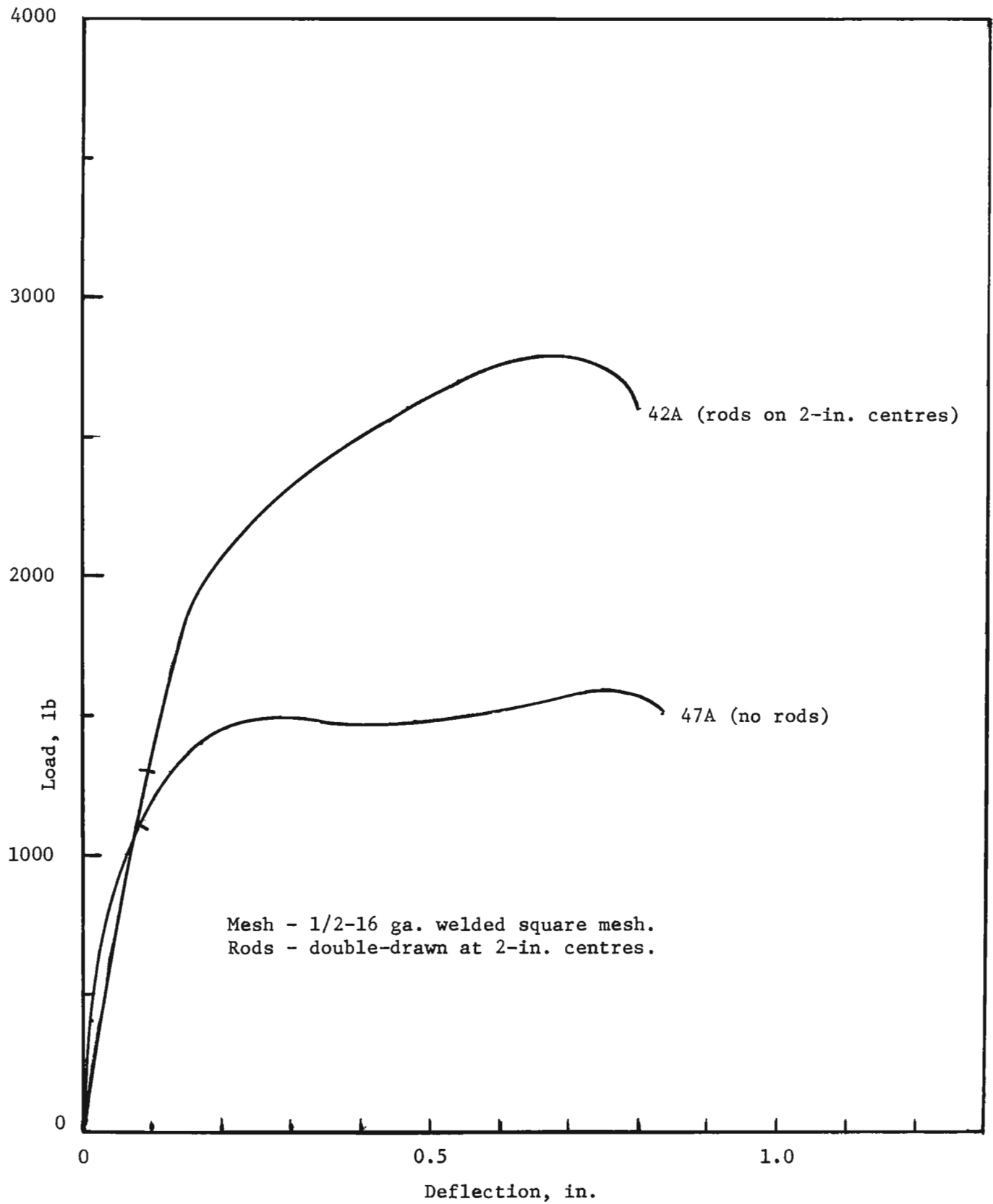


Fig. 18. Effect of rods on flexural strength.

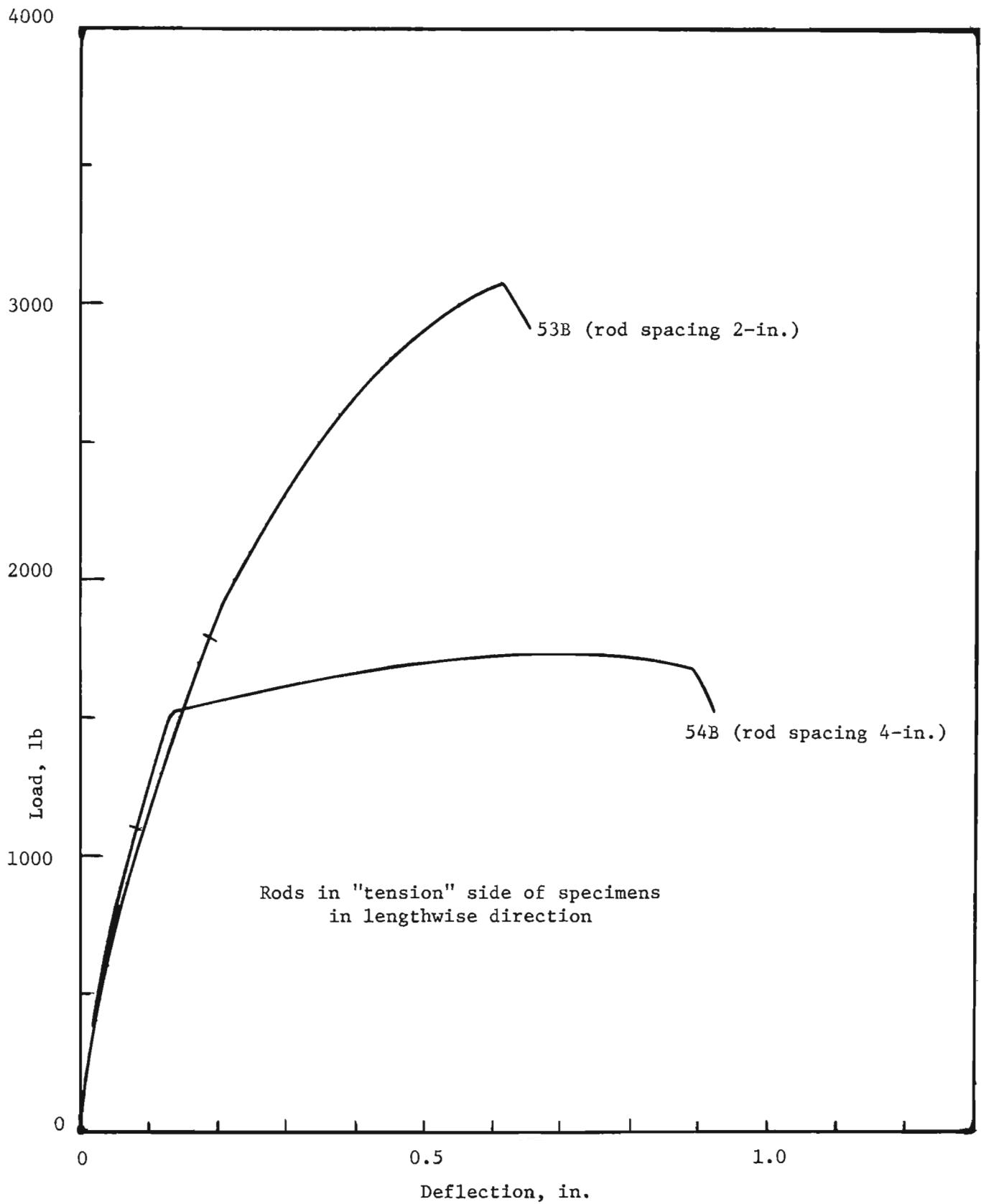


Fig. 19. Effect of rod spacing on flexural strength.

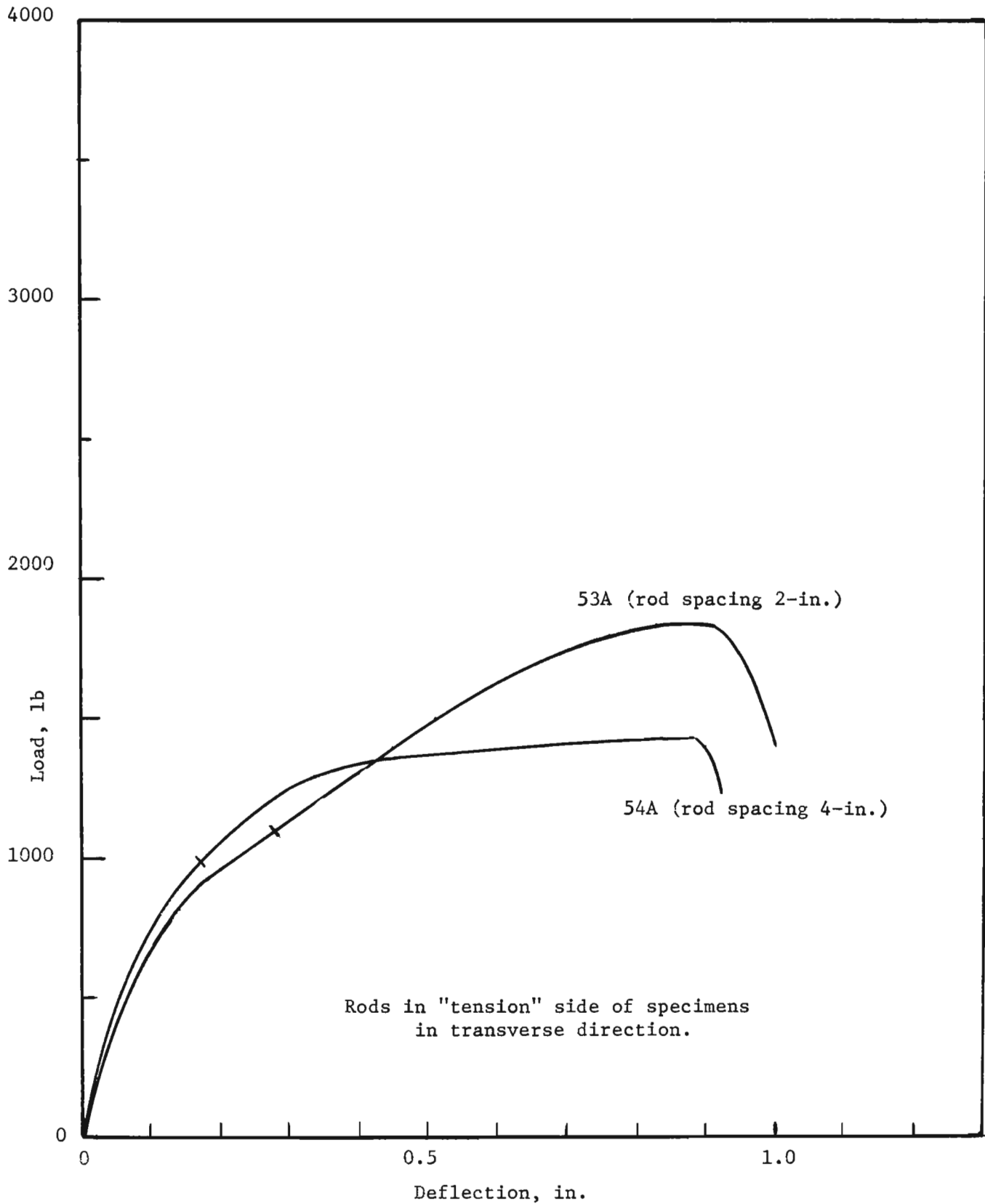


Fig. 20. Effect of rod spacing on flexural strength.

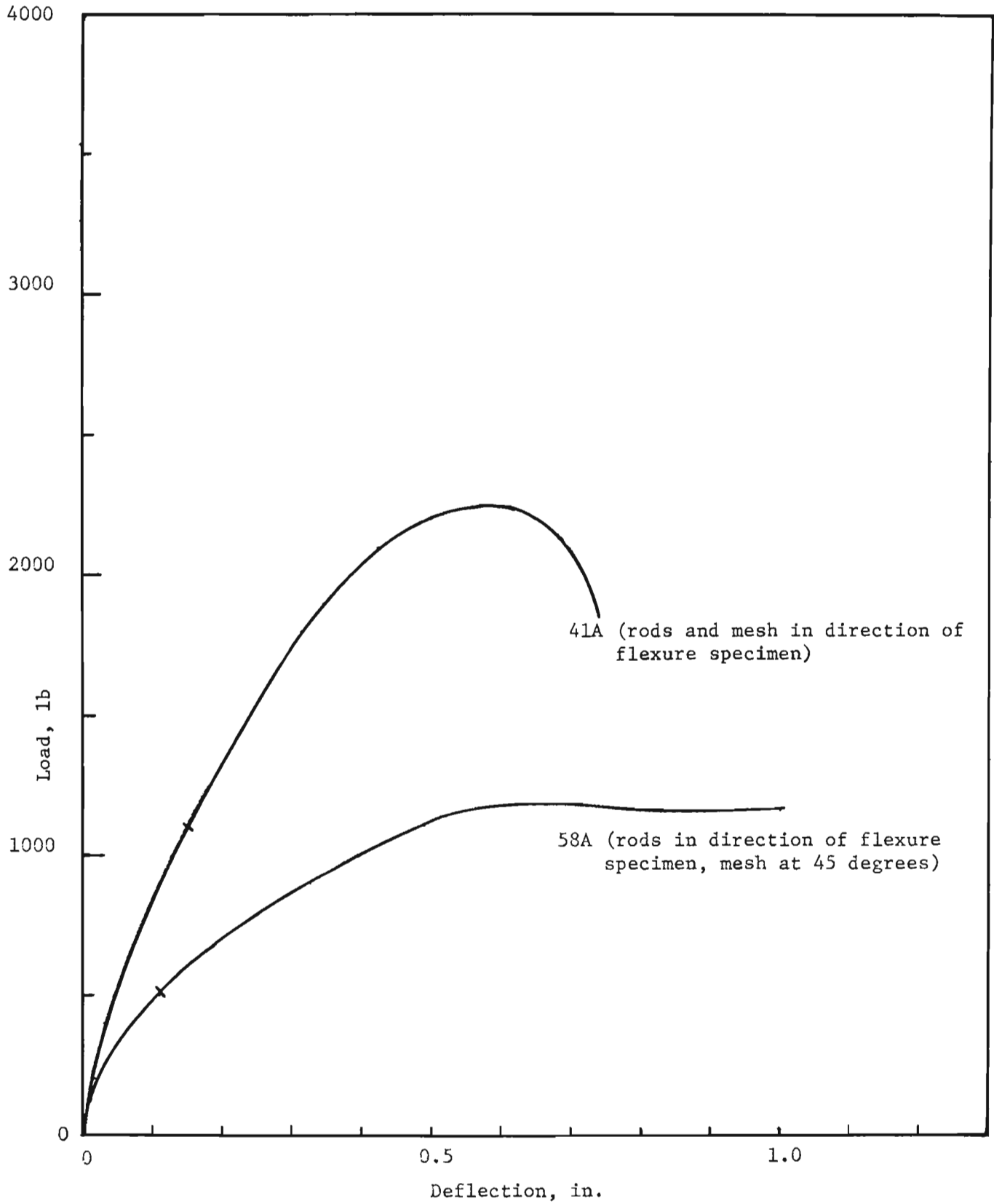


Fig. 21. Effect of mesh orientation on flexural strength.

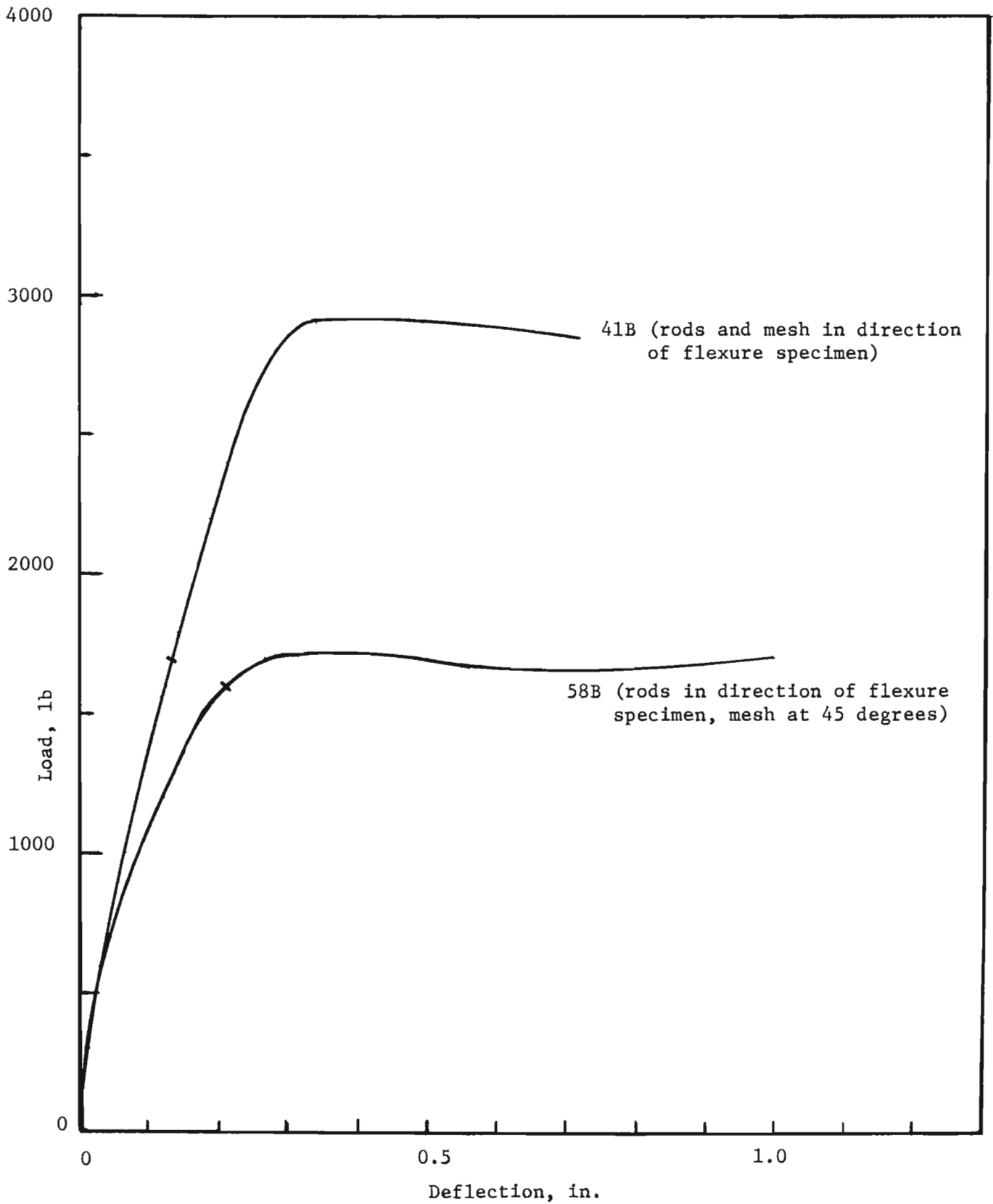


Fig. 22. Effect of mesh orientation on flexural strength.

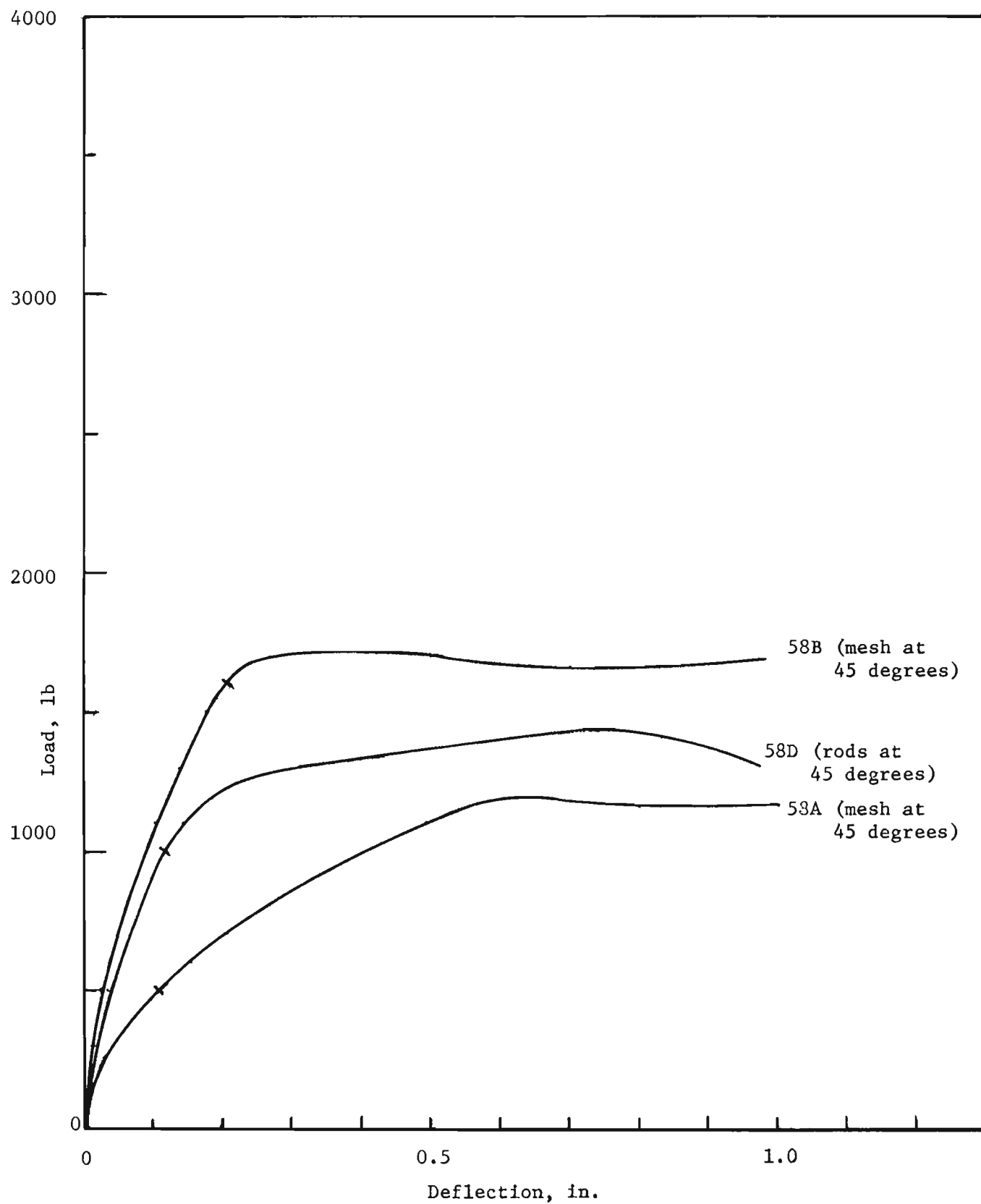


Fig. 23. Effect of rod and mesh orientation on flexural strength.

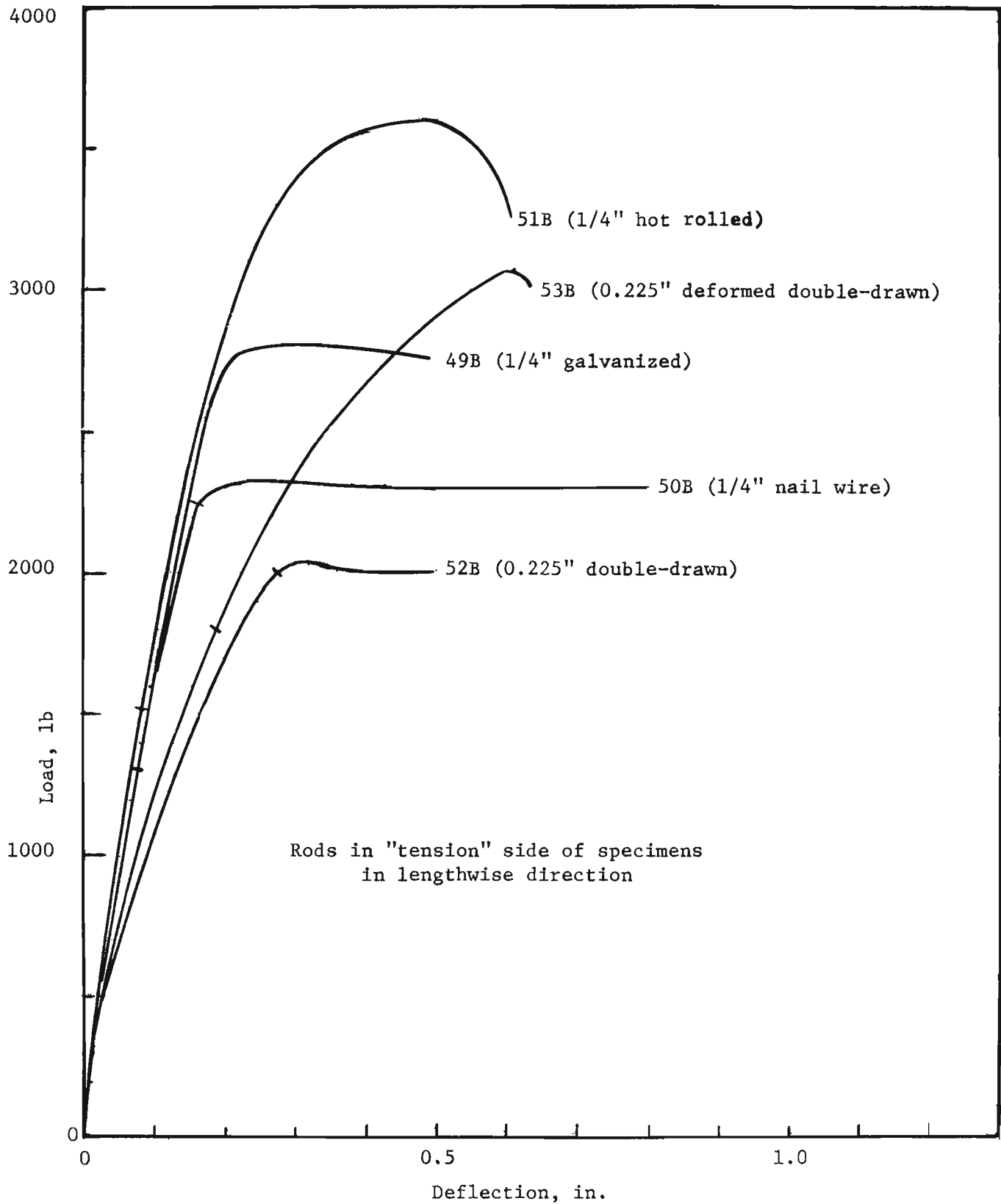


Fig. 25. Effect of type of rod reinforcement on flexural strength.

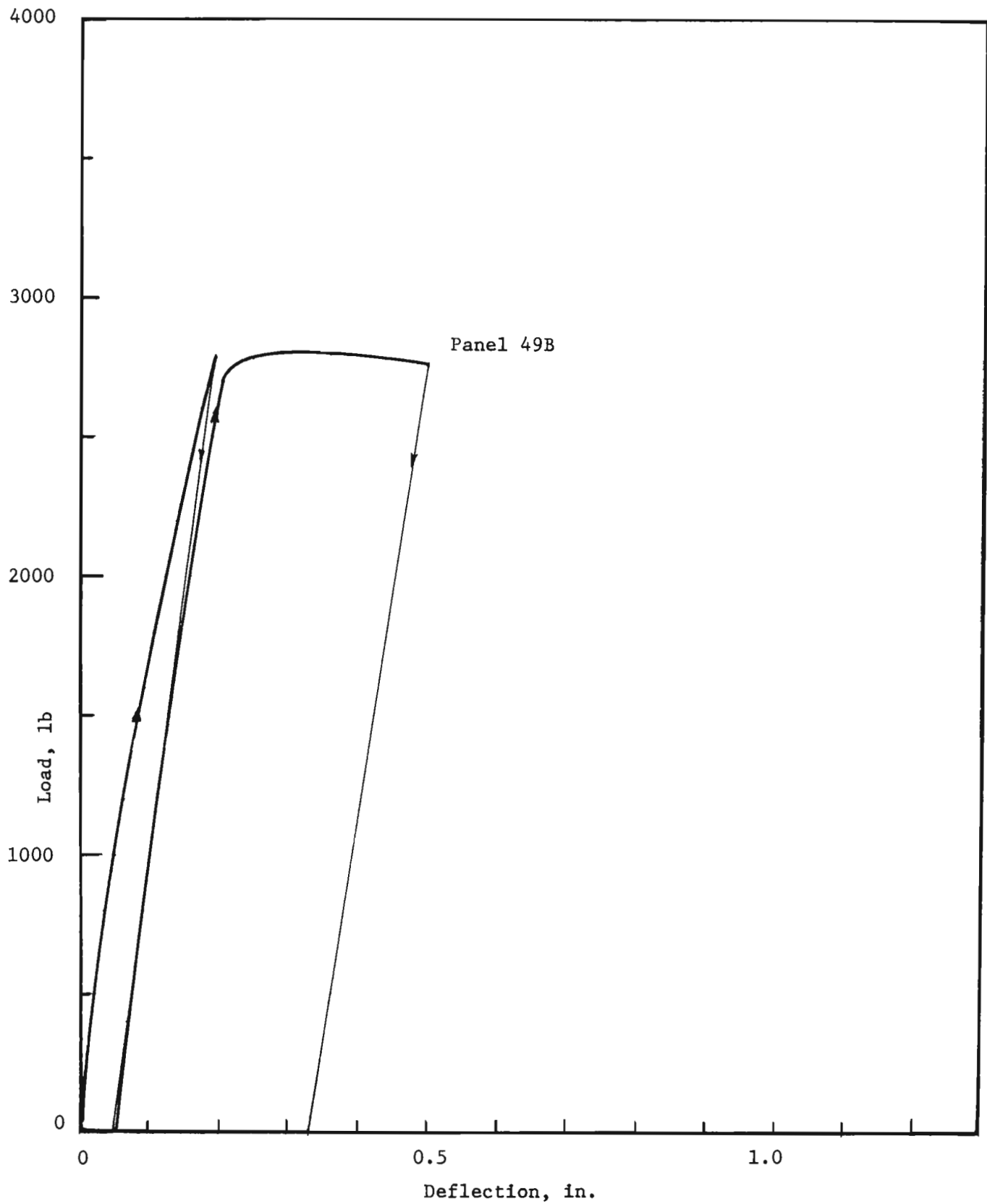


Fig. 26. Effect of unloading flexural test specimen after indication that maximum load attained and reloading.

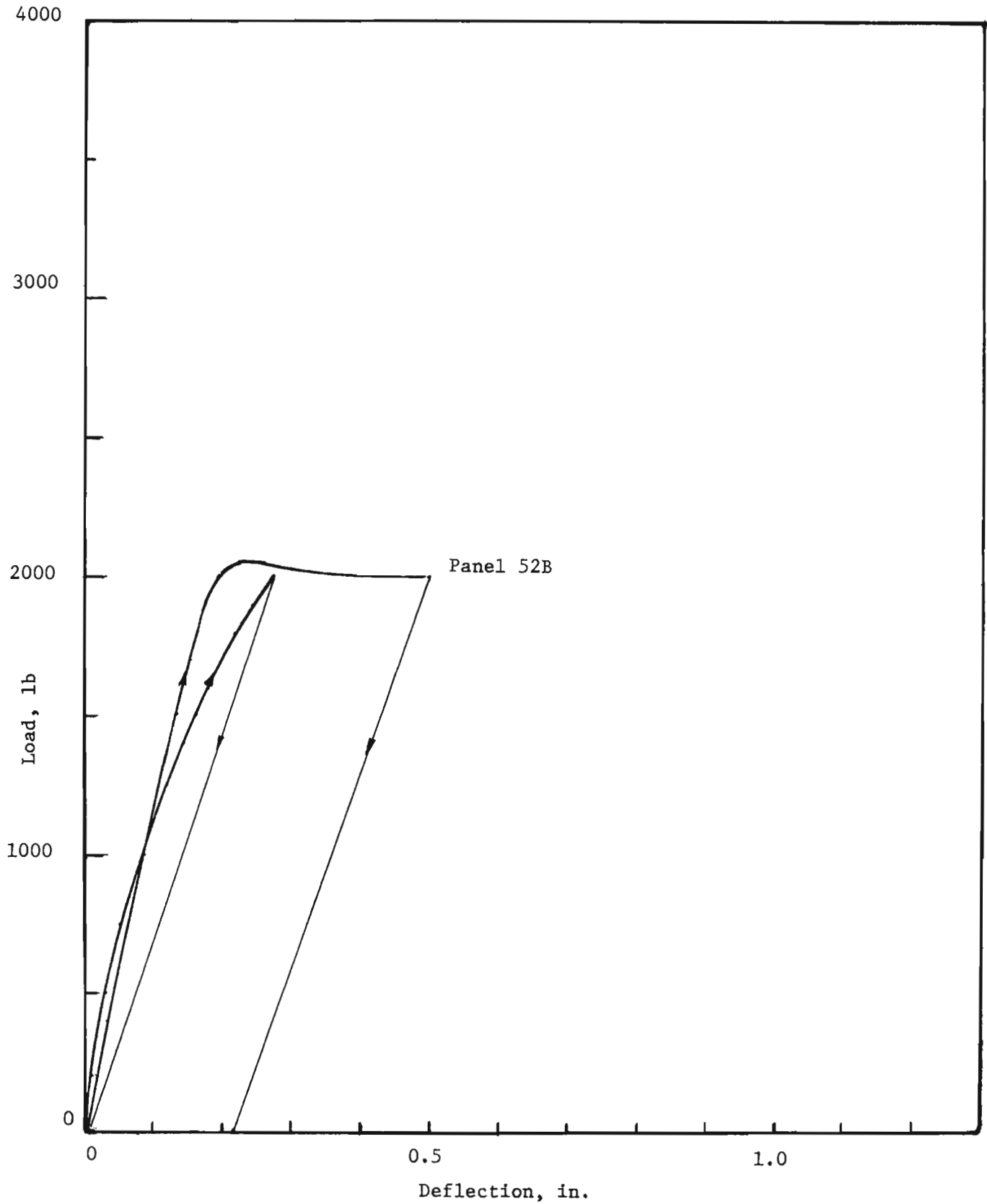


Fig. 27. Effect of unloading flexural test specimen at 2000 lb level and reloading.



Fig. 28. Breakdown of unreinforced coupons after 350 freeze-thaw cycles.

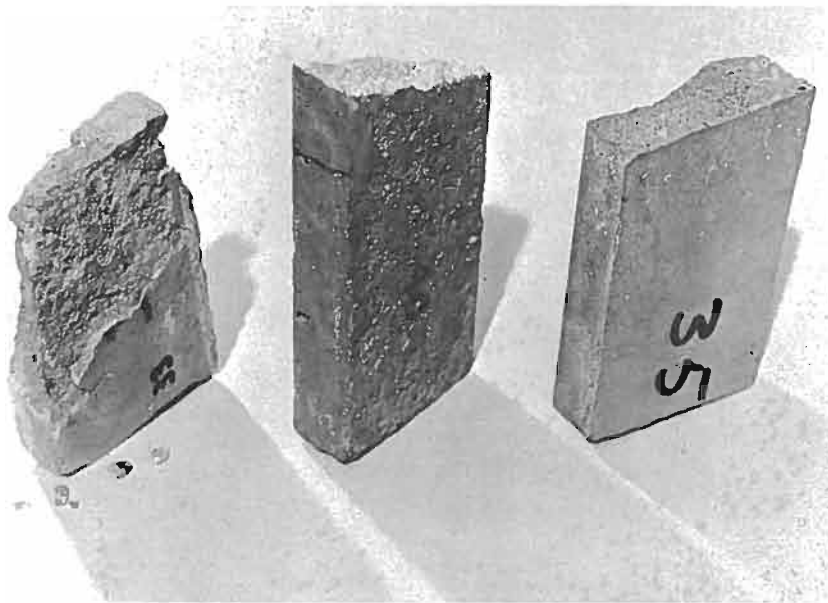


Fig. 29. Breakdown of unreinforced coupons from panels 33, 40, and 35 after 350 freeze-thaw cycles.

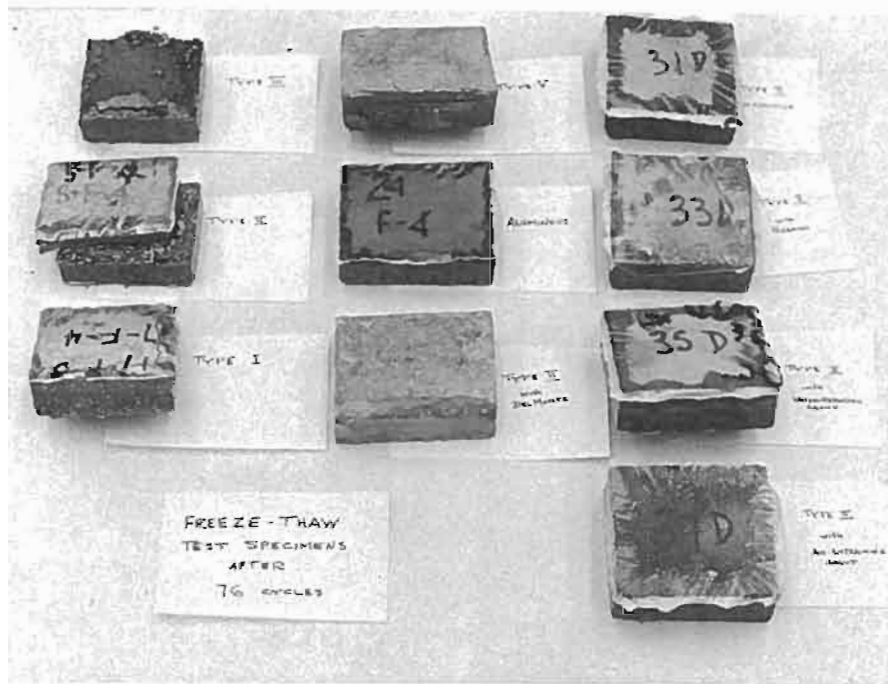


Fig. 30. Mesh-reinforced specimens after 76 freeze-thaw cycles.

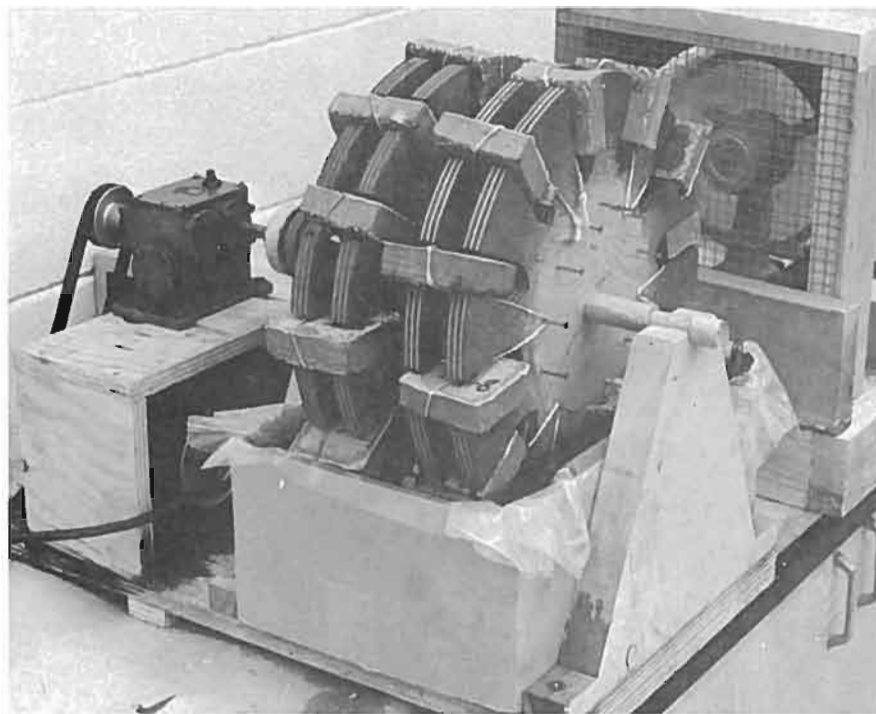


Fig. 31. Seawater exposure tests.

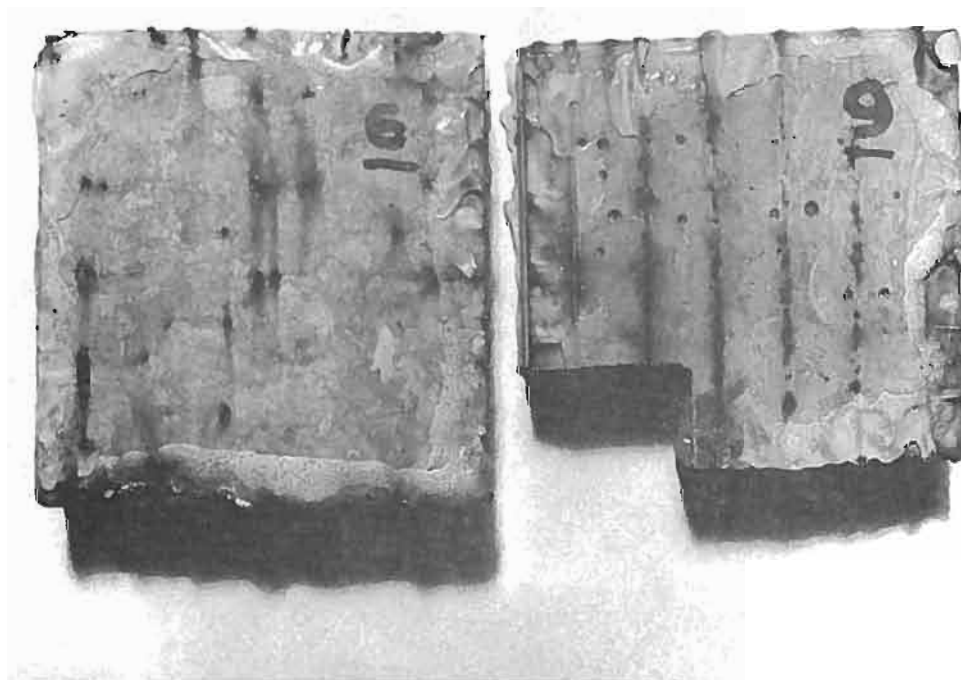


Fig. 32. Rust staining on bottom surface of coupons containing (a) 1/2-22 ga. hexagonal mesh with light zinc coating and (b) 1/2-ga. welded square mesh with zinc coating removed.

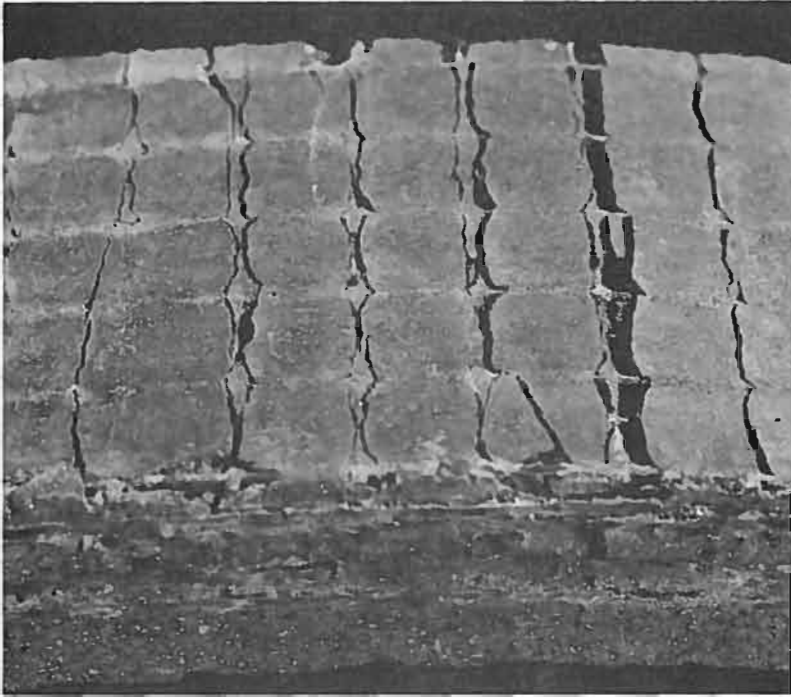


Fig. 33. Cracked coupon containing galvanized wire mesh after 48 hours immersion in seawater.

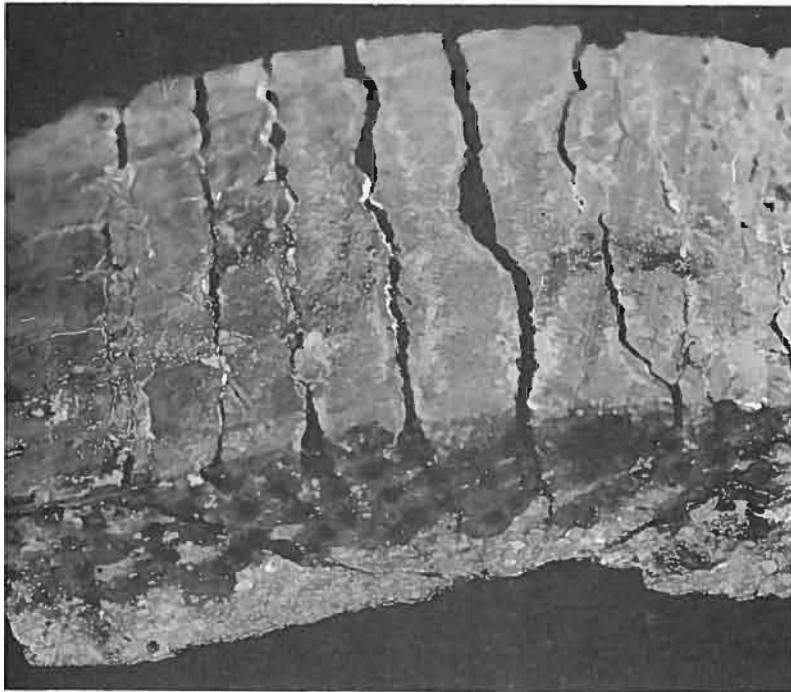


Fig. 34. Cracked coupon containing ungalvanized wire mesh after 48 hours immersion in seawater.

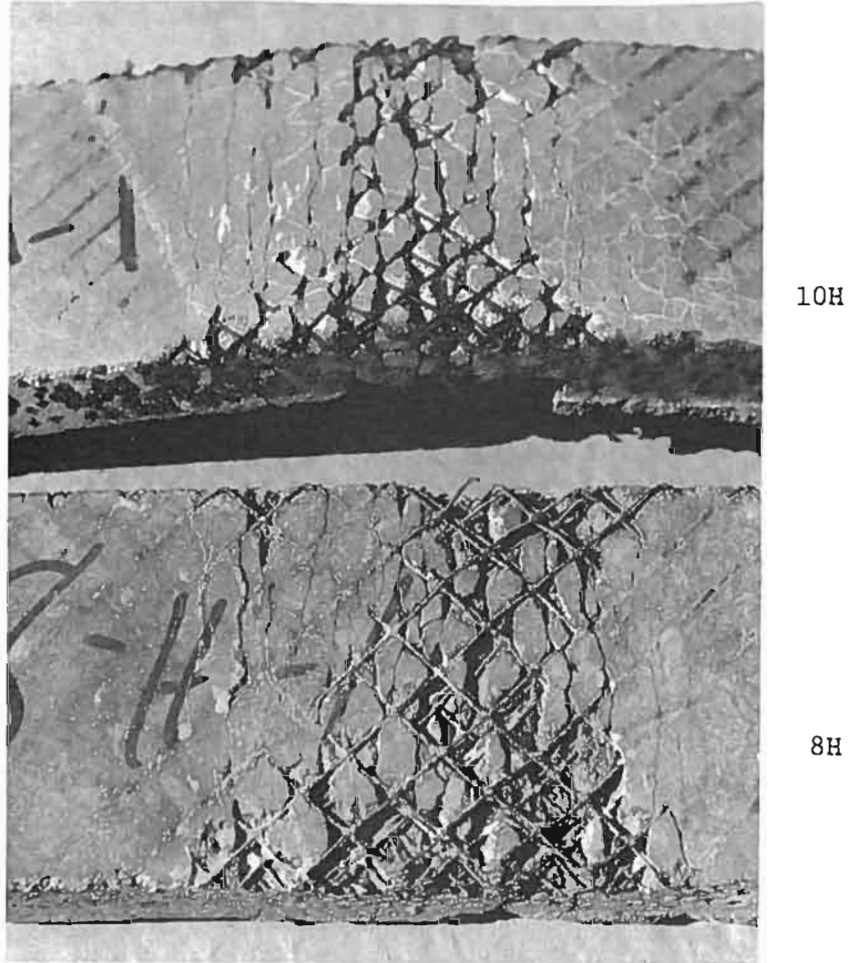


Fig. 35. Damaged bend test specimens containing ungalvanized 3/8-19 ga. mesh (10H) and galvanized 1/2-19 ga. hardware cloth (8H) after 48 hours in seawater.

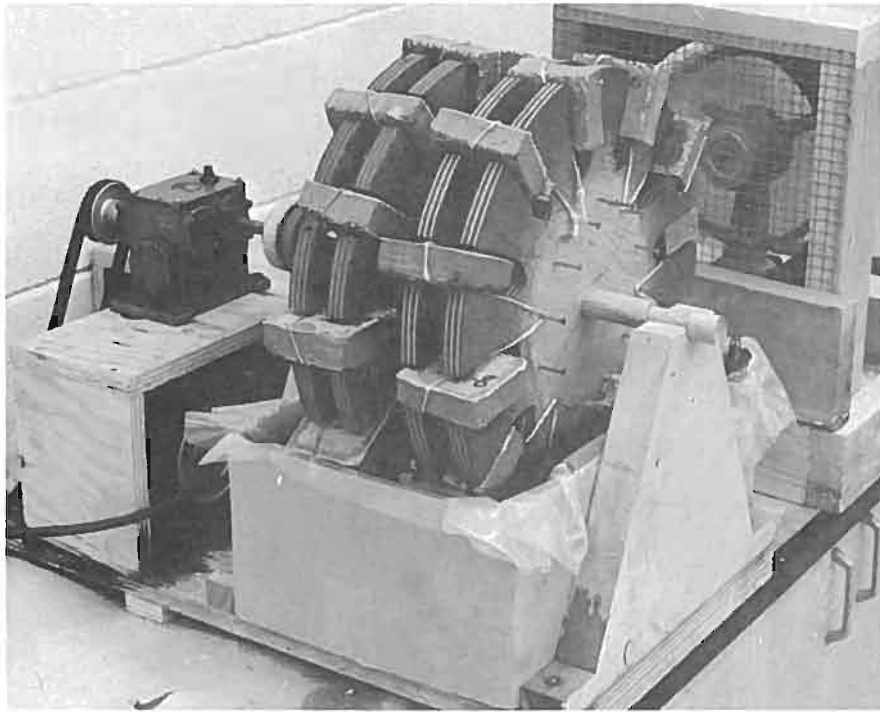


Fig. 31. Seawater exposure tests.



Fig. 32. Rust staining on bottom surface of coupons containing (a) 1/2-22 ga. hexagonal mesh with light zinc coating and (b) 1/2-ga. welded square mesh with zinc coating removed.

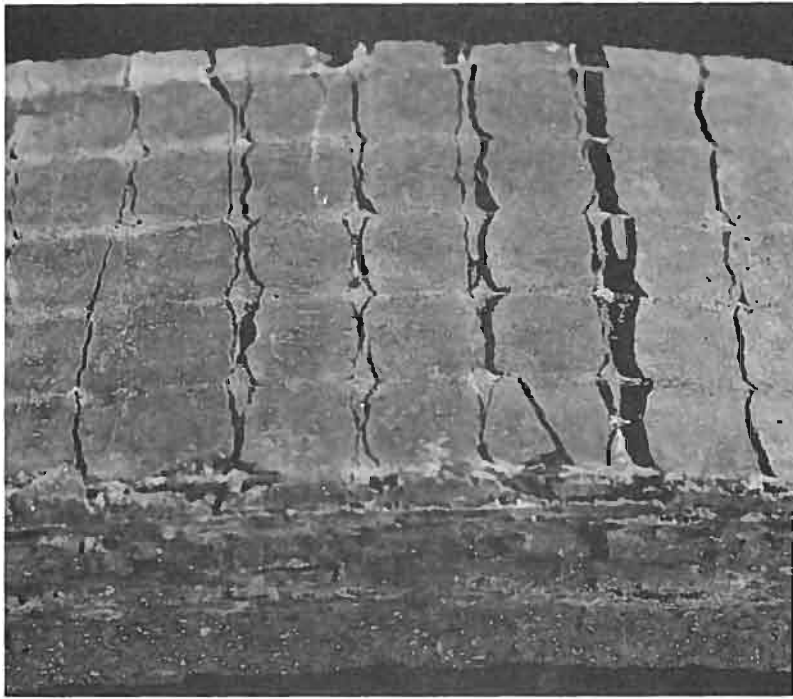


Fig. 33. Cracked coupon containing galvanized wire mesh after 48 hours immersion in seawater.

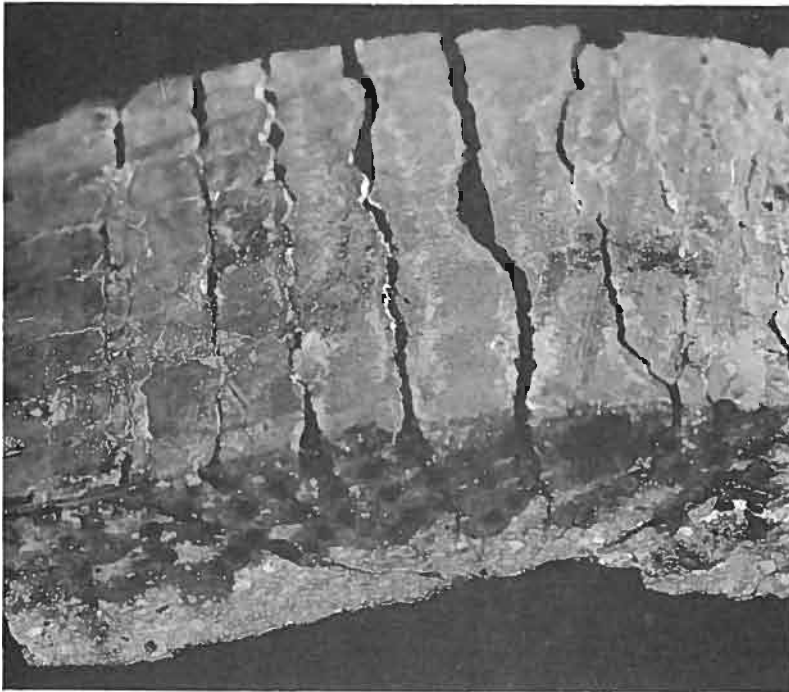


Fig. 34. Cracked coupon containing ungalvanized wire mesh after 48 hours immersion in seawater.

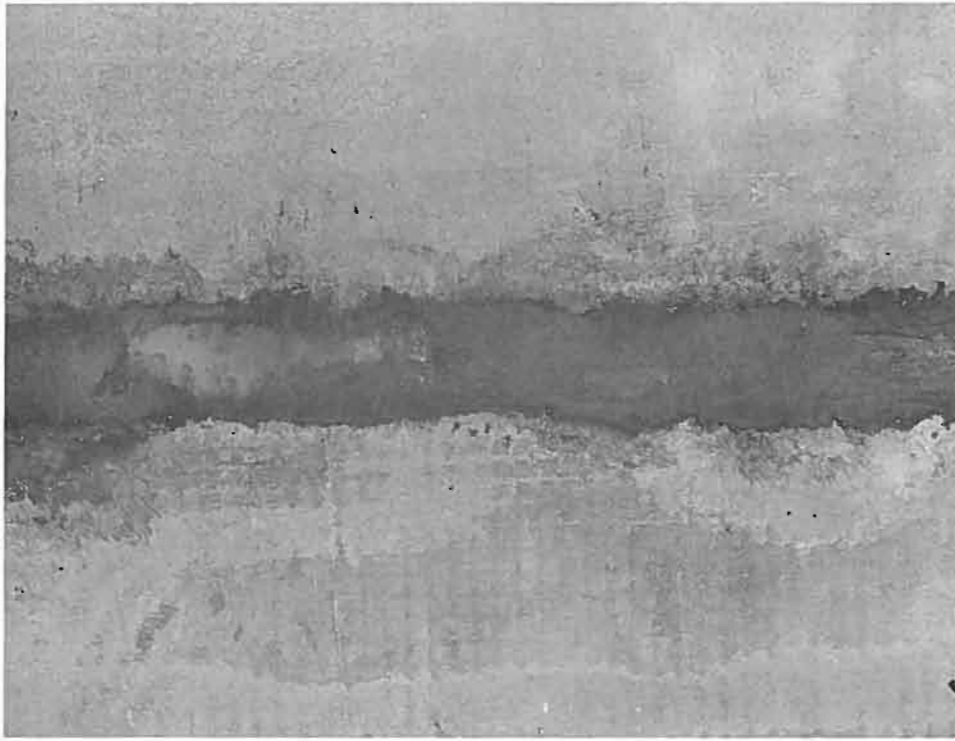


Fig. 37. Joint formed in panel during interrupted mortaring.

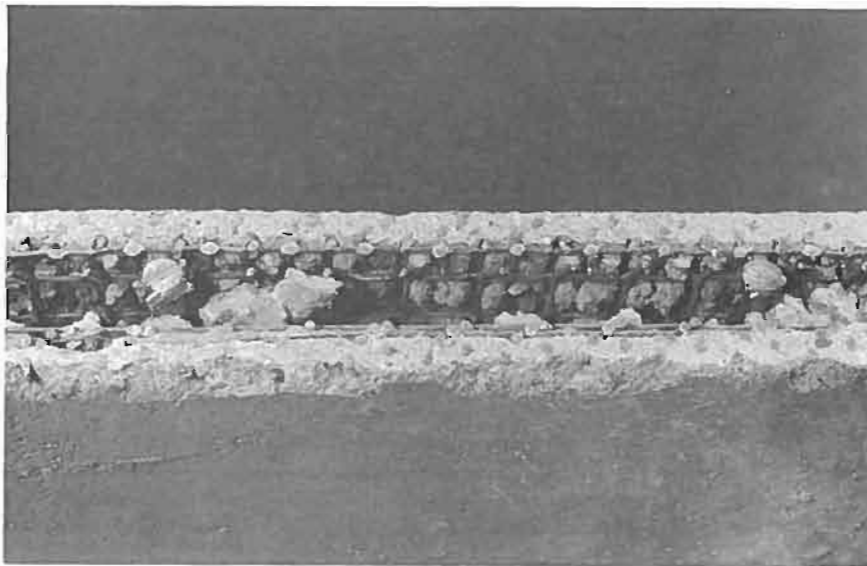


Fig. 38. Incomplete penetration of mortar resulting from too many layers of mesh for the workability of the mortar.

PART II - DEVELOPMENT OF A MATHEMATICAL MODEL
(by John D. Smith, P.Eng.*)

A. INTRODUCTION.

The available literature on ferro-cement boat building mainly concentrates on construction techniques developed through experience for specific types of reinforcement, with little information on design methods to aid the naval architect. Architects with experience in ferro-cement design tend to regard their methods as trade secrets. The more technical articles on ferro-cement are often qualitative comparisons of results of tests in which various strengths of mortar, mesh sizes and types, percentages of steel, and reinforcing rods were used. Also, most investigators emphasize the ultimate strengths achieved. It is only with great difficulty that the naval architect can find design information in a form useful to him.

The naval architect needs to know:

1. What working stress can be used for designing under tension, compression, shear, and bending and what is the effect of combined loading.
2. What deflection will be produced by a given load. At times the most significant criteria will be deflection rather than stress.
3. What type of failure will occur from accidents such as grounding (possible high local loads), or hitting a rock or log (impact loads). If the damage will seriously affect the water-tight integrity of the hull, he may want to allow extra material to compensate.

One approach to determining the required design information is to make and test a sufficient number of panels covering the range of likely reinforcement combinations under various load conditions. Since test results for reinforced concrete typically show a wide spread the number of specimens of each type must be large enough to define performance adequately and to allow the range of deviations to be determined. It should be kept in mind that a small defect in a small specimen will have a greater effect than the same defect in a large panel. Therefore, a greater number of small specimens may be required.

It is evident that this approach will be lengthy and expensive. This method could lead to greater confidence in, and acceptance of ferro-cement as a boatbuilding material, but it could also retard the evolution of new and better reinforcing materials and combinations.

*Mr. John D. Smith was formerly associated with B.C. Research, but is now at Defence Research Establishment Pacific, Esquimalt, B.C.

An alternative approach is to develop a mathematical model for the behaviour of ferro-cement. This model could then be proven or improved by the results of a limited number of test specimens. If successful, this approach could effect a considerable saving in time and money and allow new combinations of reinforcement materials to be checked out on paper. Only the most promising combination need then be chosen for experimental verification.

Experimental methods would still be required to investigate such factors as labour requirements, the effect of joints (hull to deck, frames to hull, etc.), ease of fabrication, and behaviour under impact loads.

The object is to develop the simplest model for the behaviour of ferro-cement which will give results agreeing fairly well with observed experimental results. Since the loading conditions to be experienced by a vessel during its lifetime can only be guessed at and since there can be large variations in actual strength due to workmanship, it is doubtful that a large increase in complication to achieve a small increase in accuracy is justified. The model and its application methods should also indicate the effects of changes due to increasing mortar strength and in the type, quantity, and distribution of the reinforcement.

The development of a mathematical model can be divided into four convenient stages:

1. A linear model in which both the mortar and steel are assumed to behave in a linear fashion. The linear model should result in the least complicated solutions. Since working loads will be considerably lower than ultimate loads, it is probable that non-linear effects will not be significant and that a linear model will be adequate in this region. The analysis of natural frequencies and resonances will be much simpler if a suitable linear model can be used.
2. The linear model is extended to account for the non-linearities of the mortar. The steel is still assumed to behave linearly.
3. The loads and deformations, where yielding of the steel or limited compressive failure of the concrete occur, is investigated. It is important to know when permanent deformation occurs and what the properties will be after a partial failure. With suitable assumptions it is probable that a linear model can be used to describe the behaviour of the section under low loads after some permanent deformation has occurred.

4. The analysis of ultimate failure and prediction of the mode of failure would be investigated.

In the following sections, only the first two stages will be investigated.

B. DEVELOPMENT OF THE MODEL.

Muhlert⁽¹⁾ at the University of Michigan has applied methods used in the design of reinforced concrete beams to an analysis of ferro-cement bend test specimens. His results have been fairly consistent, but conservative. Mowat⁽²⁾ at the University of Calgary attempted to predict the performance of ferro-cement through a non-linear analysis. Most of his calculations were to obtain ultimate loads, and he used the ratio of actual moment at failure to the predicted moment as a measure of the efficiency of the reinforcement. One criticism of his results is that in calculating his ultimate loads he has assumed that the mortar at the compression face has reached the maximum strain before compression failure occurs. He also computes the height of the neutral axis and the steel strains on this basis. Therefore, if the steel fails in tension before this occurs the efficiency calculated will be low. A better criteria would be the ratio between the percentage of effective steel and the ultimate load.

Both Muhlert and Mowat used relatively simple computer programs, using successive approximations, to perform the calculations. However, in this study graphical methods will be used as much as possible to make it easier to visualize the effects of changing mortar strengths and reinforcement quantities.

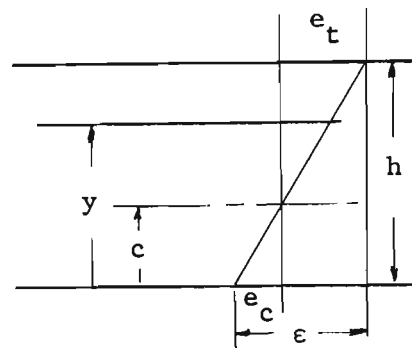
Linear model.

All loads and stresses are calculated as a function of the total strain (the sum of the absolute values of the strains at the tension and compression faces) since the ratio of thickness to the total strain is equal to the radius of curvature and proportional to the deflection.

(1) Muhlert, H.F., Analysis of Ferro-cement in Bending, The University of Michigan, Paper No. 043, January 1970.

(2) Mowat, D.L., Flexural Testing of Ferro-cement Planks, Thesis for M.Sc. in Civil Engineering, University of Calgary, Canada, January 1970.

It will be assumed that the mortar can exert only a compressive force. Shah⁽³⁾ has reported that once cracking has occurred, the modulus of elasticity in tension of ferro-cement is close to that determined from the steel alone. Since fine surface cracks have been observed on new hulls (possibly due to settling during curing or to shrinkage stress) it is reasonable to assume the cracked condition.



e_t = strain at tension face
 e_c = strain at compression face
 ϵ = total strain
 h = thickness
 c = height of neutral axis above compression face
 y = height of any element above compression face

At any point the strain is given by:

$$e = (y - c) \frac{\epsilon}{h}, \text{ taking elongation as positive.}$$

Also define the following dimensionless parameters:

$$Y = \frac{y}{h} ; C = \frac{c}{h}$$

$$\text{Therefore } e = (Y - C)\epsilon$$

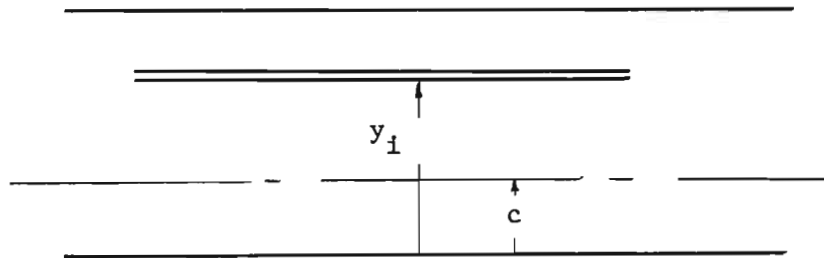
To achieve equilibrium the sum of the forces in the steel, F_s , and in the mortar, F_m , must equal zero for pure bending.

$$F_s + F_m = 0$$

(3) Shah, S.P., Ferro Cement as a New Engineering Material, College of Engineering Report No. 70-11, University of Illinois, Dec. 1970.

Linear steel.

For one layer of steel reinforcement:



The force on the layer is given by

$$F_i = \frac{(y_i - c)}{h} \epsilon A_i E_s \quad \text{where } A_i = \text{area/inch width}$$

$$y_i = \text{height of layer}$$

$$E_s = \text{modulus of elasticity}$$

and the net steel force is

$$F_s = \sum_i \frac{n (y_i - c)}{h} \epsilon A_i E_s \quad n = \text{number of layers}$$

$$F_s = \frac{\epsilon E_s}{h} [\sum y_i A_i - c \sum A_i]$$

However,

$$z = \frac{\sum y_i A_i}{\sum A_i} \quad \text{where } z = \text{height of the centroid of the steel}$$

Define $Z = \frac{z}{h}$ and $A_s = \sum A_i$

$$F_s = [Z - C] \epsilon E_s A_s.$$

The moment for the steel is given by:

$$M_s = \sum \frac{(y_i - c)^2}{h} A_i \epsilon E_s$$

$$= \frac{\epsilon E_s}{h} \times \text{moment of the steel about the neutral axis of the beam.}$$

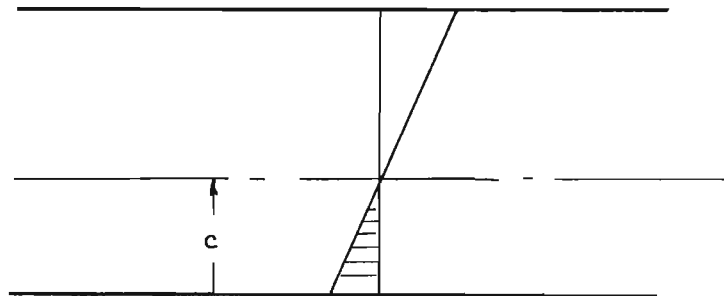
If I_s = moment of the steel about the centroid of the steel

$$M_s = [I_s + (z - c)^2 A_s] \frac{\epsilon E_s}{h}$$

$$M_s = \left[\frac{I_s}{h^2} + (Z - C)^2 A_s \right] \epsilon E_s h$$

Linear mortar.

The mortar is assumed to exert a force only in compression and the force is assumed to be linear with strain.



The stress at the compressive face S_c is given by:

$$S_m = -\frac{c}{h} \epsilon E_m \quad \text{where } E_m = \text{modulus of elasticity in compression for the mortar.}$$

The mortar force is then

$$F_m = - \left(\frac{c}{h} \epsilon E_m \right) \frac{c}{2}$$

$$= - \frac{C^2 \epsilon E_m h}{2}$$

and the moment for the mortar is

$$M_m = F_c \left(- \frac{2}{3} c \right)$$

$$M_m = \frac{C^3 E_m \epsilon h^2}{3}$$

For equilibrium the sum of the steel and mortar forces must equal zero

$$F_s = [Z - C] \epsilon E_s A_s ; F_m = - \frac{C^2 \epsilon E_m h}{2}$$

dividing both by (ϵh) and equating

$$\frac{F_s}{\epsilon h} + \frac{F_m}{\epsilon h} = \frac{Z - C}{h} E_s A_s - \frac{C^2 E_m}{2} = 0$$

$$\text{or } \frac{Z - C}{h} E_s A_s = \frac{C^2 E_m}{2}$$

We can then solve for C by plotting both sides of the equation as a function of C.

It should be noted that at this stage no account has been made of the concrete displaced by the steel on the compression side of the neutral axis. The effect of this will be investigated with an example later.

The moment equations obtained were:

$$M_s = \left[\frac{I_s}{h^2} + (Z - C)^2 A_s \right] \epsilon E_s h$$

and

$$M_m = \frac{C^3 E_m \epsilon h^2}{3}$$

Dividing both by ϵh^2 we get

$$\frac{M_s}{\epsilon h^2} = \left[\frac{I_s}{h^3} + (Z - C)^2 \frac{A_s}{h} \right] E_s$$

and

$$\frac{M_m}{\epsilon h^2} = \frac{C^3 E_m}{3}$$

As an example it would be convenient to use Mowat's results for his Series 3 Plank 9. This plank contained 13 layers of 1/2" x 1/2" welded and was strain-gauged top and bottom. The gauges remained intact for the full range of loads allowing us to find both the total strain and the height of the neutral axis for each bending moment.

Table 1 presents Mowat's data and the derived total strains and heights for the neutral axis. These are also plotted in Fig. 1A.

To calculate the height of the neutral axis we must have a value of Modulus of Elasticity for the mortar.

Mowat used a stress strain relationship.

$$f_c = f_{cu} \left[1 - \left(\frac{e_{cu} - e_c}{e_{cu}} \right)^\lambda \right]$$

where: f_c = mortar stress
 f_{cu} = ultimate mortar stress
 e_{cu} = ultimate mortar strain
 e_c = mortar strain

$$\lambda = \frac{25}{1.25 + f_c \text{ (ksi)}}$$

$$\text{Taking } E_m = \frac{d f_c}{d e_c} \bigg|_{e_c = 0} = \frac{f_{cu} \lambda}{e_{cu}}$$

Mowat used a value of 0.38% for e_{cu} . For

$$f_{cu} = 5000 \text{ psi, we get}$$

$$E_m = 5.26 \times 10^6 \text{ psi.}$$

Since the steel is symmetrically arranged $Z = 0.50$ and

$$\frac{Z E_s A_s}{h} = 0.539 \times 10^6$$

The functions $\frac{Z - C}{h} E_s A_s$ and $\frac{C^2 E_m}{2}$ are plotted in the top half of Fig. 2A. The curves intersect at $C = 0.293$.

The curves for

$$\frac{M_m}{\epsilon h^2} = \frac{C^3 E_m}{3}$$

$$\text{and each part of } \frac{M_s}{\epsilon h} = \frac{I_s E_s}{h^3} + \frac{(Z - C)^2 E_s A_s}{h}$$

are also plotted. Taking the values from the curves

$$\begin{aligned} \frac{M}{\epsilon h^2} &= (0.045 + 0.077 + 0.045) \times 10^6 \\ &= 0.167 \times 10^6 \end{aligned}$$

for $\epsilon = 0.2\%$ and $h = 1.0$ in.

$$\begin{aligned} M &= 0.167 (0.002)(1)^2 \times 10^6 \\ &= 334 \text{ in.-lb/in.} \end{aligned}$$

This corresponds to a load of 365 lb which is much lower than the value of 530 lb taken from Fig. 1A. However, if the load vs. strain for the linear model is drawn on Fig. 1A it will be seen that the calculated strain curve is offset from the experimental load/strain curve but nearly parallel to it.

Before commenting further, the effect of the concrete displaced by the steel on the compression side of the neutral axis should be considered. This can be done by replacing the area

$$A_i \text{ by } \frac{E_s - E_m}{E_s} A_i \text{ for those layers.}$$

For this case the corrected $A_s = 0.033$ sq in.

$$Z = 0.518$$

The corrected line for $(Z - C) E_s \frac{A_s}{h}$ is shown in Fig. 2A by a dashed line.

The corrected $I_s = 0.00229$ in.⁴/in. and the corrected moment is:

$$M = 326 \text{ in.-lb/in. for } \epsilon = 0.2\%$$

This is a change of 5.4%, which is small compared to the extra work involved.

Non-Linear mortar.

It will be assumed that the steel behaves linearly as in the last section. However, the effect of a non-linear stress/strain relationship for the mortar will be investigated.

The mortar force will be given by:

$$F_m = - \alpha f_{cu} c$$

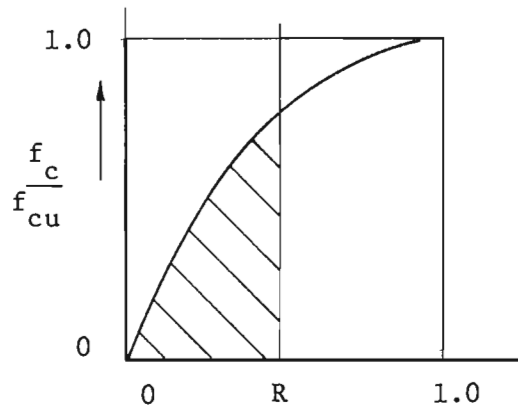
$$\frac{F_m}{\epsilon h} = - \alpha f_{cu} \frac{C}{\epsilon}$$

α = a stress block factor defined as the ratio of the average mortar stress to the ultimate stress f_{cu} .

The stress/strain relationship from page 100:

$$\frac{f_c}{f_{cu}} = 1 - (1 - R)^\lambda \text{ where } R = \frac{e_c}{e_{cu}} \text{ will be used.}$$

This is plotted in Fig. 3A.



For a given R

$$\alpha = \text{average value of } \frac{f_c}{f_{cu}} \text{ between 0 and R.}$$

$$= \frac{\text{shaded area}}{R}$$

This gives $\alpha = 1 - \frac{1 - (1 - R)^{\lambda + 1}}{(\lambda + 1)R}$ and is plotted in Fig. 4A.

$$\text{Now } R = \frac{e_c}{e_{cu}} \text{ and } e_c = C \epsilon$$

Therefore $\frac{F}{\epsilon h} = -\alpha f_{cu} \frac{C}{\epsilon}$ is now a function of ϵ as well as C and a separate curve can be plotted for each value of ϵ . This is done for $\epsilon = 0.01\%$, 0.2% and 0.4% in Fig. 5A. It can be seen that the height of the neutral axis increases as the total strain increases, which is opposite to the trend shown in Fig. 1A for Mowat's specimen 3.9.

Improved linear mortar model.

Previously it was assumed that the mortar could only exert a force in compression. If we assume that the mortar has a limited tensile strength and characterize this by an ultimate tensile

strain e_{tu} . The mortar force now becomes

$$\begin{aligned} \frac{F_m}{\epsilon h} &= \frac{C^2 E_m}{2} - \left(\frac{e_{tu}}{\epsilon}\right)^2 \frac{E_m}{2} \\ &= \frac{E_m}{2} \left[C^2 - \left(\frac{e_{tu}}{\epsilon}\right)^2 \right] \end{aligned}$$

and the mortar moment becomes

$$\frac{M_m}{\epsilon h^2} = \frac{E_m}{3} \left[C^3 - \left(\frac{e_{tu}}{\epsilon}\right)^3 \right]$$

When $\epsilon \gg e_{tu}$ the force and moment approach those for the previous linear model. The height of the neutral axis now decreases for increasing strain, approaching the value given by the earlier linear model. This is demonstrated in Fig. 6A.

C. DISCUSSION.

The linear model resulted in simple expressions for forces and moments. The graphical method employed (Fig. 2A) in solving for the height of the neutral axis and moments clearly shows the effect of varying parameters such as steel area, mortar modulus of elasticity and beam thickness.

Using Mowat's Series 3 Plank 9 as an example gave calculated moments lower than the experimental results. However, the calculated load/strain curve was roughly parallel to the experimental. It appeared that the calculated values could be improved by choosing a higher value for the modulus of elasticity for the mortar. This would lower the calculated neutral axis height, as well as increasing the calculated moment.

The non-linear model indicated that the height of the neutral axis above the compression face would increase with increasing strain as long as the steel did not yield. This result was inconsistent with the experimental result.

Compared to the linear model, the non-linear mortar approximation gave a greater neutral axis height and would give a lower bending moment, thus resulting in an even poorer agreement with the experiment.

The improved linear model which accounted for some tensile strength in the mortar correctly forecast the trend for decreased neutral axis height with increasing strain and gave a higher mortar moment than the previous models. It is felt that with a suitable adjustment of the parameters E_m and e_{tu} a good fit with the experimental result could be attained.

No attempt was made to fit the experimental curves more closely since this should be done using the results of many tests rather than one isolated example, and the values chosen were adequate to illustrate trends.

The correction of the linear model for the volume of concrete displaced by the steel in the compression zone did not result in a large change in neutral axis height or calculated moment.

D. CONCLUSIONS AND RECOMMENDATIONS.

Either the linear or the improved linear model promises to be a satisfactory basis for a design procedure for ferro-cement in the working stress range. Further development of the method will require the determination of appropriate constants by comparison with experimental results.

Strain measurements on both tension and compression faces are an essential requirement to determine the behaviour of the test specimens. The effects of cracking at the tension face on the strain gauge readings must be considered.

There exists enough experimental data and information on standard practices to establish a standard mortar to be used for design purposes. This would be the first step in establishing an approved design procedure. Design charts and standards could then be developed for this standard mortar. When advances in cement technology permit mortars of higher properties to be produced consistently, a second standard mortar could then be established.

Using the standard mortar for test specimens, experimental results could be used to establish points on the curves for $\frac{F}{ch}$ and $\frac{M}{ch^2}$.

Initially the points could be fitted to a C^2 function for mortar forces and a C^3 function for moment. As the experimental data increased, empirical curves could be established and values of E_s to be used with basic types of reinforcement could be determined. The final stage would be to determine whether an improved linear mortar model would be an improvement. It is likely that the experimental data will show a great enough spread that a more complicated model would not be justified.

Rather than establishing working stresses for design purposes, the possibility of determining strain limits for tension and compressive strains under design loads should be investigated.

Most of the available data gives load/strain or load/deflection curves for specimens loaded progressively to failure. Since boat hulls will occasionally experience high loads and the effects may be cumulative, it is essential to monitor specimens through repeated load cycles to high loads and through cycles of alternating loads. A design procedure must consider the strains and strengths of the material after many years of service, not just for the new condition.

TABLE 1. Mowat's Data for Series 3 Plank 9.

13 layers 1/2" x 1/2" welded mesh - assumed evenly distributed.

Wire dia = 0.042 in.

Thickness 1 in.

Width 6 in.

Length 33 in.

Total longitudinal wire = 0.00276 sq in./in./layer

= 0.0359 sq in./in.

Moment of steel about steel centroid $I_s = 0.00257 \text{ in.}^4/\text{in.}$

Mortar compressive strength = 4830 psi.

Load (lb)	Defl. (in.)	Compressive Strain (in./in.)	Tension Strain (in./in.)	Total Strain (in./in.)	Neutral Axis height/thickness
150	.035	0.010	0.02	0.030	0.30
300	.129	0.027	0.06	0.087	0.31
450	.260	0.045	0.114	0.159	0.283
600	.385	0.061	0.176	0.237	0.257
750	.529	0.080	0.241	0.320	0.250
900	.719	0.107	0.950	0.457	0.234
1050	1.19	0.157	0.642	0.819	0.192
1090	Failure				

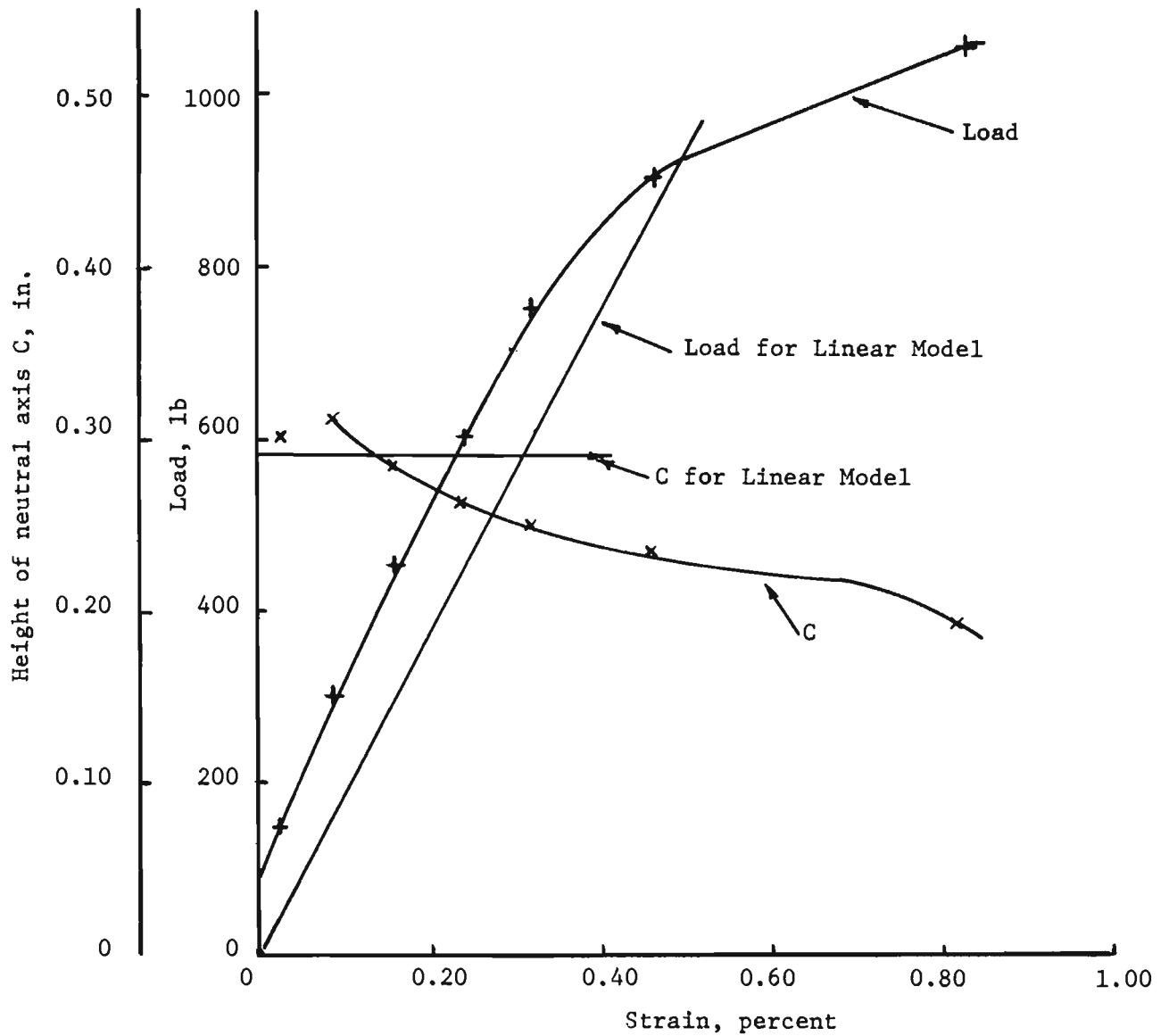


Fig. 1A. The derived height of neutral axis, $C = c/h$ and derived loads at various strain levels compared with measured values by Mowat (Series 3, Plank 9)*

*Mowat, D.L., Flexural Testing of Ferro-cement Planks, Thesis for Master of Science in Civil Engineering, University of Calgary, Calgary, Canada, Jan. 1, 1970.

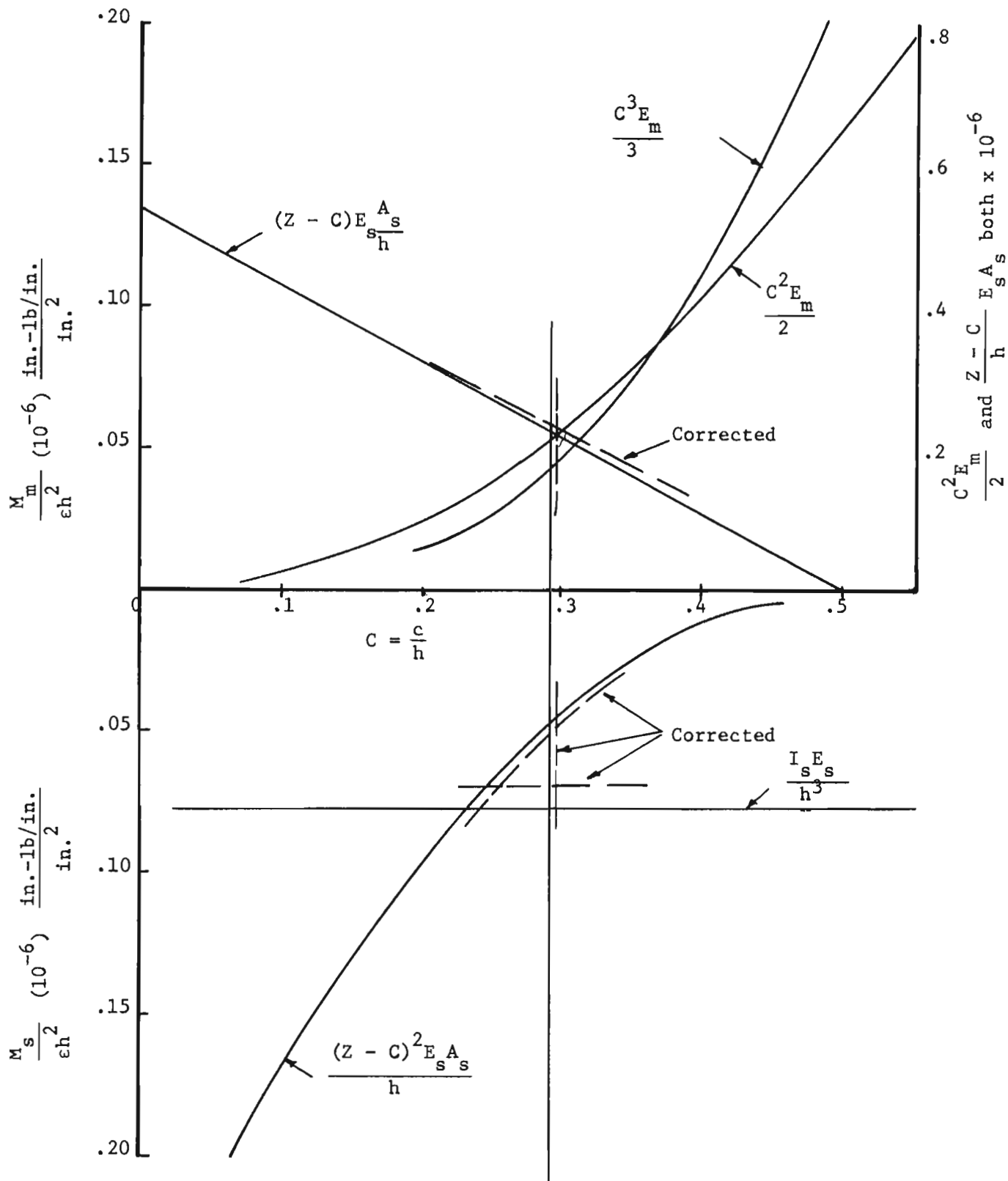


Fig. 2A. Plot of modulus functions vs strain to obtain the value of C and hence location of neutral axis.

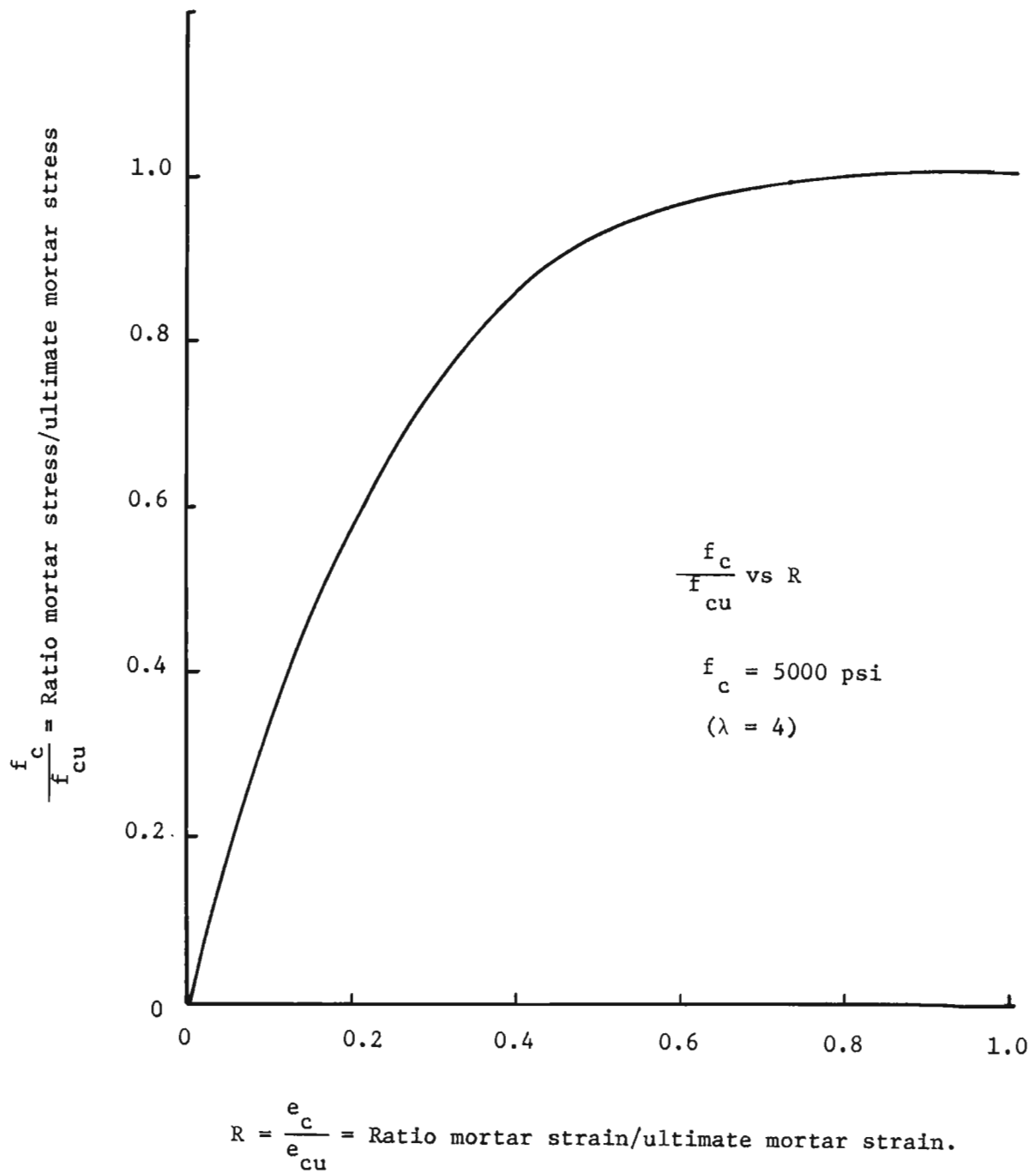
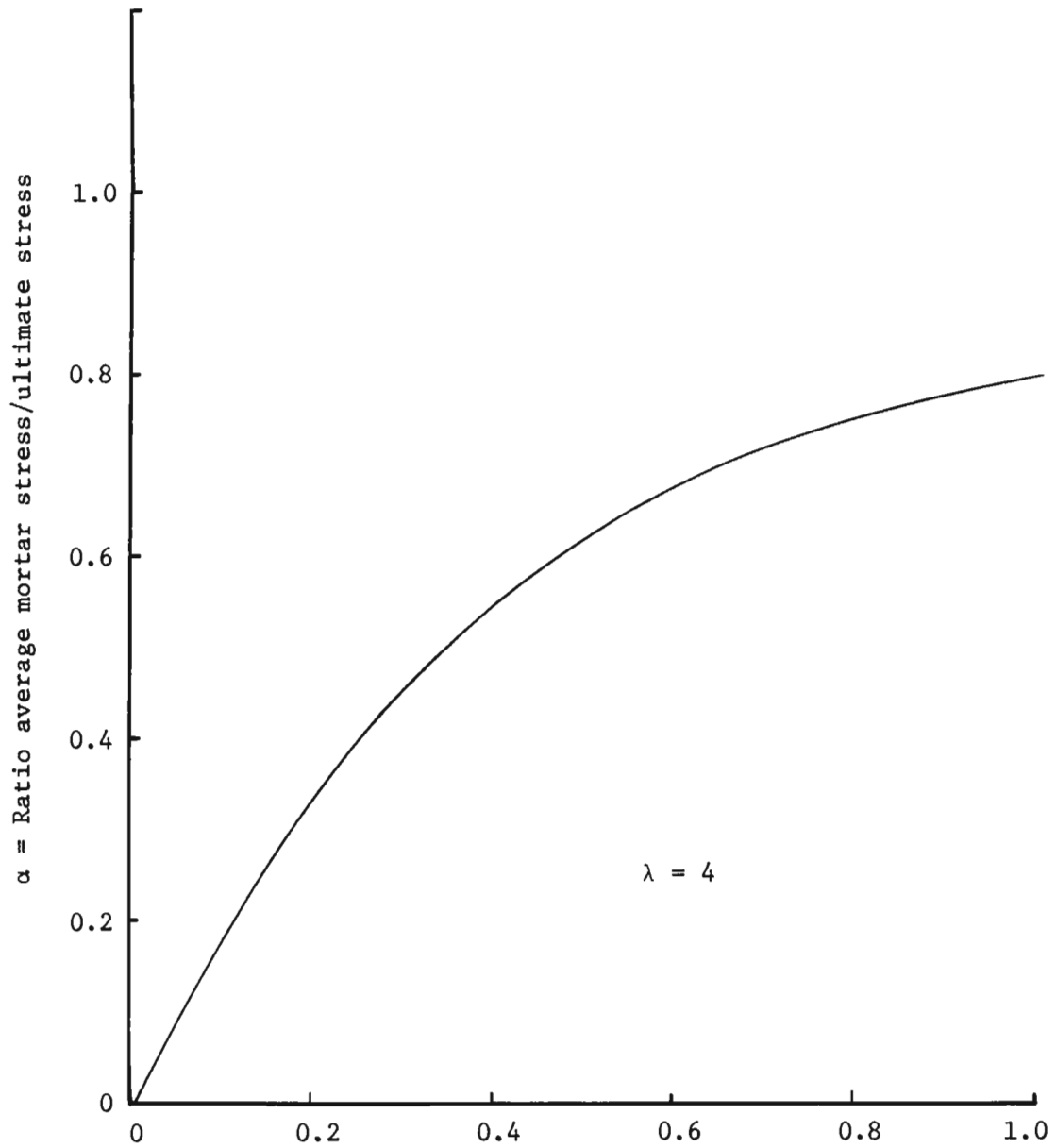


Fig. 3A. Stress Ratio vs Strain Ratio R .



$$R = \frac{e_c}{e_{cu}} = \text{Ratio mortar strain/ultimate mortar strain}$$

Fig. 4A. Stress ratio α vs strain ratio R .

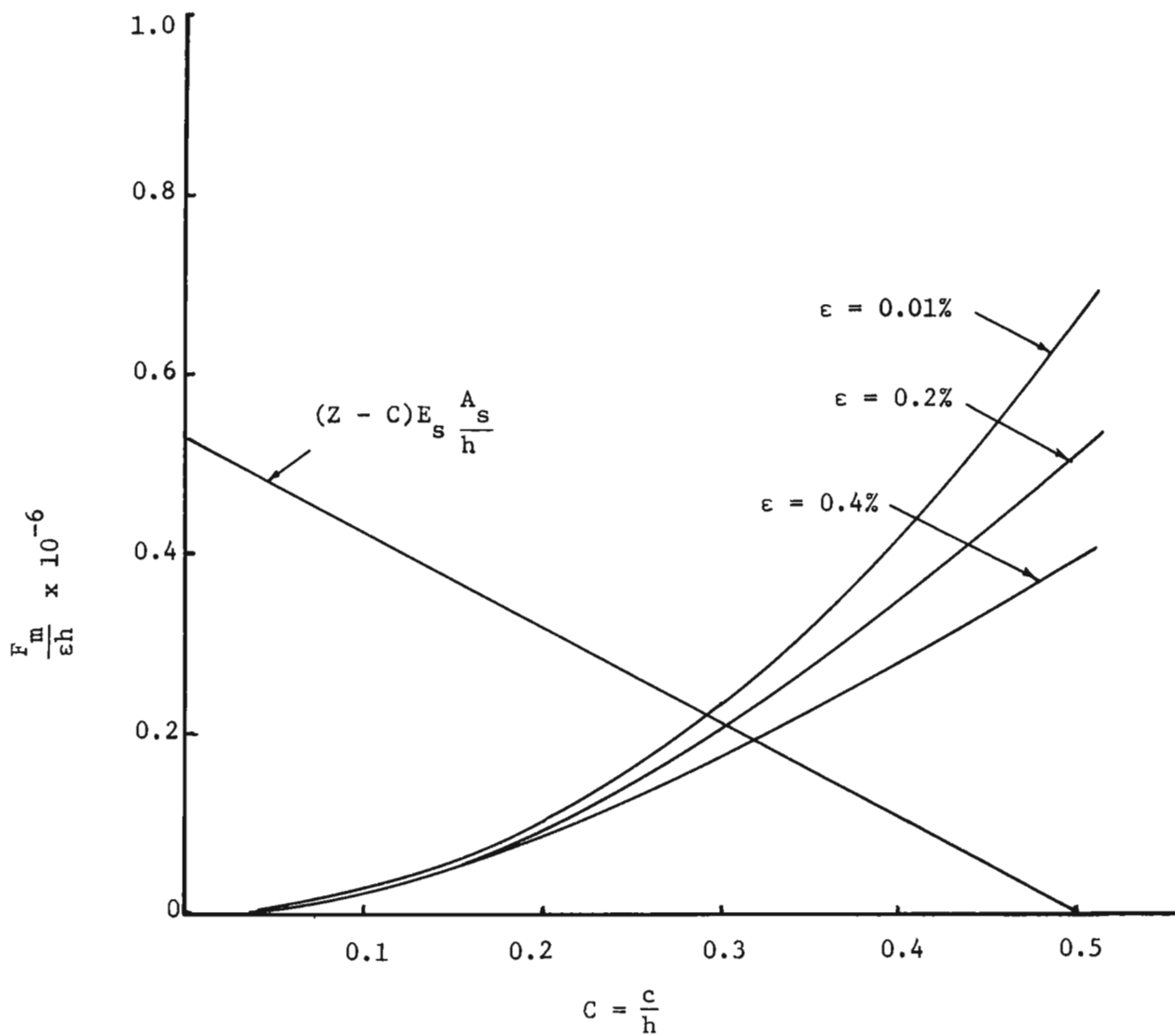


Fig. 5A. $\frac{F_m}{\epsilon h}$ vs C for Non-linear Mortar.

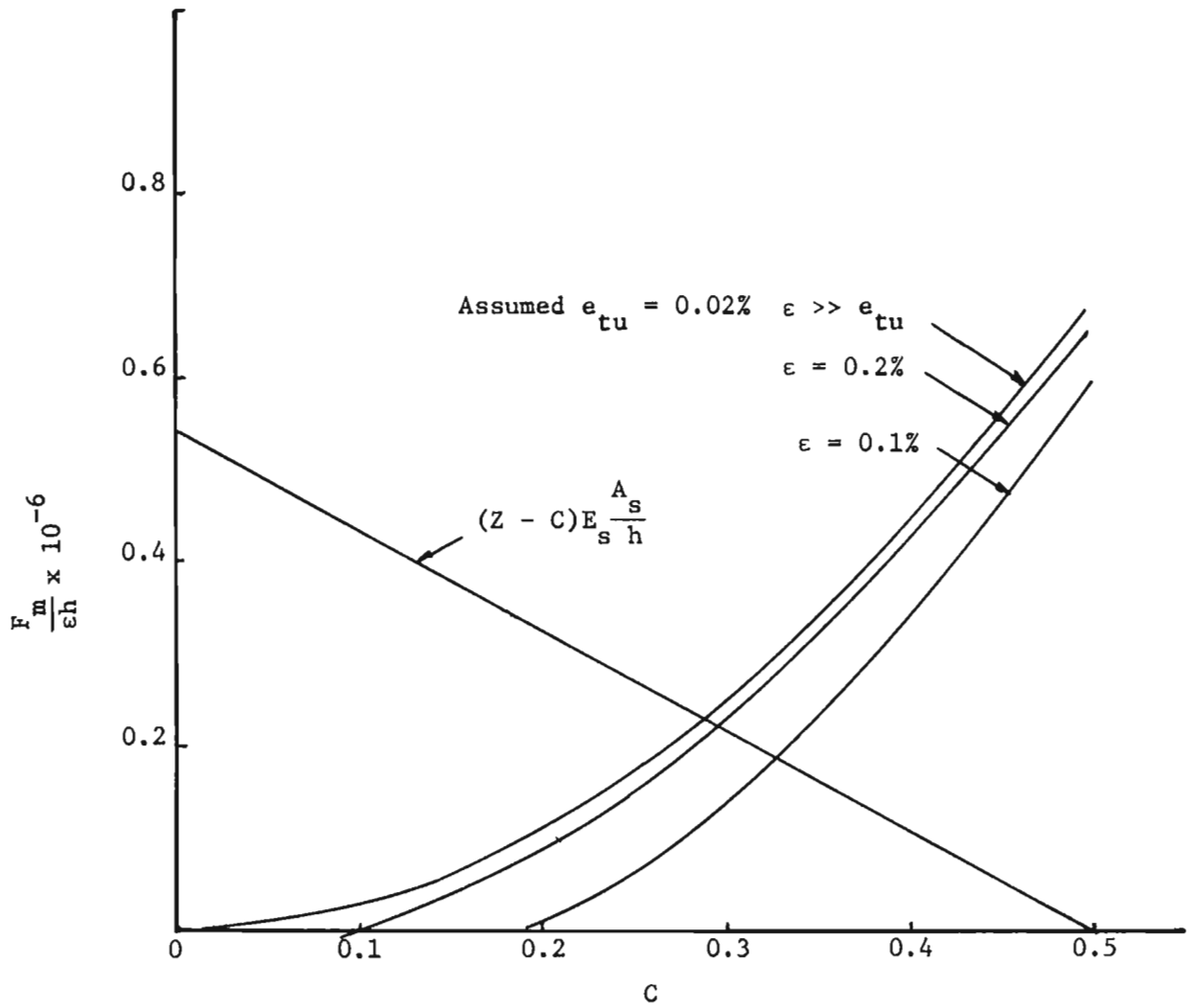


Fig. 6A. $\frac{F_m}{\epsilon h}$ vs C for Improved Linear Model.